

University of Missouri, St. Louis

IRL @ UMSL

Dissertations

UMSL Graduate Works


10-25-2011

Rational Ligand Design for Potential Applications in Transition Metal Catalysis

Sergey L. Sedinkin

University of Missouri-St. Louis

Follow this and additional works at: <https://irl.umsl.edu/dissertation>

 Part of the [Chemistry Commons](#)

Recommended Citation

Sedinkin, Sergey L., "Rational Ligand Design for Potential Applications in Transition Metal Catalysis" (2011). *Dissertations*. 410.

<https://irl.umsl.edu/dissertation/410>

This Dissertation is brought to you for free and open access by the UMSL Graduate Works at IRL @ UMSL. It has been accepted for inclusion in Dissertations by an authorized administrator of IRL @ UMSL. For more information, please contact marvinh@umsl.edu.

Rational Ligand Design for Potential Applications in Transition Metal Catalysis

Sergey L. Sedinkin

M.S. in Chemistry, University of Missouri-St. Louis, 2009

M.S. in Chemistry, Higher Chemical College of the Russian Academy of Sciences,
2006

A Thesis Submitted to The Graduate School at the University of Missouri – St. Louis in
partial fulfillment of the requirements for the degree
Doctor of Philosophy in Chemistry

August 2011

Advisory Committee

Eike Bauer, Ph.D.
Chairperson

Christopher Spilling, Ph.D.

James Chickos, Ph.D.

Keith Stine, Ph.D.

Table of Contents

LIST OF ABBREVIATION.....	V
LIST OF FIGURES.....	VI
LIST OF TABLES	III
ABSTRACT	IX
CHAPTER I Rational Ligand Design for Transition Metal Catalysis	
1.1. INTRODUCTION	1
1.2. INFLUENCE OF THE METAL COMPLEX ON THE CATALYTIC EFFICIENCY.....	2
1.3. LIGAND DESIGN.....	3
1.3.1. STERIC AND ELECTRONIC EFFECTS.....	5
1.3.1.1. <i>Steric tuning of ligands</i>	5
1.3.1.2. <i>Electronic tuning of ligands</i>	7
1.4 GOALS OF THE CURRENT PROJECT	10
1.5. CONCLUSION	11
1.6. REFERENCES	11
CHAPTER II Investigation of Amino-dithiaphosphanes as a New Class of Ligands	
2.1. AIM OF THE CHAPTER	16
2.2. INTRODUCTION	16

2.3. SYNTHESIS AND STUDIES OF THE LIGANDS	18
2.3.1. ELECTRONIC PROPERTIES AND CHEMICAL STABILITY	20
2.3.2. STERIC PROPERTIES AND CHEMICAL STABILITY	23
2.3.3. OVERVIEW OF THE CHEMICAL STABILITY OF THE SYNTHESIZED AMINO-DITHIAPHOSPHOLANES	28
2.4. ANALYSIS OF PROPERTIES OF THE NEW AMINO-DITHIAPHOSPHOLANES	30
2.4.1. PREPARATION OF SELENIUM DERIVATIVES.....	31
2.4.2. ANALYSIS OF THE NMR DATA	33
2.4.3. ANALYSIS OF THE SPECTROSCOPIC DATA OF AMINO-DITHIAPHOSPHOLANES IN METAL COMPLEXES.....	35
2.5. CONCLUSION	40
2.6. REFERENCES	40
CHAPTER II Experimental Section	
GENERAL METHODS	44
SYNTHESES	44
CHAPTER III Investigation of Steric and Electronic Tuning of Phosphinooxazoline Ligands	
3.1. AIM OF THE CHAPTER	49
3.2. INTRODUCTION	49
3.3. SYNTHESIS OF PHOSPHINOXAZOLINES	51

3.4. ANALYSIS OF THE LIGANDS' PROPERTIES	63
3.4.1. NEW IRON PHOSPHINOXAZOLINE COMPLEXES	64
3.4.2. ELECTRONIC PROPERTIES OF THE LIGANDS	67
3.4.3. STERIC PROPERTIES OF THE LIGANDS	72
3.5. CONCLUSION	74
3.6. REFERENCES	75
CHAPTER III Experimental Section	
GENERAL METHODS	79
SYNTHESES	79
CHAPTER IV Investigation of New Non-Heme Complexes for Iron Catalyzed Oxidation Reactions	
4.1. AIM OF THE CHAPTER	97
4.2. INTRODUCTION	97
4.3. SYNTHESIS OF THE LIGANDS	99
4.4. APPLICATION OF THE NEW LIGANDS IN CATALYSIS	111
4.4.1. PREPARATION OF THE IRON BASED CATALYTIC SYSTEMS	112
4.4.1.1. <i>Characterization of the new iron complexes</i>	115
4.4.2. STUDIES OF THE ACTIVITIES OF THE CATALYSTS	119
4.4.2.1. <i>Comparison of catalytic activities of the complexes</i>	120
4.4.2.2. <i>Mechanistic considerations of the oxidation reactions</i>	123
4.4.2.3. <i>Determination of isolated yields</i>	124

4.5. CONCLUSION	127
4.6. REFERENCES	128
CHAPTER IV Experimental Section	
GENERAL METHODS	132
SYNTHESES	132
CATALYTIC EXPERIMENTS.....	141
GENERAL PROCEDURE FOR COMPARATIVE CATALYTIC OXIDATIONS.....	141
DETERMINATION OF ISOLATED YIELDS	141

List of Abbreviation

Bn.....	Benzyl
DCM	Dichloromethane
DMAP	4-(Dimethylamino)pyridine
DMF.....	<i>N,N</i> -Dimethylformamide
DMSO.....	Dimethyl Sulfoxide
Et ₃ N.....	Triethylamine
Et ₂ O.....	Diethyl Ether
FAB.....	Fast Atom Bombardment
IR.....	Infrared
Me.....	Methyl
MeCN.....	Acetonitrile
MS.....	Mass spectrometry
3-NBA.....	3-Nitrobenzyl Alcohol
NMR.....	Nuclear Magnetic Resonance
OTf.....	Triflate (OSO ₂ CF ₃)
Ph.....	Phenyl
PhMe.....	Toluene
ppm.....	Parts per Million
THF	Tetrahydrofuran
TLC	Thin Layer Chromatography
TsCl.....	<i>m</i> -Toluenesulfonyl Chloride

List of Figures

Figure 1.1	6
Figure 1.2	7
Figure 1.3	8
Figure 2.1	17
Figure 2.2	18
Figure 2.3	20
Figure 2.4	21
Figure 2.5	24
Figure 2.6	24
Figure 2.7	26
Figure 2.8	27
Figure 2.9	29
Figure 2.10	32
Figure 2.11	35
Figure 2.12	36
Figure 3.1	50
Figure 3.2	51
Figure 3.3	52
Figure 3.4	52
Figure 3.5	53
Figure 3.6	55

Figure 3.7	57
Figure 3.8	58
Figure 3.9	60
Figure 3.10	61
Figure 3.11	64
Figure 3.12	66
Figure 4.1	98
Figure 4.2	100
Figure 4.3	100
Figure 4.4	103
Figure 4.5	104
Figure 4.6	106
Figure 4.7	107
Figure 4.8	108
Figure 4.9	111
Figure 4.10	114
Figure 4.11	115
Figure 4.12	118
Figure 4.13	119
Figure 4.14	120
Figure 4.15	120
Figure 4.16	125

List of Tables

Table 2.1	33
Table 2.2	37
Table 3.1	67
Table 3.2	69
Table 3.3	71
Table 3.4	73
Table 4.1	122
Table 4.2	126

Abstract

Strategies to influence the steric and electronic properties of three classes of ligands were investigated. First, a compound class known as amino-dithiaphospholanes was studied. It is structurally related to phosphoramidites, which have been successfully applied in catalysis. The synthesis of amino-dithiaphospholanes was envisaged as an approach to electronically tuned phosphoramidites. General access to a variety of structurally modified amino-dithiaphospholanes from commercially available starting materials was developed. The investigation of their chemical reactivities indicated that a combination of electronic, steric and physical properties determined the stability of the target ligands. The electron donating properties of the new ligands were characterized by NMR. They were found to be more basic and, thus, more electron donating than the corresponding phosphoramidites. The coordination chemistry of amino-dithiaphospholanes was investigated by synthesis of a series of iridium and rhodium complexes. Analysis of the physical data obtained for the complexes confirmed the increase in the electron density at the metal centers as a consequence of the increased basicity of the ligands.

Second, a series of new, as well as known, phosphinooxazoline (PHOX) ligands was synthesized. A systematic study of structure-property relationships was performed with the PHOX ligands. It was shown that electronic tuning of the ligands is possible by varying the substituents on the phenyl ring. However, the tuning was seen to have unexpected, and often only minor influence on the electronic properties of the metal complexes from those ligands due to the structural diversity and the back-

bonding abilities of the PHOX ligands. The efficiency of steric tuning was investigated by evaluation of X-ray structure analysis data of new iron PHOX complexes synthesized for the study. It was shown that the presence of substituents in the position α to the nitrogen atom of the oxazoline ring had the most profound impact on the geometries of the corresponding metal complexes.

Finally, five new multidentate N,O donating ligands (**L**) were synthesized and characterized. Their coordination chemistry was investigated by preparation of new iron complexes mimicking naturally occurring non-heme enzymes. The general formulation $[\text{Fe}(\mathbf{L})_2](\text{OTf})_2$, $[\text{Fe}(\mathbf{L})(\text{OTf})_2]$ or $[\text{Fe}(\mathbf{L})(\text{OTf})](\text{OTf})$ was established for the new complexes, and formation of only one isomer was confirmed for one of the complexes. The catalytic activity of the new compounds was demonstrated in the oxidation of activated methylene groups and alcohols to the corresponding ketones.

Chapter I

Rational Ligand Design for Transition Metal Catalysis

1.1. Introduction

With the society's driving need to establish and practice environmentally benign chemical processes, catalytic reactions have become a highly dynamic field in chemical research. Indeed, the threat of global warming has escalated the requirement of global industries to develop catalytic reactions for the regio- and enantioselective synthesis of sophisticated targets from simple starting materials. This is due to a strong and overriding belief that the development of efficient catalysts for industrial-scale reactions will significantly reduce energy consumption and waste production.

Stoichiometric and catalytic reactions of transition metals, in particular, have generated considerable interest due to their versatile and numerous applications in industrial and pharmaceutical settings. With the expanding utility of transition metal catalysis in the pharmaceutical and petrochemical industries, a major driving force was provided for the study and development of transition metal-catalyzed reactions. Catalysts of this type provide critical assistance in thermodynamically feasible processes by opening a lower activation energy pathway, often one that was symmetry forbidden.¹ These metal-centered reactions are mostly characterized by one or more elementary reactions, i.e. ligand substitution, oxidative addition, reductive elimination, migratory insertion, hydrogen exchange, β -hydrogen transfer, σ -bond metathesis, and nucleophilic addition.²

There are several reasons why transition metal complexes have become popular in this field. First, many of them are stable and easy to handle on any scale. For

example, the L-DOPA synthesis, discovered by Knowles,³ was taken to a commercial process in 1974 by the Monsanto Corporation. It utilizes a stable rhodium complex, which is required in large quantities for bulk syntheses. Secondly, by employing chiral ligands, these catalysts can promote highly stereoselective reactions. A good example is the use of chiral BINAP ligands in ruthenium complexes for the hydrogenation of β -keto carboxylic esters. The reported enantiomeric excess was nearly 100%.⁴ Thirdly, transition metal catalysts can be sterically and electronically “fine-tuned” by appropriate choice of the metal center and by manipulating the type and structure of the ligands. Finally, understanding of the mechanisms of the catalytic transformation and the influence of the ligands on the properties of the metal center can be used to improve the performance of the catalysts.

1.2. Influence of the metal complex on the catalytic efficiency

The effectiveness of a catalytic reaction depends on the following considerations: (1) the selectivity of the transformation (chemo-, regio-, and stereo-), (2) the rate of the conversion, and (3) the yield of the desired product. One of the main advantages of organometallic catalysts is the ability to be “tuned” to the desired level of activity and selectivity. This can be accomplished in two main ways. First, the choice of the metal for the complex heavily influences what kind of chemical transformations the complex could catalyze efficiently. Thus, rhodium and iridium are common choices for homogeneous hydrogenation;⁵ manganese,^{6,7} titanium^{8,9} and recently iron¹⁰⁻¹⁴ are widely employed in oxidation reactions; palladium is the most prevalent metal for catalyzing carbon-carbon bond formation in cross coupling reactions;¹⁵ and

ruthenium carbene complexes catalyze olefin metathesis.¹⁶ The second important part of a metal complex are its ligands. Most of the complexes' characteristics, including catalytic activity, are defined through the nature of the ligand attached – i.e. the steric and electronic properties of a ligand are usually translated to the complexes. Thus, since the catalytic properties of metal complexes are highly dependent on the nature of the ligand, it is thereby reasonable to assume that the design of a ligand that exhibits the desired steric and electronic property will lead to an efficient catalyst for a particular process. Consequently, it is important to realize that the outcome of reactions catalyzed by organometallic complexes can be influenced by the nature of a metal complex and the selection and design of the chiral ligand.¹ Therefore, the targeted design of ligands can lead to synthesis of metal complexes with desired properties, which is especially beneficial for application in organometallic catalysis.

1.3. Ligand design

There are several characteristics to be considered for the structure of a ligand to be employed in synthesis of a metal complex. The design of a ligand starts with the selection of an atom that would participate in formation of a coordination bond to the metal. Typical choices are phosphorus, nitrogen, oxygen or sulfur. These atoms typically are part of structurally complex ligands unlike halogens that are ligands on their own. The coordinating atom plays an important role in the overall behavior of a molecule as a ligand. The energy of the coordination bond depends on interaction of the metal center with the coordinating atom. The “hard and soft acid and base”

concept can be used to describe that dependency.¹⁷ It was shown that “softer” transition metals (platinum, palladium, ruthenium, rhodium, etc.) form stronger bonds with ligands bearing “softer” coordinating atoms (phosphorus, sulfur) rather than “harder” oxygen or nitrogen atoms. The opposite holds true for the “harder” alkali metals.¹⁸

Next factor is the number of atoms that participate in formation of coordination bonds with a metal center. Ligands with only one of such an atom are called monodentate. Ligands with two or more atoms capable of forming coordination bonds to a metal are called polydentate. Upon formation of a complex, these ligands generate chelating rings including the metal center.¹⁹ Chelation complexes are thermodynamically more stable mainly due to an overall increase in entropy during their formation.²⁰ The stabilization is known as “chelate effect”.²¹ That is usually a beneficial outcome for complex synthesis because it often allows the preparation of compounds that are more stable and thus easier to handle without special precautions. However, in some cases the stability of a complex can limit its practical applications. Thus, for catalysis, a complex in a catalytic cycle should be able to open a coordination site through one of the mechanisms mentioned above,² but strongly bonded ligands can potentially inhibit that process.

With type and number of coordinating atoms selected, the next aspect of the design is the organic core structure that would contain these atoms. The choice of the organic compound class ultimately defines the molecule’s performance as a ligand and the kind of steric and electronic properties that would be translated to the metal complex.

1.3.1. Steric and electronic effects

As mentioned above, ligands exert steric and electronic influences on the metal center. Thus, they not only influence the stereo- and regioselective outcome of the reaction to be catalyzed, they also affect the catalytic efficiency. Metal-ligand interactions have a big influence on the electron density of the metal center and thus impact the catalytic behavior of the metal complex.²²

Ligand-metal bonds consist of σ - (usually donor interaction) and π - (usually acceptor interaction) components. The contribution of each component to bonding depends on the electronic characteristics of the ligand.²³⁻²⁵ Consequently, considerable research efforts have been devoted to the fine-tuning of the electronic characteristics of a ligand by incorporating a variety of electron withdrawing or electron donating groups. On the other hand, bulky groups on a ligand exert steric effects on the metal center. These thereby influence catalytic activity by changing the geometry of the complex and by controlling the accessibility of the metal center.

1.3.1.1. Steric tuning of ligands

Varying the steric properties of ligands is most commonly employed strategy in improving the performance of metal complexes.²⁶ One of the first systematic investigations of steric properties was performed by Tolman who introduced his concept of a cone angle Θ for phosphorus containing ligands (**Figure 1.1, I**).²⁷ Later, an additional probe for assessing steric properties was developed by Casey and Whiteker for bidentate ligands (**Figure 1.1, II**). They introduced the concept of a bite angle β_n .²⁸ However, it was shown that effects of the bite angle of ligands are

not exclusively steric but could have an electronic component.²⁹ While these concepts are applicable for relatively simple systems, most of the more complex ligands cannot be analyzed by these concepts.

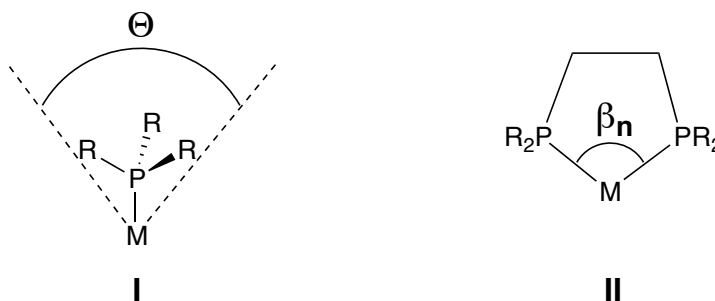


Figure 1.1. The cone angle Θ (I) and bite angle β_n (II) concepts

Fundamental steric properties of ligands are defined by their skeletal core structure, but minor alternations can be achieved by varying substituents, usually alkyl groups, on the basic configuration. Placement of the substituents plays an important role with the most logical positions being nearby the coordinating atom (or atoms in case of multidentate ligands). For example, the chromium based complex **III** (**Figure 1.2**) employed in asymmetric epoxidation of *trans*- β -methylstyrene was shown to induce higher enantioselectivity when substituents in *ortho*- positions to the coordinating groups (R^1 and R^4 , **Figure 1.2**) were present.^{30,31} On the contrary, a shift of the substitution to the R^2 and R^3 positions with R^1 and R^4 being hydrogens resulted in a drop of the selectivity. This finding was ascribed to greater influence on the properties of the complex by steric effects, when the substituents are situated closer to the coordinating oxygen and nitrogen atoms. Steric “fine tuning” of the catalyst **III** was performed by varying the size of

the substituents R¹. Very bulky *t*-butyl groups were shown to provide the highest stereoselectivity.³⁰

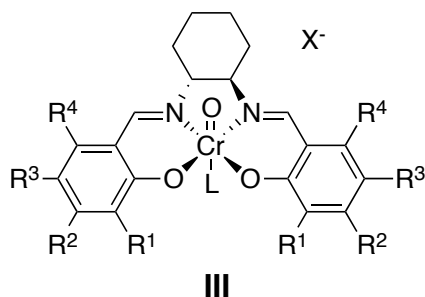


Figure 1.2. Sterically tuned chromium complex III

Several approaches to study steric properties of ligands and their effects on the metal center of complexes are known in literature.^{27,32-34} Analysis of theoretical models is often employed in order to describe steric characteristics of known ligands and possibly predict steric influence of new compounds.^{33,34} While molecular mechanics methods were employed in the literature to assist investigation of potentially practical catalysts,³⁵ employment of X-Ray structural analysis remained a more common technique.³⁶⁻³⁸

1.3.1.2. Electronic tuning of ligands

Modifications of the electronic properties of ligands for known catalytic systems are not as widely employed as “adjustments” of the steric environment caused by ligands. This is generally due to more challenging electronic tuning of most practically used ligands, which often do not allow a convenient modification of their structure.²⁶ Nevertheless, studies of new catalytic systems and the influence of the electronic properties of ligands on their efficiency have been reported in the literature.^{22,39}

The purpose of electronic tuning of ligands is to influence the ability of the coordinating atom to donate electron density to the metal center of a complex.

Electronic tuning effects can be divided into two aspects: (1) selection of the compounds class to bear principal electronic properties and (2) electronic fine-tuning.

Similarly to sterics, the key electronic properties of ligands are defined by the initial choice of the compound class. The substitution pattern around the coordinating atom shows the largest influence on the electronic properties of the ligand. For example, in a series of phosphorus containing ligands, a change from strong electron-donation to moderate electron-withdraw was observed when the increasing number of oxygen atoms was attached to the phosphorus (**Figure 1.3**).²³

Among nitrogen based ligands, amines perform as σ -donors but presence of a double bond at a nitrogen (imines, pyridines, etc.) makes them also effective π -acceptors.^{40,41}

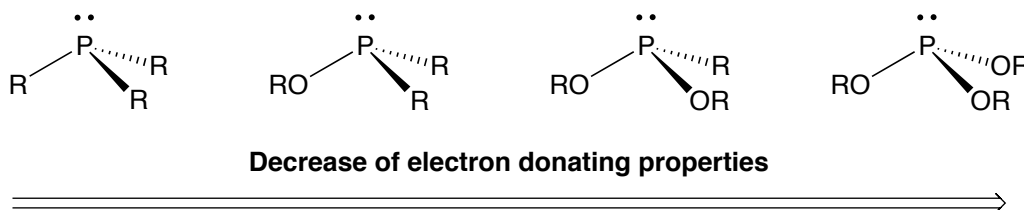


Figure 1.3. Influence of the substitution pattern around a phosphorus atom on the donating properties of the ligands

At the point when the general electronic properties have been set, fine electronic tuning can be performed by placing electron-donating or electron-withdrawing groups in the backbone while the core skeletal structure remains the same.

Properties of these substituents translate to electronic changes at the coordinating

atom through either inductive or resonance effects.⁴² Therefore, the type and position of a substituent in a molecule plays an important role in the overall outcome of the electronic tuning. The inductive effect strongly depends on the number of bonds separating the coordinating atom and the substituent. It decreases very rapid with increasing distance. Hence, the position of the substituent should be close to the coordinating atom to have an effect on its electron density. However, that placement can interfere with the steric properties of the molecule.^{30,31} On the model metal complex **III** (**Figure 1.2**) it was shown that its catalytic activity significantly decreased with moving the electron withdrawing chloride substituent farther from the coordinating oxygen atom (from $R^1 = Cl$ to $R^3 = Cl$).³¹

There are several ways how the effects of electronic tuning of ligands can be studied. One of the most common procedures is based on employing the ligands in the synthesis of a series of related metal complexes carrying a carbonyl ligand. Analysis of the IR spectra gives information about the electron density at the metal, as increasing stretching frequencies of the carbonyl ligand indicate increasing electron donating properties of the ligands.^{41,43-46}

Applications of cyclic voltammetry method for identification of oxidation potentials were described for metal complexes and ligands. A correlation between donating properties of ligands and $\nu_{C=O}$ stretching frequencies was found. A linear increase of the oxidation potentials was shown to result in the decrease of $\nu_{C=O}$ stretching frequencies in a similar linear manner that was connected to the decline of the electron donating abilities of the ligands.²³

Nuclear magnetic resonance was employed to determine coupling constants between magnetically active coordinating atoms (usually ^{31}P) and a metal center (Rh, W, Hg).⁴⁷⁻⁵¹ A decrease in the coupling constant (^{31}P -M) values was observed with increasing donating properties of ligands. Also, extensive application was found for values of ^{31}P - ^{77}Se couplings due to their good correlation with donating properties of the phosphorus atoms.^{43,52-58}

1.4. Goals of the current project

The main goal stated for this project is to investigate pathways to influence steric and electronic properties of three classes of ligands. The first target of the investigation is a class of compounds known as amino-dithiaphospholanes.⁵⁹ They are structurally related to phosphoramidites, which have successfully been applied in catalysis.⁶⁰ Therefore, amino-dithiaphospholanes can be seen as electronically tuned phosphoramidites. However, very little is known about their properties and their coordination chemistry has not been reported in the literature. The second objective is to systematically investigate the possibility of steric and electronic tuning of the phosphinoxazolines.⁶¹ While they are a known class of ligands, a comprehensive study of their structure-properties relationship cannot be found in the literature. The final part of the project is dedicated to the synthesis of several new multidentate ligands and their corresponding iron complexes mimicking naturally accruing non-heme enzymes.⁶² A probe of the catalytic activity of the new complexes is going to be performed using oxidation reactions of activated methylene groups and alcohols.

1.5. Conclusion

Irrespective of the application, the synthetic pathway to a metal complex consists of several stages. Ligands design is one of the most substantial steps in the process. Its importance is often underestimated. However, the ligand is a significant part of a metal complex and defines many of its principal properties. A better understanding of steric and electronic properties exerted by known ligands helps to develop complexes with desired characteristics. On the other hand, introduction of new classes of compounds as potential ligands broadens the selection of building blocks that can be used for designing new metal complexes. These are the main ways for the expansion and improvement of practical implementation of metal complexes that will lead to the continuous evolution of coordination chemistry.

1.6. References

- (1) Niu, S.; Hall, M. B. *Chem. Rev.* **2000**, *100*, 353.
- (2) Crabtree, R. H. *The Organometallic Chemistry of the Transition Metals*; John Wiley & Sons: New York, 1988.
- (3) Knowles, W. S. *Acc. Chem. Res.* **1983**, *16*, 106.
- (4) Noyori, R.; Ohkuma, T.; Kitamura, M.; Takaya, H.; Sayo, N.; Kumobayashi, H.; Akutagawa, S. *J. Am. Chem. Soc.* **1987**, *109*, 5856.
- (5) Vries, J. G. d.; Elsevier, C. J. *Handbook of Homogeneous Hydrogenation*; WILEY-VCH Verlag GmbH & Co. KGaA: Weinheim, Germany, 2007.

- (6) Zhang, W.; Loebach, J. L.; Wilson, S. R.; Jacobsen, E. N. *J. Am. Chem. Soc.* **1990**, *112*, 2801.
- (7) Linker, T. *Angew. Chem., Int. Ed.* **1997**, *36*, 2060.
- (8) Katsuki, T.; Sharpless, K. B. *J. Am. Chem. Soc.* **1980**, *102*, 5974.
- (9) Johnson, R. A.; Sharpless, K. B. *Comp. Org. Syn.* **1991**, *7*, 389.
- (10) Bauer, E. B. *Curr. Org. Chem.* **2008**, *12*, 1341.
- (11) Shejwalkar, P.; Rath, N. P.; Bauer, E. B. *accepted* **2011**.
- (12) Shejwalkar, P.; Rath, N. P.; Bauer, E. B. *Molecules* **2010**, *15*, 2631.
- (13) Lenze, M.; Bauer, E. B. *J. Mol. Catal. A: Chem.* **2009**, *309*, 117.
- (14) Lenze, M.; Rath, N. P.; Bauer, E. B. *in preparation*.
- (15) Yin, L.; Liebscher, J. *Chem. Rev.* **2006**, *107*, 133.
- (16) Astruc, D. *New J. Chem.* **2005**, *29*, 42.
- (17) Pearson, R. G. *J. Am. Chem. Soc.* **1963**, *85*, 3533.
- (18) Hancock, R. D.; Martell, A. E. *Chem. Rev.* **1989**, *89*, 1875.
- (19) Morgan, G. T.; Drew, H. D. K. *J. Chem. Soc., Trans.* **1920**, *117*, 1456.
- (20) Greenwood, N. N.; Earnshaw, A. In *Chemistry of the Elements*; 2nd ed.; Butterworth-Heinemann: Oxford, 1997, p 910.
- (21) Schwarzenbach, G. *Helv. Chim. Acta* **1952**, *35*, 2344.
- (22) RajanBabu, T. V.; Casalnuovo, A. L.; Ayers, T. A.; Nomura, N.; Jin, J.; Park, H.; Nandi, M. *Curr. Org. Chem.* **2003**, *7*, 301.
- (23) Rahman, M. M.; Liu, H. Y.; Eriks, K.; Prock, A.; Giering, W. P. *Organometallics* **1989**, *8*, 1.

- (24) Rahman, M. M.; Liu, H. Y.; Prock, A.; Giering, W. P. *Organometallics* **1987**, *6*, 650.
- (25) Golovin, M. N.; Rahman, M. M.; Belmonte, J. E.; Giering, W. P. *Organometallics* **1985**, *4*, 1981.
- (26) Jacobsen, E. N.; Zhang, W.; Guler, M. L. *J. Am. Chem. Soc.* **1991**, *113*, 6703.
- (27) Tolman, C. A. *Chem. Rev.* **1977**, *77*, 313.
- (28) Casey, C. P.; Whiteker, G. T. *Israel J. Chem.* **1990**, *30*, 299.
- (29) Freixa, Z.; van Leeuwen, P. W. N. M. *Dalton Trans.* **2003**, 1890.
- (30) Ryan, K. M.; Bousquet, C.; Gilheany, D. G. *Tetrahedron Lett.* **1999**, *40*, 3613.
- (31) O'Mahony, C. P.; McGarrigle, E. M.; Renehan, M. F.; Ryan, K. M.; Kerrigan, N. J.; Bousquet, C.; Gilheany, D. G. *Org. Lett.* **2001**, *3*, 3435.
- (32) Tolman, C. A. *J. Am. Chem. Soc.* **1970**, *92*, 2953.
- (33) Fernandez, A.; Reyes, C.; Wilson, M. R.; Woska, D. C.; Prock, A.; Giering, W. P. *Organometallics* **1997**, *16*, 342.
- (34) Joerg, S.; Drago, R. S.; Sales, J. *Organometallics* **1998**, *17*, 589.
- (35) Denmark, S. E.; Gould, N. D.; Wolf, L. M. *J. Org. Chem.* **2011**, *76*, 4337.
- (36) Denmark, S. E.; Gould, N. D.; Wolf, L. M. *J. Org. Chem.* **2011**, *76*, 4260.
- (37) Denmark, S. E.; Kalyani, D.; Collins, W. R. *J. Am. Chem. Soc.* **2010**, *132*, 15752.
- (38) Zehnder, M.; Schaffner, S.; Neuburger, M.; Plattner, D. A. *Inorg. Chim. Acta* **2002**, *337*, 287.

- (39) Flanagan, S. P.; Guiry, P. J. *J. Organomet. Chem.* **2006**, *691*, 2125.
- (40) Ho, T. C.; Katritzky, A. R.; Cato, S. *Ind. Chem. Res.* **1992**, *31*, 1589.
- (41) Moloy, K. G.; Petersen, J. L. *J. Am. Chem. Soc.* **1995**, *117*, 7696.
- (42) McNaught, A. D.; Wilkinson, A. *IUPAC. Compendium of Chemical Terminology*; 2nd ed.; Blackwell Scientific Publications: Oxford, 1997.
- (43) Jeulin, S.; De Paule, S. D.; Ratovelomanana-Vidal, V.; Genêt, J. P.; Champion, N.; Dellis, P. *Angew. Chem., Int. Ed.* **2004**, *43*, 320.
- (44) Huang, A.; Marcone, J. E.; Mason, K. L.; Marshall, W. J.; Moloy, K. G.; Serron, S.; Nolan, S. P. *Organometallics* **1997**, *16*, 3377.
- (45) Clarke, M. L.; Ellis, D.; Mason, K. L.; Orpen, A. G.; Pringle, P. G.; Wingad, R. L.; Zaher, D. A.; Baker, R. T. *Dalton Trans.* **2005**, 1294.
- (46) Grotjahn, D. B.; Zeng, X.; Cooksy, A. L.; Kassel, W. S.; DiPasquale, A. G.; Zakharov, L. N.; Rheingold, A. L. *Organometallics* **2007**, *26*, 3385.
- (47) Grim, S. O.; Shah, D. P.; Haas, C. K.; Ressler, J. M.; Smith, P. H. *Inorg. Chim. Acta* **1979**, *36*, 139.
- (48) Grim, S. O.; Singer, R. M.; Johnson, A. W.; Randall, F. J. *J. Coord. Chem.* **1978**, *8*, 121
- (49) Grim, S. O.; Lui, P. J.; Keiter, R. L. *Inorg. Chem.* **1974**, *13*, 342.
- (50) Grim, S. O.; Wheatland, D. A.; McFarlane, W. *J. Am. Chem. Soc.* **1967**, *89*, 5573.
- (51) Grim, S. O.; Keiter, R. L.; McFarlane, W. *Inorg. Chem.* **1967**, *6*, 1133.
- (52) Pinnell, R. P.; Megerle, C. A.; Manatt, S. L.; Kroon, P. A. *J. Am. Chem. Soc.* **1973**, *95*, 977.

- (53) Kroshefsky, R. D.; Weiss, R.; Verkade, J. G. *Inorg. Chem.* **1979**, *18*, 469.
- (54) Suárez, A.; Méndez-Rojas, M. A.; Pizzano, A. *Organometallics* **2002**, *21*, 4611.
- (55) Bilenko, V.; Spannenberg, A.; Baumann, W.; Komarov, I.; Börner, A. *Tetrahedron: Asymmetry* **2006**, *17*, 2082.
- (56) Adams, D. J.; Bennett, J. A.; Duncan, D.; Hope, E. G.; Hopewell, J.; Stuart, A. M.; West, A. J. *Polyhedron* **2007**, *26*, 1505.
- (57) Enthaler, S.; Erre, G.; Junge, K.; Schröder, K.; Addis, D.; Michalik, D.; Hapke, M.; Redkin, D.; Beller, M. *Eur. J. Org. Chem.* **2008**, 3352.
- (58) Erre, G.; Junge, K.; Enthaler, S.; Addis, D.; Michalik, D.; Spannenberg, A.; Beller, M. *Chem.-Asian J.* **2008**, *3*, 887.
- (59) Farschtschi, N.; Gorenstein, D. G. *Tetrahedron Lett.* **1988**, *29*, 6843.
- (60) de Vries, A. H. M.; Meetsma, A.; Feringa, B. L. *Angew. Chem., Int. Ed.* **1996**, *35*, 2375.
- (61) Helmchen, G.; Pfaltz, A. *Acc. Chem. Res.* **2000**, *33*, 336.
- (62) Bruijninx, P. C. A.; van Koten, G.; Klein Gebbink, R. J. M. *Chem. Soc. Rev.* **2008**, *37*, 2716.

Chapter II

Investigation of Amino-dithiaphospholanes as a New Class of Ligands

2.1. Aim of the chapter

Electronic tuning of phosphoramidite ligands.

It has been our experience that one of the most employed ligand class in our laboratory, phosphoramidites,¹⁻⁵ lacked the ability of effective electronic tuning,^{3,4} when performed by electron donating or accepting substituents on the aryl rings connected to the phosphorus. Therefore, a different approach to adjust the electronic properties was required. A new class of ligands structurally related to phosphoramidites was investigated in which the oxygen in phosphoramidites was replaced with sulfur. The aim of the investigation was to establish a general procedure for the synthesis of the new ligands, characterization, determination of their chemical stability and investigation of their electronic properties.

Coordination chemistry and impact of the new ligands on the electron density at the metal center were also investigated.

2.2. Introduction

Phosphoramidites (**I** in **Figure 2.1**) have been employed in the synthesis of a variety of catalytically active organometallic complexes.⁶ Our laboratory has already shown that phosphoramidite complexes of ruthenium can efficiently catalyze the formation of β -oxo esters⁴ and the Mukaiyama aldol reaction.³ However, it was shown that electronic tuning of the phosphoramidites had only a slight effect when performed on the backbone of the ligand.^{3,4} Consequently, we were interested in investigating the electronic influences of the atoms directly attached to the phosphorus center on

the properties of the ligands. We decided to study the sulfur analogs of phosphoramidites, known in the literature as amino-dithiaphospholanes (**III**) if the phosphorus and the sulfur atoms are incorporated in a five membered ring, or phosphoramidodithioites (**II**) in all other cases (**Figure 2.1**).⁷ Significantly, this class of compounds is known, but it has not been applied in transition metal coordination chemistry.

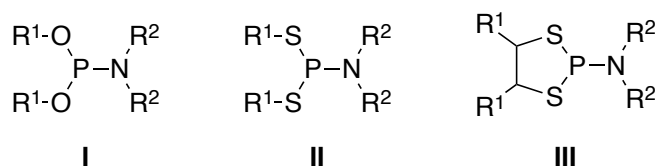


Figure 2.1. Phosphoramidites I, phosphoramidodithioites II and amino-dithiaphospholanes III

Amino-dithiaphospholanes have first been reported in the literature but, their synthetic applications have been limited.⁸ Only a few structures have been synthesized,⁷ therefore the knowledge of their chemistry and reactivity is limited. Up to now, only a few applications of this class of compounds in research gave information about their reactivity. The P-N bond in amino-dithiaphospholanes is sensitive to hydrolysis⁹ or alcoholysis,^{7,10} a property that has been used for the phosphorylation of nucleotides.^{7,8,11} While the instability of the P-N bond is useful in these cases, for purposes of our research we needed to access more stable structures of that compound class.

2.3. Synthesis and studies of the ligands

Due to the lack of literature examples for amino-dithiaphospholane synthesis, we applied modified methodologies developed earlier in our laboratory for the preparation of phosphoramidites.^{3,4} The general procedure consisted of a two step substitution of the chloride atoms in PCl_3 that were performed one pot (**Figure 2.2**).

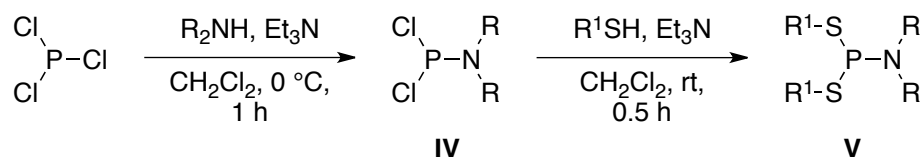


Figure 2.2. General method for amino-dithiaphospholane synthesis

As shown in **Figure 2.2**, the intended synthesis of the targeted ligands started with the exchange of one of the chlorides in PCl_3 with a disubstituted nitrogen atom (the NR_2 unit) to give compound **IV**. It was performed by slow dropwise addition of one equivalent of a secondary amine to a solution of PCl_3 in CH_2Cl_2 in the presence of Et_3N as a base. In order to prevent overheating of the reaction mixture and possible formation of di- and tri- substituted side products, the addition was performed at 0°C (ice/water bath). The reaction proceeded very fast but in order to ensure complete conversion, the mixture was stirred for an hour in the ice bath. At that time, the next step was performed to yield the target compound **V**. After addition of a slight excess (2.1 equivalents) of the thiol R^1SH at 0°C , the reaction mixture was warmed to room temperature and stirred for 30 minutes. A crude ^{31}P NMR was recorded to check for the presence of the desired product. The reaction mixture was quickly washed with aqueous solutions of NaHSO_4 and NaHCO_3 in order to separate unreacted amine and thiol starting materials, if present, and potential basic

or acidic byproducts. Final purification was accomplished either by precipitation of the target compound out of a solution in CH_2Cl_2 by addition of a Et_2O /hexanes solvent mixture or by column chromatography. The synthesis of the ligands and their characterization is detailed below.

For further investigations we first needed to understand the chemical behavior of the potential ligands. Therefore, an appropriate selection of target structures was performed to achieve that objective. Due to the aforementioned ability of amino-dithiaphospholanes to undergo decomposition through a nucleophilic attack on the phosphorus atom, an investigation of the influence of the molecular structure on the stability of the compounds was required. There are two main factors that can play a role in the ability of the phosphorus atom to suffer nucleophilic attack. The first factor relates to the electronic properties of the potential reaction centers. For a nucleophilic attack, the phosphorus atom has to perform as an electrophile, so the electron density at the atom must be low for the attack to proceed. Consequently, an increase of the electron density at the phosphorus should result in a less reactive compound, and thus a more stable molecule. The second important factor for reactivity is the steric environment around the phosphorus center. A nucleophile has to be able to reach the atom in order for an attack to take place. By increasing the steric congestion around the phosphorus atom, amino-dithiaphospholanes should become less prone to nucleophilic attack. In our targeted ligands, both effects mainly depend on the substituents on the nitrogen and the sulfur atoms. Therefore, by exploiting structural modifications of the ligands, we should be able to identify optimal substituents to increase the stability of our targets. This part of the

project was divided into two sections. The electronic effects were studied first, followed by an investigation of the steric influence on the ligand stabilities.

2.3.1. Electronic properties and chemical stability

The electron density at the phosphorus atom in amino-dithiaphospholanes can be tuned by varying the substituent on the sulfur and nitrogen atoms. According to the method chosen for the general synthesis of the compounds (**Figure 2.2**), those variations were implemented by employing amine and thiol starting materials with different electronic properties.

Five readily available thiols **2.1-2.5** were used for the synthesis (**Figure 2.3**). We were interested in comparing the impact of different alkyl (**2.1**) and aryl substituents (**2.2-2.5**) on the ligand properties. In addition, introduction of substituents on the aryl ring were expected to change the electron-donating properties of the sulfur atom. Therefore, along with the parental thiophenol **2.2**, thiols with a strongly electron-donating methoxy group (**2.5**), a weakly electron-donating methyl substituent (**2.3**) and an electron-withdrawing chloride substituent (**2.4**) were selected for the synthesis of the corresponding amino-dithiaphospholanes.

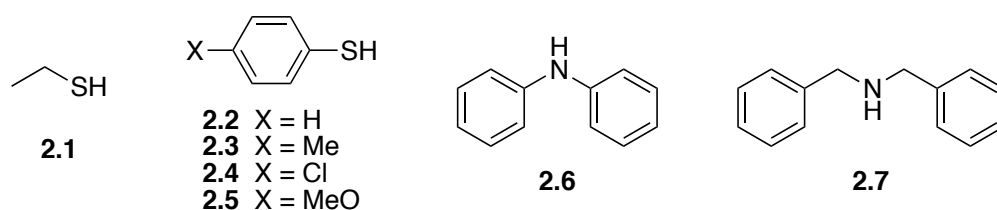


Figure 2.3. Electronically modified thiol and amine starting materials

At the nitrogen side of the molecule, a modification of the electronic properties was intended to be achieved by use of a dialkyl and a diaryl amine. In an attempt to only probe the electronic effect without triggering steric interactions, two structurally similar secondary amines were selected, diphenylamine **2.6** and dibenzylamine **2.7** (**Figure 2.3**). All the compounds chosen for the study are commercially available. With this series of starting materials, we moved to employing them in the synthesis of amino-dithiaphospholanes according to the general procedure described above (**Figure 2.2**). In order to get insight in the relationships between the structure and the stability of amino-dithiaphospholanes, we employed all possible combinations of the starting materials in synthesis (**Figure 2.4**). To obtain preliminary data, test reactions were performed and the reaction mixtures analyzed spectroscopically.

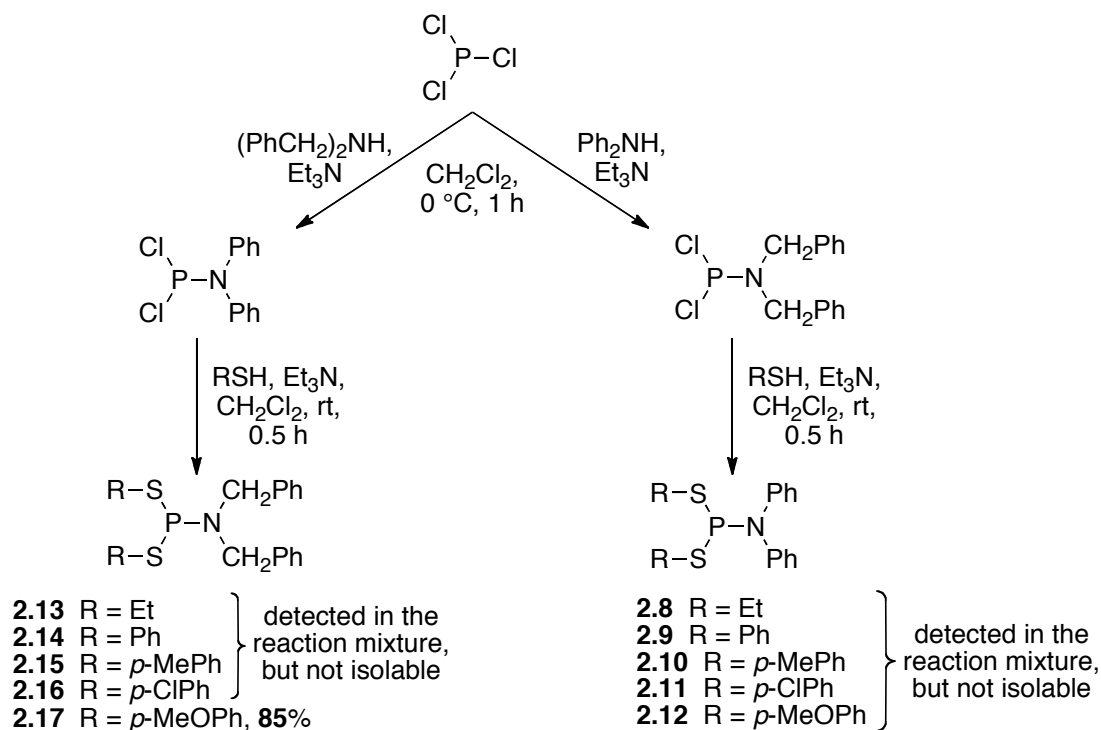


Figure 2.4. Targets for probing of electronic effects

Accordingly, after reaction, a small aliquot of the crude reaction mixture was taken from each of the ten reaction mixtures. Crude ^{31}P NMR spectra were obtained and confirmed the absence of either the PCl_3 starting material or any chloro-containing intermediates. Each sample showed a major peak with various amounts of minor signals. The chemical shifts for the main signal in the ^{31}P NMR spectra ranged between 120 and 135 ppm, and were in the region expected for the target molecules.¹⁰ Unfortunately, even from the crude NMR data we observed ongoing decomposition for many of the desired compounds. A large number of signals with high intensities, exceeding in total the intensity of the major peak, was observed in the crude spectra from the syntheses of compounds **2.8-2.12**. Due to the aniline derivative (**2.7**) employed in the synthesis, all those molecules were expected to contain a NPh_2 group on the phosphorus, which is significantly less electron donating than the NBn_2 group, therefore a nucleophilic attack on the phosphorus potentially proceeded at a higher rate. While we observed that aryl substituents on the nitrogen atom caused fast decomposition of the molecules **2.8-2.12**, a trend for their relative stability was nevertheless noticed based on the analysis of the data obtained from ^{31}P NMR spectra of the crude reaction mixtures over a period of a couple hours. Thus, compound **2.12** was found to decompose at the lowest rate among the molecules in the series.

Those findings were consistent with similar data obtained for compounds **2.13-2.17**. In that series, overall a higher stability was observed for molecules bearing dialkylamino substituent at the phosphorus atom, with the amino-dithiaphospholane **2.17** being the most stable one.

After acquisition of preliminary information about the stability of the amino-dithiaphospholanes **2.8-2.17**, numerous attempts to separate and purify the synthesized compounds in **Figure 2.4** were undertaken. First, aqueous work up of the reaction mixtures was necessary to separate the ammonium salts and some of the side products. Then, precipitation of the desired target molecules was attempted. For that purpose, the crude materials obtained from the aqueous work up were redissolved in a minimal amount of CH_2Cl_2 followed by slow addition of Et_2O /hexanes mixtures with various ratios of the two solvents. Column chromatography was also investigated for purification of the products. Several sorbents were examined, including silica gel, alumina and Florisil®. Hexanes/ethyl acetate or toluene/ethyl acetate solvent systems with 3% Et_3N were used for elution. Unfortunately, almost all efforts to separate the desired products from the reaction mixtures failed due to ongoing decomposition of the compounds. Only the target molecule **2.17** was shown to be stable enough to “survive” washing with H_2O , and purification by column chromatography to afford the product in 85% yield as a colorless oil.

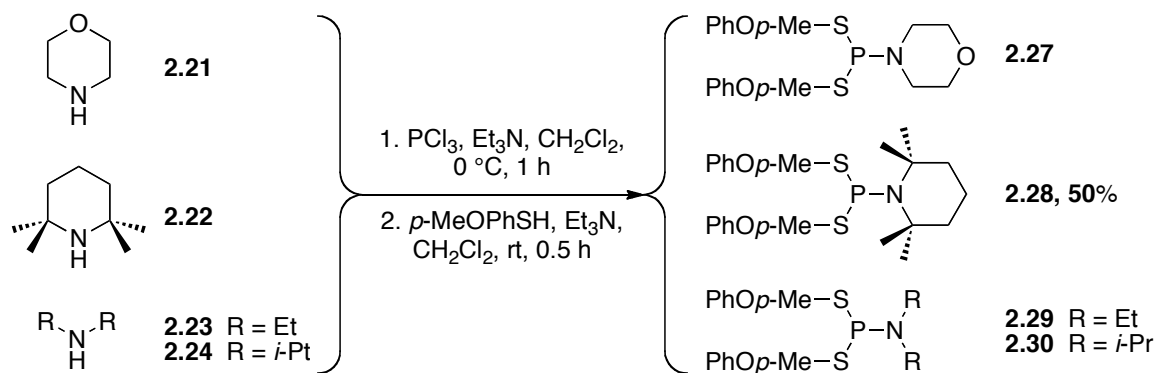
2.3.2. Steric properties and chemical stability

Similar to probing the electronic tuning effects, investigations of the influence of the steric environment around the phosphorus center on the stability of the amino-dithiaphospholanes were performed by employing sterically modified thiols and secondary amines in their synthesis.

Due to the presence of two sulfur atoms connected to the phosphorus center in the target molecules, the choice of the sulfur containing starting materials allowed the

temperature and upon dilution with a large amount of H₂O, yellow crystals of the desired intermediate product **2.26** formed. In order to remove excess CS₂ the mixture was kept at around 70 °C for an hour. The crystalline product was separated by filtration, was spectroscopically pure, and was used in the next step without further purification. Reduction of the cyclic trithiocarbonate **2.26** with LiAlH₄ in THF gave complete conversion to the dithiol **2.19** after 3 hours of reflux. Washing of the reaction mixture with diluted HCl was performed to destroy unreacted LiAlH₄ and aluminum byproducts of the reaction. After extraction with Et₂O and evaporation of the solvent, the product **2.19** was obtained with base line NMR purity in 83% yield and was used without further purification.

All the starting materials were next employed in the amino-dithiaphospholane syntheses according to the general methodology (**Figure 2.2**). The previously obtained data showed that the use of *para*-methoxythiophenol **2.5** and dibenzylamine **2.7** gave more stable products. Therefore, at this phase of the study, they were used as coupling partners to obtain the corresponding target molecules with different levels of steric congestion. We started with the synthesis of phosphoramidodithioites **2.27-2.30** (**Figure 2.7**).



Compounds **2.27**, **2.29**, and **2.30** were detected in the reaction mixture, but not isolable

Figure 2.7. Targets for probing the steric effects of the substituents on nitrogen on the ligand stabilities

The reactions and workups were performed as described above (**Figure 2.2**). Upon completion of the reactions, an investigation of the number of products was performed by ^{31}P NMR of the crude mixtures. It showed that the crude compound **2.28** gave the least number of ^{31}P signals not related to the expected product and the highest ratio between the intensity of the major product signal at 133.2 ppm and the combined intensities of the minor peaks. A reverse trend was seen in the ^{31}P NMR data of the compounds **2.27**, **2.29** and **2.30**. The spectra for those mixtures contained a significant number of signals in the region between 40 to 0 ppm, suggesting ongoing hydrolysis with formation of compounds containing P-O bond and ultimately phosphoric acid. Purification attempts increased the intensity of those peaks. The amino-dithiaphospholane **2.28** was separated from the reaction mixture by extraction and purified by column chromatography in 50% overall yield as a colorless oil. The three other targets (**2.27**, **2.29** and **2.30**) from **Figure 2.7** were too reactive and all efforts to separate them from hydrolysis byproducts resulted in ongoing decomposition.

Our last synthetic targets were the cyclic amino-dithiaphospholanes **2.31-2.33**

(**Figure 2.8**). The dithiols **2.18-2.20** were utilized for their synthesis.

Dibenzylamine **2.7**, that was shown above to give potentially more stable products, was used as the nitrogen source.

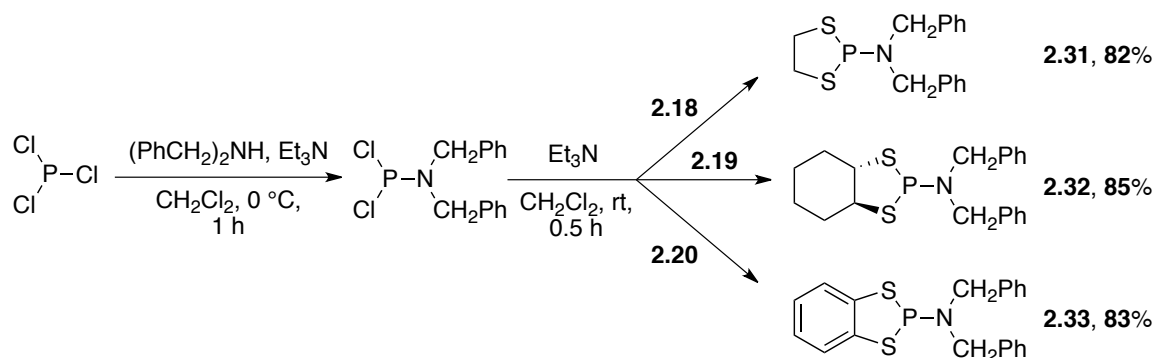


Figure 2.8. Targets for probing the steric effects of substituents on sulfur

The syntheses were performed under the standard condition described above (**Figure 2.2**). The products **2.31-2.33** were found to be crystalline. Therefore, their separation was performed by precipitation. Attempts to exclude potentially destructive aqueous work up and to precipitate the amino-dithiaphospholanes **2.31-2.33** straight from their corresponding reaction mixtures did not result in successful separations. Significant amounts of hydrolysis byproducts were observed during aqueous workup, which precipitated along with the crystalline materials as oils. However, the byproducts were separated by washing with H_2O and saturated aqueous NaHCO_3 , and the resulting crude products were redissolved in CH_2Cl_2 . The compounds **2.31-2.33** were successfully precipitated out of the solutions by slow addition of Et_2O followed by Et_2O /hexanes mixtures. The crystalline materials were separated from the solvent by filtration and, upon drying, afforded the

spectroscopically pure amino-dithiaphospholanes **2.31-2.33** in 82%, 85%, and 83% yields, respectively, as colorless, crystalline materials.

2.3.3. Investigation of the chemical stability of the synthesized amino-dithiaphospholanes

Overall, five amino-dithiaphospholanes (**2.17**, **2.28**, **2.31-2.33**) were isolated in spectroscopically pure form with yields ranging from 50 to 85%. In general, it was found that for this class of compounds, a combination of factors afforded isolable products with stabilities sufficient to obtain analytically pure materials. Increase of the electron density at the phosphorus atom produced compound **2.17**, which is less vulnerable to hydrolysis than **2.8-2.12**. In addition to the electron-donating substituents on the sulfur atoms, the molecule **2.28** carries two quaternary carbon atoms next to the nitrogen that we believe causes a significant steric barrier for a potential nucleophilic attack on the phosphorus atom, thus making the structure relatively stable. The physical state of the desired products was also found to play an important role in successful isolation and purification of the compounds. The ligands **2.31-2.33** are crystalline and precipitated out of the solutions of the crude mixtures. However, all other crude mixtures required purification by column chromatography, which is more “demanding” with respect to the stability of the target molecules. Therefore, from the large series of the attempted syntheses, only two non-crystalline products (**2.17** and **2.28**) were successfully isolated. The relative chemical stability of the synthesized compounds **2.17**, **2.28**, **2.31-2.33** was investigated by ^{31}P NMR measurements in presence of nucleophiles over time.

The experiments were conducted in NMR tubes. The compounds were dissolved in CDCl_3 and around 10 volume percent of MeOH or H_2O were added to the solutions. Water is not miscible with CDCl_3 , therefore the tubes were shaken to form emulsions. The ^{31}P NMR data for the solutions were recorded before the addition of the nucleophiles and after 15, 30, 60 minutes and after one day. Analysis of the relative rates of decomposition of the molecules resulted in the following row of stability for the synthesized amino-dithiaphospholanes (**Figure 2.9**).

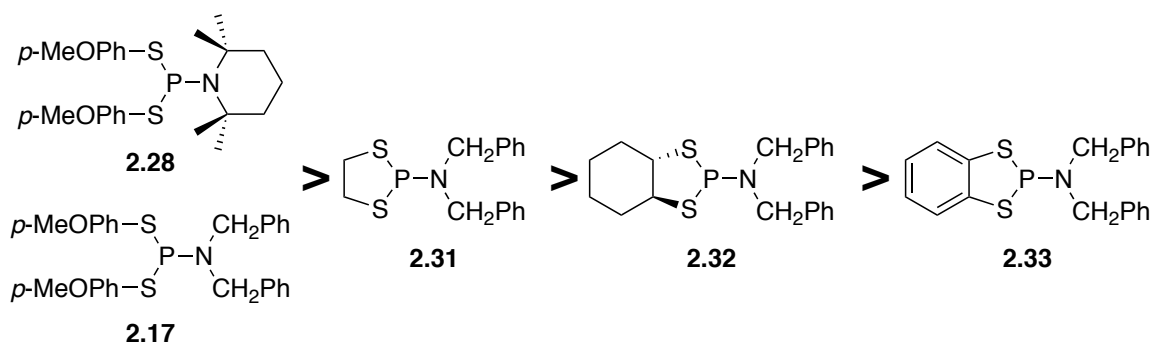


Figure 2.9. Chemical stability row for the synthesized compounds 2.17, 2.28, 2.31-2.33

The amino-dithiaphospholane **2.17** was found to be the most stable among the synthesized compounds, closely followed by the molecule **2.28**. Both compounds showed only small amounts of decomposition after 60 minutes in CDCl_3 solutions in the presence of MeOH or H_2O . However, after 24 hours the intensities of the ^{31}P signals corresponding to the compounds **2.17** and **2.28** were significantly lower than the combined intensities of the other peaks in the NMR spectra. These data supported increased stability of the products **2.17** and **2.28**, while still confirming their sensitivity towards hydrolysis and alcoholysis over time in solution.

The three amino-dithiaphospholanes **2.31-2.33**, which incorporate the phosphorus atom into a cyclic structure, were observed to be indefinitely stable in crystalline form, but were seen to rapidly decompose in solution. The NMR study of their behavior in presence of the nucleophiles showed almost complete disappearance of the ^{31}P signal for compounds **2.31-2.33** 60 minutes after addition of MeOH or H₂O. The relative degradation rate of compound **2.33** was noticeably higher than that of the compounds **2.31** and **2.32**, while the amino-dithiaphospholane **2.31** was found to be stable in the solution for at least 30 minutes.

2.4. Analysis of the properties of the new amino-dithiaphospholanes

With the purified and sufficiently stable ligands **2.17**, **2.28**, **2.31-2.33** in hand, we started the next part of the project. As mentioned above, the coordination chemistry of this class of compounds has previously not been reported. Therefore, electronic factors relevant for coordination to a metal center were investigated first. At first, the electron-donating abilities of the new ligands were compared with those of structurally related phosphoramidites, which was accomplished by NMR. A relationship between the chemical shift and the electron density at the atom is very complex for heavy elements, such as phosphorus, due to the large influence of paramagnetic shielding components on the chemical shift. On the other hand, coupling constants to another nucleus were shown to correlate well with the electron density at phosphorus. For phosphorus containing ligands, analysis of the

coupling constants was previously performed to assess the electron density and basicity on the phosphorus.¹⁴ Basicity trends obtained from $^1J(^{31}\text{P-M})$ coupling constants in metal complexes showed a dependency on the metal¹⁴ and the structure of the complexes.^{15,16} Thus, it was observed that with increase of the electron donating properties of a ligand, the $^{31}\text{P-}^{195}\text{Pt}$ ¹⁷ and $^{31}\text{P-}^{183}\text{W}$ ^{18,19} coupling constants decreased, but a reversed effect was observed for $^1J(^{31}\text{P-}^{199}\text{Hg})$.^{20,21} Similar relationships were found for selenium derivatives of phosphines. The isotope ^{77}Se is NMR active and has a spin of $\frac{1}{2}$, leading to spin-spin interactions with ^{31}P , which results in splitting of the phosphorus signals to a doublet. It was described that the value of the $^{31}\text{P-}^{77}\text{Se}$ coupling constant increases with decreasing basicity of the phosphorus atom.^{16,22-28} Correlations based on those trends were found to be more reliable due to only very slight deviations of the structures of phosphorus compounds upon introduction of selenium.¹⁶ Therefore we employed selenium derivatives in order to characterize the electronic properties of the new amino-dithiaphospholanes.

2.4.1. Preparation of selenium derivatives

Phosphines and other compounds containing trivalent phosphorus readily react with elemental selenium to form the corresponding selenides,^{26,29} which are analogs of phosphinoides derivatives. For the purpose of collecting $^{31}\text{P-}^{77}\text{Se}$ coupling constants, we found that NMR tube experiments are the fastest and easiest way to achieve that goal. To perform the tests, we followed a general procedure specifically developed to determine those coupling constants (**Figure 2.10**).

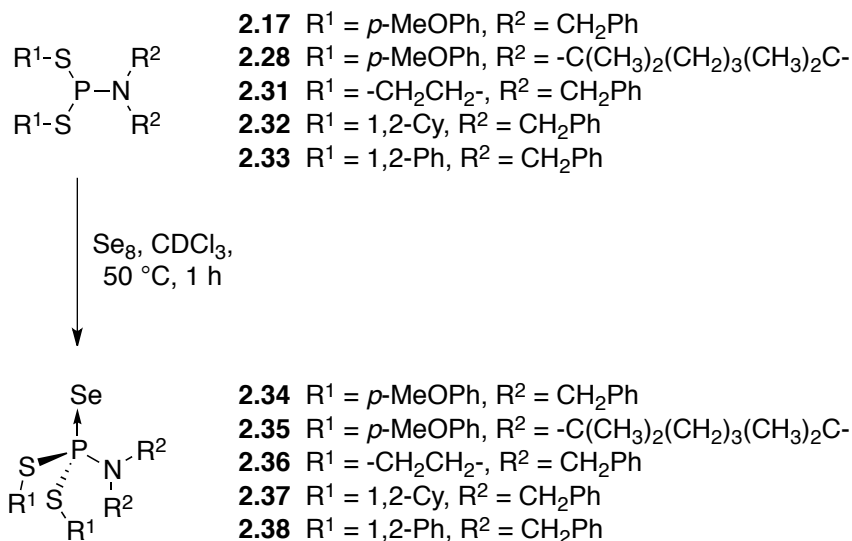


Figure 2.10. A general procedure for synthesis of the selenium derivatives of the amino-dithiaphospholanes 2.17, 2.28, 2.31-2.33

A 20 mg sample of the phosphorus-containing ligands **2.17**, **2.28**, **2.31-2.33** was dissolved in CDCl₃ and placed into an NMR tube. The amount of selenium added to the solution was 15 mg. The molar ratio between the reactant and selenium varied depending on the molecular weight of the molecule to be tested, but the added amount of selenium was always in 2 to 4 fold excess. It was found that different amino-dithiaphospholanes reacted at slightly different rates at room temperature except for the compound **2.28** that did not give noticeable conversion to **2.35** even after several hours, as assessed by NMR. The other ligands afforded the expected selenium derivatives between 2 and 4 hours at room temperature. The substantial difference in the reactivity of **2.28** was ascribed to the very high steric hindrance of the phosphorus center in that compound. Therefore, to assure complete conversion to the corresponding selenide for each molecule, all reactions were carried out at 50 °C for one hour. The formation of the selenides **2.34-2.38** was confirmed by FAB-

MS showing corresponding molecular ion peaks in the spectra. ^{31}P NMR spectra were recorded next. The natural abundance of the ^{77}Se isotope is low (7.63%),³⁰ thus a doublet caused by ^{31}P - ^{77}Se coupling, which appeared as satellites of the main phosphorus signal. Hence, usually an extended number of scans (256 to 512) was required in order to obtain a good signal to noise ratio.

2.4.2. Analysis of the NMR data

The $^1J(^{31}\text{P}$ - $^{77}\text{Se})$ coupling constants along with the ^{31}P chemical shifts of free amino-dithiaphospholanes are compiled in **Table 2.1**. For comparison, corresponding data for the phosphoramidite **VI** ($\text{R}^1 = \text{BINOL}$, $\text{R}^2 = \text{Bn}$ in structure **I**, **Figure 2.1**)²⁷ and $(\text{PhO})_3\text{P}$,³¹ $(\text{MeO})_3\text{P}$,^{22,31} and Ph_3P ^{16,31} are provided as well.

Table 2.1. ^{31}P NMR data for the new amino-dithiaphospholanes and their Se-derivatives

Ligand	^{31}P chemical shift, ppm	Selenium derivative	$^1J(^{31}\text{P}$ - $^{77}\text{Se})$, Hz
2.17	133.2	2.34	858
2.28	133.2	2.35	832
2.31	108.8	2.36	841
2.32	102.0	2.37	837
2.33	88.0	2.38	862
VI	149.4	VI-Se	971 ²⁷
$(\text{PhO})_3\text{P}$	127.5 ³¹	$(\text{PhO})_3\text{PSe}$	1025 ³¹
$(\text{MeO})_3\text{P}$	139.8 ³¹	$(\text{MeO})_3\text{PSe}$	954 ²²
Ph_3P	-7.4 ³¹	Ph_3PSe	735 ¹⁶

We were expecting that the exchange of the two oxygen atoms in phosphoramidites by sulfur would lead to an increase of electron density at the phosphorus atom, thus making it more basic. Overall, the ^{31}P chemical shifts of the synthesized amino-dithiaphospholanes were observed at higher field (88.0-133.8 ppm) than phosphoramidites normally resonate (145.2-152.3 ppm).³² This finding was consistent with previously reported NMR properties of phosphorus containing compounds, where more electronegative substituents caused a downfield shift of the corresponding ^{31}P signals.³³ However, no correlation was found for the chemical shifts of the $^{31}\text{P}\{^1\text{H}\}$ and the structures of the synthesized compounds **2.17**, **2.28**, **2.31-2.33**. As was expected, a more reliable trend for analysis of the electron donating properties was obtained from the ^{31}P - ^{77}Se coupling constants of the selenium derivatives **2.34-2.38** of the corresponding amino-dithiaphospholanes. The compound **2.28** was found to be the most basic ($^1J(^{31}\text{P}-^{77}\text{Se}) = 832$ Hz) and the molecule **2.33** was the least donating ($^1J(^{31}\text{P}-^{77}\text{Se}) = 862$ Hz) among the synthesized amino-dithiaphospholanes. The electron donating properties of the other three compounds **2.17**, **2.31** and **2.32** were shown to be in between the molecules **2.28** and **2.33** according to the $^1J(^{31}\text{P}-^{77}\text{Se})$ values, which ranged from 837 to 858 Hz for their selenium derivatives **2.34**, **2.36** and **2.37**. In general, amino-dithiaphospholanes were found to be less basic than PPh_3 ($^1J(^{31}\text{P}-^{77}\text{Se}) = 735$ Hz), but more basic than phosphoramidites ($^1J(^{31}\text{P}-^{77}\text{Se}) = 971$ Hz) and phosphites ($^1J(^{31}\text{P}-^{77}\text{Se}) = 954$ - 1025 Hz).

2.4.3. Analysis of the spectroscopic data of amino-dithiaphospholanes in metal complexes

The investigation of the coordination capabilities of the new ligands was performed in follow up studies by applying them in the synthesis of new iridium and rhodium metal complexes.^{9,34} Initial investigations concerning the chemical stability of the new amino-dithiaphospholanes upon coordination to the metal center were explored utilizing the least stable compound **2.33**. Rhodium and iridium complexes **2.39** and **2.40** containing the ligands **2.33** with structures shown in **Figure 2.11** were synthesized⁹ and their stabilities towards nucleophilic attack were assessed by NMR.

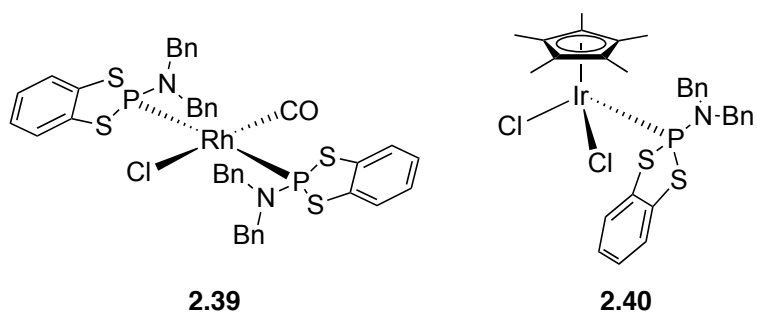


Figure 2.11. Iridium and rhodium complexes for investigation of the chemical stability of amino-dithiaphospholanes upon coordination

To probe the chemical stability of the ligand upon coordination to the metal center, solutions of the complexes **2.39** and **2.40** in CDCl_3 were treated with a drop of H_2O followed by recording of ^1H and ^{31}P NMR spectra. As described above, the decomposition of the free ligand **2.33** started immediately upon the addition of H_2O and resulted in complete hydrolysis after 60 minutes. For the complexes **2.39** and **2.40**, the disappearance of their corresponding ^{31}P signals in NMR spectra

proceeded at a noticeably lower rate. However, 2-3 hours after the addition of H₂O, the solutions, they did not contain detectable amounts of the starting materials **2.39** and **2.40**. Several resonances assigned to hydrolysis products were observed in the ¹H NMR spectra. The presence of broad signals around 5 ppm most likely corresponded to SH groups formed by cleavage of the P-S bonds. Free dibenzylamine was detected in the mixtures due to the signal of its CH₂ groups at 3.9 ppm. Therefore, coordination of the ligand **2.33** slightly increased the time required for complete hydrolysis, but did not have a dramatic influence on its stability towards nucleophilic attack. Most interestingly, an opposite result was obtained for the second least stable amino-dithiaphospholane **2.32** when applied in a similar stability investigation.⁹ The corresponding metal complexes structurally related to **2.39** and **2.40** decomposed much faster, as shown by NMR.

In order to finalize the introduction of the amino-dithiaphospholanes as new potential ligands, extra information was obtained from a series of rhodium complexes synthesized in a follow up study.³⁴ The compounds **2.17**, **2.28**, **2.31**, and **2.32** were employed in the synthesis of square planar rhodium complexes with general structures presented in **Figure 2.12**.³⁴

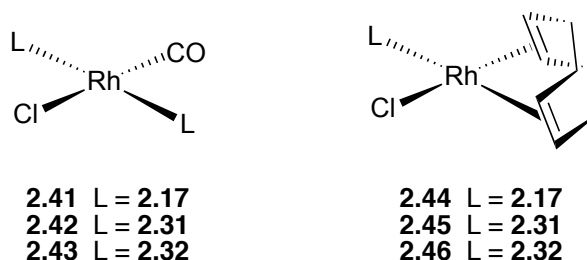


Figure 2.12. Rhodium amino-dithiaphospholanes complexes³⁴

The first noteworthy finding concerned the ligand **2.28**. As mentioned above, during preparation of its selenium derivative **2.35** the reaction did not proceed at room temperature unlike for all other amino-dithiaphospholanes. Therefore, the phosphorus might be sterically hindered due to the presence of the quaternary carbon atoms next to the nitrogen. Hence, it was expected that the compound **2.28** would form complexes slowly, but no coordination was observed at all in attempts to employ it as a ligand to obtain rhodium complexes comparable to those shown in **Figure 2.12**. Application of the amino-dithiaphospholanes **2.17**, **2.31** and **2.32** resulted in six rhodium complexes **2.41-2.46**. The compounds were analyzed by NMR and IR. All complexes contained a rhodium metal center, which is magnetically active with a spin of $\frac{1}{2}$, and three of the compounds **2.41-2.43** bear CO ligands. Therefore, measurements of the Rh-P coupling constants were obtained along with values for ν_{CO} stretching frequencies. The data are compiled in **Table 2.2**.

Table 2.2. Spectroscopical data for the rhodium complexes 2.41-2.46

Ligand	Complex	ν_{CO} , cm^{-1}	$^1J(^{31}\text{P}-^{103}\text{Rh})$, Hz
2.17	2.41	1972	166
2.31	2.42	1980	161
2.32	2.43	1983	164
2.17	2.44	-	197
2.31	2.45	-	194
2.32	2.46	-	194

It is known from the literature that ν_{CO} stretching frequencies can be used to analyze the electron density at the metal center. It was shown that electron rich metal centers decrease ν_{CO} stretching frequencies through back bonding from the metal to the CO ligand.^{24,35-38} Previously, the analysis of the electron donating properties of free ligands (**Table 2.1**) revealed that the compound **2.32** should be the most basic one followed by the amino-dithiaphospholane **2.31** and the least electron donating molecule **2.17**. Therefore, the corresponding rhodium complexes **2.41-2.43** were expected to follow a similar trend. However, a reverse dependency of electron density at the rhodium center on the proposed donating properties of the ligands was observed based on the ν_{CO} stretching frequencies in the complexes **2.41-2.43**. Thus, the compound **2.43** bearing the most basic ligand **2.32** was found to have a relatively electron poor rhodium center ($\nu_{\text{CO}} = 1983 \text{ cm}^{-1}$) and the least donating ligand **2.17** corresponded to the complex **2.41** with the smallest ν_{CO} stretching frequency (1972 cm^{-1}). IR frequencies data are highly structure dependent, hence direct comparison of the stretching frequencies is only possible for structurally related compounds.³⁹ The complexes **2.41-2.43** have a square planar geometry, but their ligands **2.17**, **2.31** and **2.32** created significantly different steric environments around the carbonyl ligands, consequently influencing their stretching frequencies. While the observations of the relative electronic properties of the amino-dithiaphospholanes **2.17**, **2.31** and **2.32** in the complexes **2.41-2.46** were not consistent with the previous findings, the overall impact of changing the oxygen atoms in phosphoramidites to sulfur resulted in the expected increase of the basicity of the corresponding compounds. The literature values of the ν_{CO} stretching

frequencies in related square planar rhodium complexes containing phosphoramidite or phosphite ligands ranged from 1983 to 2017 cm^{-1} ,³⁴ which are higher than those observed for amino-dithiaphospholanes complexes (1972-1983 cm^{-1}).

The coupling constants between the phosphorus atom and the rhodium center were investigated in the literature as a way to describe electron donating properties of the ligands. It was shown that the $^1J(^{31}\text{P}-^{103}\text{Rh})$ values decreased in complexes with increased basicity of their ligands.⁴⁰ However, as mentioned above, metal-ligand interactions are highly dependent on the structures of the complexes and the steric and electronic properties of the ligands. Hence, even for complexes with similar geometries ($[(\text{L})_3\text{RhPR}_3]$), a linear trend for a basicity – $^1J(^{31}\text{P}-^{103}\text{Rh})$ relationship was not observed.¹⁵ The two groups of the investigated structurally related complexes **2.41-2.43** and **2.44-2.46** showed nearly identical $^1J(^{31}\text{P}-^{103}\text{Rh})$ coupling constants regardless of their respective ligands (161-166 Hz and 194-197 Hz, respectively), but overall, they were found to be significantly lower (29-46 Hz) than the coupling constants of corresponding complexes bearing structurally related phosphoramidite ligands.³⁴

Overall, the spectroscopic analysis of rhodium complexes bearing thio analogs of the phosphoramidite ligands showed increased electron density at the metal centers supporting our assumption that the amino-dithiaphospholanes are more basic and, thus, more electron donating ligands than phosphoramidites.

2.5. Conclusion

A general approach to access a variety of electronically and structurally modified amino-dithiaphospholanes from commercially available starting materials was introduced. First, the investigation of their chemical stability was performed. A combination of electronic, steric and physical properties of the target molecules was shown to dictate the stability of the desired compounds. Overall, five new amino-dithiaphospholanes were found to be stable enough to be obtained analytically pure compounds and their application in coordination chemistry was subsequently investigated. The electron donating properties of the ligands were analyzed by NMR and IR. They were found to be more basic and, thus, more electron donating than the corresponding phosphoramidites. The coordination chemistry of the amino-dithiaphospholanes was investigated by synthesis of a series of iridium and rhodium complexes. Analysis of the spectroscopic data of the complexes confirmed increased electron density at the metal centers compared to related phosphite and phosphoramidite complexes.

Overall, amino-dithiaphospholanes were shown to be easily accessible and more basic alternatives to phosphoramidite ligands. However, their stability depends on electronic and steric factors about the phosphorus center.

2.6. References

- (1) Costin, S.; Rath, N. P.; Bauer, E. B. *Inorg. Chim. Acta* **2009**, *362*, 1935.
- (2) Costin, S.; Rath, N. P.; Bauer, E. B. *Tetrahedron Lett.* **2009**, *50*, 5485.

- (3) Costin, S.; Rath, N. P.; Bauer, E. B. *Inorg. Chim. Acta* **2008**.
- (4) Costin, S.; Rath, N. P.; Bauer, E. B. *Adv. Synth. Catal.* **2008**, 350, 2414.
- (5) Shejwalkar, P.; Rath, N. P.; Bauer, E. B. *Molecules* **2010**, 15, 2631.
- (6) de Vries, A. H. M.; Meetsma, A.; Feringa, B. L. *Angew. Chem., Int. Ed.* **1996**, 35, 2375.
- (7) Farschtschi, N.; Gorenstein, D. G. *Tetrahedron Lett.* **1988**, 29, 6843.
- (8) Miller, G. P.; Silverman, A. P.; Kool, E. T. *Bioorg. Med. Chem.* **2008**, 16, 56.
- (9) Costin, S.; Sedinkin, S. L.; Bauer, E. B. *Tetrahedron Lett.* **2009**, 50, 922.
- (10) Kostin, V. P.; Sinyashin, O. G.; Karelov, A. A.; Batyeva, E. S.; Pudovik, A. *N. Zh. Obshch. Khim.* **1985**, 55, 2175.
- (11) Okruszek, A.; Sierzchala, A.; Zmudzka, K.; Stec, W. J. *Nucleosides, Nucleotides Nucleic Acids* **2001**, 20, 1843.
- (12) Iqbal, S. M.; Owen, L. N. *J. Chem. Soc.* **1960**, 1030.
- (13) Culvenor, C. C. J.; Davies, W.; Pausacker, K. H. *J. Chem. Soc.* **1946**, 1050.
- (14) Allman, T.; Goel, R. G. *Can. J. Chem.* **1982**, 60, 716.
- (15) Tolman, C. A. *Chem. Rev.* **1977**, 77, 313.
- (16) Pinnell, R. P.; Megerle, C. A.; Manatt, S. L.; Kroon, P. A. *J. Am. Chem. Soc.* **1973**, 95, 977.
- (17) Grim, S. O.; Keiter, R. L.; McFarlane, W. *Inorg. Chem.* **1967**, 6, 1133.
- (18) Grim, S. O.; Wheatland, D. A.; McFarlane, W. *J. Am. Chem. Soc.* **1967**, 89, 5573.

- (19) Grim, S. O.; Singer, R. M.; Johnson, A. W.; Randall, F. J. *J. Coord. Chem.* **1978**, *8*, 121
- (20) Grim, S. O.; Lui, P. J.; Keiter, R. L. *Inorg. Chem.* **1974**, *13*, 342.
- (21) Grim, S. O.; Shah, D. P.; Haas, C. K.; Ressner, J. M.; Smith, P. H. *Inorg. Chim. Acta* **1979**, *36*, 139.
- (22) Kroshefsky, R. D.; Weiss, R.; Verkade, J. G. *Inorg. Chem.* **1979**, *18*, 469.
- (23) Suárez, A.; Méndez-Rojas, M. A.; Pizzano, A. *Organometallics* **2002**, *21*, 4611.
- (24) Jeulin, S.; De Paule, S. D.; Ratovelomanana-Vidal, V.; Genêt, J. P.; Champion, N.; Dellis, P. *Angew. Chem., Int. Ed.* **2004**, *43*, 320.
- (25) Bilenko, V.; Spannenberg, A.; Baumann, W.; Komarov, I.; Börner, A. *Tetrahedron: Asymmetry* **2006**, *17*, 2082.
- (26) Adams, D. J.; Bennett, J. A.; Duncan, D.; Hope, E. G.; Hopewell, J.; Stuart, A. M.; West, A. J. *Polyhedron* **2007**, *26*, 1505.
- (27) Enthaler, S.; Erre, G.; Junge, K.; Schröder, K.; Addis, D.; Michalik, D.; Hapke, M.; Redkin, D.; Beller, M. *Eur. J. Org. Chem.* **2008**, 3352.
- (28) Erre, G.; Junge, K.; Enthaler, S.; Addis, D.; Michalik, D.; Spannenberg, A.; Beller, M. *Chem.-Asian J.* **2008**, *3*, 887.
- (29) Peer, M.; Jong, J. C. d.; Kiefer, M.; Langer, T.; Rieck, H.; Schell, H.; Sennhenn, P.; Sprinz, J.; Steinhagen, H.; Wiese, B.; Helmchen, G. *Tetrahedron* **1996**, *52*, 7547.
- (30) Bohlke, J. K.; de Laeter, J. R.; De Bievre, P.; Hidaka, H.; Peiser, H. S.; Rosman, K. J. R.; Taylor, P. D. P. *J. Phys. Chem. Ref. Data* **2005**, *34*, 57.

- (31) Socol, S. M.; Verkade, J. G. *Inorg. Chem.* **1984**, *23*, 3487.
- (32) Zhang, H.; Fang, F.; Xie, F.; Yu, H.; Yang, G.; Zhang, W. *Tetrahedron Lett.* **2010**, *51*, 3119.
- (33) Iggo, J. A. *NMR Spectroscopy in Inorganic Chemistry*; Oxford University Press: New York, 1999.
- (34) Shejwalkar, P.; Sedinkin, S. L.; Bauer, E. B. *Inorg. Chim. Acta* **2011**, *366*, 209.
- (35) Moloy, K. G.; Petersen, J. L. *J. Am. Chem. Soc.* **1995**, *117*, 7696.
- (36) Huang, A.; Marcone, J. E.; Mason, K. L.; Marshall, W. J.; Moloy, K. G.; Serron, S.; Nolan, S. P. *Organometallics* **1997**, *16*, 3377.
- (37) Clarke, M. L.; Ellis, D.; Mason, K. L.; Orpen, A. G.; Pringle, P. G.; Wingad, R. L.; Zaher, D. A.; Baker, R. T. *Dalton Trans.* **2005**, 1294.
- (38) Grotjahn, D. B.; Zeng, X.; Cooksy, A. L.; Kassel, W. S.; DiPasquale, A. G.; Zakharov, L. N.; Rheingold, A. L. *Organometallics* **2007**, *26*, 3385.
- (39) Smith, B. C. *Fundamentals of Fourier Transform Infrared Spectroscopy*; CRC Press: Boca Raton, Florida, 1995.
- (40) Otto, S.; Mzamane, S. N.; Roodt, A. *Acta Crystallogr., Sect. C* **1999**, *55*, 67.

Chapter II

Experimental Section

General Methods

Chemicals were treated as follows: THF, toluene, diethyl ether, distilled from Na/benzophenone; CH₂Cl₂, distilled from CaH₂. Benzene-1,2-dithiol (**2.20**), phosphorus trichloride, triethyl amine, dibenzyl amine (**2.7**), 1,2-ethanedithiol (**2.18**), 4-methoxy thiophenol (**2.5**), 2,2,6,6-tetramethyl piperidine (**2.22**) (all Aldrich) were used as received. All reactions were carried out under an atmosphere of nitrogen applying Schlenk techniques.

NMR spectra were obtained at room temperature on a Bruker Avance 300 MHz or a Varian Unity Plus 300 MHz instrument (¹H: 300.13 MHz; ¹³C: 75.5 MHz; ³¹P: 121.5 MHz) and referenced to a residual solvent signal; all assignments are tentative.

GC/MS spectra were recorded on a Hewlett Packard GC/MS System Model 5988A.

Exact masses were obtained on a JEOL MStation [JMS-700] Mass Spectrometer.

Melting points are uncorrected and were taken on an Electrothermal 9100 instrument. IR spectra were recorded on a Thermo Nicolet 360 FT-IR spectrometer.

Elemental analyses were performed by Atlantic Microlab, GA, USA.

Syntheses

(rac)-N,N-2-dibenzylamino-hexahydrobenzo[d][1,3,2]dithiaphospholane, ((rac)-2.32). To a Schlenk flask containing NEt₃ (3.8 mL, 27.0 mmol) and phosphorus trichloride (1.2 mL, 13.5 mmol), CH₂Cl₂ (50 mL) was added followed by dibenzylamine (2.6 mL, 13.5 mmol), which upon addition, yielded a white smoke. The white slurry was stirred at 0 °C for 30 min upon which the color changed to

yellow. An additional portion of NEt_3 (7.5 mL, 54 mmol) was then added followed by cyclohexane-1,2-dithiol (*rac*)-**2.19** (2.00 g, 13.5 mmol). After warming up to room temperature, the slurry was stirred for 16 h. The slurry was diluted with CH_2Cl_2 (50 mL). The organic layer was washed with H_2O (50 mL), 0.2 M solution of aqueous NaHSO_4 , H_2O , with a saturated aqueous solution of NaHCO_3 and H_2O . The combined organic layers were dried over MgSO_4 and concentrated *in vacuo*. The crude product was purified by precipitation from a CH_2Cl_2 solution by addition of hexanes yielding (*rac*)-**2.32** as a white solid (4.28 g, 11.5 mmol, 85%).

NMR (δ , CDCl_3) ^1H 7.36–7.16 (m, 10 H, Ph), 4.26–4.10 (m, 2 H, NCH_2), 4.08–3.91 (m, 2 H, NCH_2), 3.25–3.11 (m, 1 H, CHS), 3.05–2.90 (m, 1 H, CHS), 2.37–2.22 (m, 2 H, Cy), 1.94–1.75 (m, 2 H, Cy), 1.72–1.52 (m, 2 H, Cy), 1.48–1.17 (m, 2 H, Cy); $^{13}\text{C}\{^1\text{H}\}$ 137.7 (s, Ph), 128.3 (d, $J_{\text{CP}} = 1.1$ Hz, Ph), 128.2 (s, Ph), 127.1 (s, Ph), 62.8 (d, $J_{\text{CP}} = 2.7$ Hz, CHS), 57.6 (s, CHS), 51.8 (d, $J_{\text{CP}} = 17.6$ Hz, NCH_2), 31.8 (s, Cy), 31.7 (s, Cy), 25.7 (s, Cy), 25.3 (s, Cy); $^{31}\text{P}\{^1\text{H}\}$ 102.0.

HRMS calcd for $\text{C}_{20}\text{H}_{24}\text{NPS}_2$ 373.1088, found 373.1093. IR (cm^{-1} , neat solid) 3019 (w), 2931 (w), 1490 (m).

N,N-dibenzylaminobenzo[d][1,3,2]dithiaphospholane, (2.33). 1,2-Benzenedithiol (**2.20**, 0.500 g, 3.52 mmol) was converted to **2.33** (1.07 g, 2.9 mmol, 83%) as described above for (*rac*)-**2.32**. Anal. calcd for $\text{C}_{20}\text{H}_{18}\text{NPS}_2$: C, 65.37; H, 4.94. Found: C, 64.83; H, 4.82.

NMR (δ , CDCl_3) ^1H 7.54 (dd, $J = 5.7, 3.3$ Hz, 2 H, aromatic), 7.34–7.22 (m, 6 H, aromatic), 7.18–7.05 (m, 6 H, aromatic), 3.77 (d, $J = 10.7$ Hz, 4 H, $2 \times \text{NCH}_2$); $^{13}\text{C}\{^1\text{H}\}$ 137.9 (s, aromatic), 136.9 (s, aromatic), 128.41 (s, aromatic), 128.38 (s, aromatic),

127.4 (s, aromatic), 125.3 (s, aromatic), 124.3 (d, $J_{CP} = 6.0$ Hz, aromatic), 52.5 (d, $J_{CP} = 17.0$ Hz, NCH_2); $^{31}P\{^1H\}$ 88.0.

HRMS calcd for $C_{20}H_{24}NPS_2$ 367.0618, found 367.0619. IR (cm^{-1} , neat solid) 3025 (w), 1441 (m).

1,2-Ethanedithio-N,N-dibenzyl-phosphoramidite (2.31). To a Schlenk flask containing triethyl amine (4.8 mL, 34 mmol) and phosphorus trichloride (0.5 mL, 5.7 mmol), CH_2Cl_2 (20 mL) was added followed by dibenzylamine (1.1 mL, 5.7 mmol), which upon addition, yielded a white smoke. The white slurry was stirred at 0 °C for 30 min upon which the color changed to yellow. 1,2-Ethanedithiol (0.58 mL, 0.65 g, 6.9 mmol) was then added. After warming up to room temperature, the slurry stirred at room temperature for 1 h. The slurry was diluted with CH_2Cl_2 (50 mL). The organic layer was washed with H_2O (50 mL), 0.2 M solution of aqueous $NaHSO_4$, H_2O , and with a saturated aqueous solution of $NaHCO_3$ and H_2O . The combined organic layers were dried over $MgSO_4$ and concentrated *in vacuo*. The crude product was purified by precipitation from an EtOAc solution by addition of hexanes yielding **2.31** as a white solid (1.5 g, 4.7 mmol, 82%). Anal. Calc. for $C_{16}H_{18}NPS_2$: C, 60.16; H, 5.68. Found: C, 60.66; H, 5.89%.

NMR (δ , $CDCl_3$) 1H 7.39–7.12 (m, 10 H, 2×Ph), 4.03 (d, $^3J_{PH} = 10.9$ Hz, 4 H, 2× NCH_2), 3.56–3.41 (m, 2 H, $CHH'CHH'$), 3.25–3.10 (m, 2 H, $CHH'CHH'$); $^{13}C\{^1H\}$ 137.6 (d, $^3J_{CP} = 1.65$ Hz, 2× NCH_2C), 128.34 (s, Ph), 128.31 (d, $J_{CP} = 3.3$ Hz, Ph), 127.2 (s, Ph), 52.0 (d, $^2J_{CP} = 17.0$ Hz, 2× NCH_2), 41.3 (s, 2× CH_2); $^{31}P\{^1H\}$ 108.8 (s).

HRMS calcd for $C_{16}H_{18}NPS_2$ 319.0618, found 319.0627. IR (cm^{-1} , neat solid) 3023(w), 2894(w), 1492(m), 1452(m).

bis(4-Methoxyphenyl)-dibenzylphosphoramidodithioite (2.17). 4-

Methoxythiophenol (1.5 mL, 1.7 g, 12 mmol) was converted to **2.17** as described above for **2.31**. The crude product was purified by flash column chromatography on SiO₂ (2×20 cm column; eluted with 1:0 v/v hexanes/EtOAc → 9:1 v/v hexanes/EtOAc) to obtain the product **2.17** (2.15 g, 4.87 mmol, 85%) as a colorless oil. Anal. Calc. for C₂₈H₂₈NO₂PS₂: C, 66.51; H, 5.58. Found: C, 66.80; H, 5.59%.

NMR (δ, CDCl₃) ¹H 7.48–7.38 (m, 4 H, aromatic), 7.25–7.10 (m, 6 H, aromatic), 6.99–6.89 (m, 4 H, aromatic), 6.87–6.79 (m, 4 H, aromatic), 4.13 (d, ³J_{PH} = 9.0 Hz, 4 H, 2×NCH₂), 3.79 (s, 6 H, 2×CH₃); ¹³C{¹H} 159.5 (d, ⁵J_{CP} = 2.2 Hz, 2×CH₃OC), 137.3 (d, J_{CP} = 2.7 Hz), 135.4 (d, J_{CP} = 4.4 Hz), 128.8 (s), 128.1 (s), 127.1 (s), 124.3 (d, J_{CP} = 12.6 Hz), 114.7 (s, aromatic), 55.3 (s, 2×CH₃), 52.1 (d, ²J_{CP} = 17.0 Hz, 2×NCH₂); ³¹P{¹H} 133.2 (s).

HRMS calcd for C₂₀H₂₈NNaO₂PS₂ 528.1197, found 528.1200. IR (cm⁻¹, neat solid) 3027(w), 2937(w), 2931(w), 2831(w), 1590(m), 1490(s).

bis(4-Methoxyphenyl)-2,2,6,6-tetramethylpiperidin-1-ylphosphonodithioite

(2.28). 2,2,6,6-Tetramethylpiperidine (0.96 mL, 0.81 g, 5.7 mmol) was converted to **2.28** as described above for **2.31**. The crude product was purified by flash column chromatography on SiO₂ (1.5×15 cm column; eluted with 1:0 v/v hexanes/EtOAc → 9:1 v/v hexanes/EtOAc) to obtain the product **2.28** (1.28 g, 50%) as a colorless oil. Anal. Calc. for C₂₃H₃₂NO₂PS₂: C, 61.44; H, 7.17. Found: C, 61.45; H, 7.13%.

NMR (δ, CDCl₃) ¹H 7.35 (d, ³J_{HH} = 7.5 Hz, 4 H, aromatic), 6.77 (d, ³J_{HH} = 8.7 Hz, 4 H, aromatic), 3.72 (s, 6 H, 2×OCH₃), 1.68 (br s, 6 H, 2×CH₃), 1.62–1.34 (m, 6 H, 3×CH₂), 1.10 (br s, 6 H, 2×CH₃); ¹³C{¹H} 159.2 (d, ⁵J_{CP} = 2.8 Hz, 2×CH₃OC), 135.8 (d, J_{CP} = 4.9

Hz), 126.1 (d, $J_{CP} = 20.3$ Hz), 114.3 (d, $J_{CP} = 1.1$ Hz), 60.2 (d, $^2J_{CP} = 9.3$ Hz, NCH₂), 58.1 (d, $^2J_{CP} = 31.8$ Hz, NCH₂'), 55.2 (s, 2×CH₃O), 42.1 (br s, CCH₂), 40.6 (broad s, CCH₂'), 33.1 (d, $^3J_{CP} = 24.2$ Hz, 2×CH₃), 31.3 (br s, 2×CH₃'), 16.9 (s, CH₂CH₂CH₂); ³¹P{¹H} 133.2 (s).

HRMS calcd for C₂₃H₃₂NNaO₂PS₂ 472.1510, found 472.1516.

Chapter III

Investigation of Steric and Electronic Tuning of Phosphinooxazoline Ligands

3.1. Aim of the chapter

As part of our long-standing research interests in transition metal catalysis, we were in search of a tunable ligand system to be employed in iron complex synthesis. We chose phosphinooxazolines (PHOX) ligands, as their versatile structure allows for fine tuning of their steric and electronic properties.

In order to establish an easy access to a variety of structurally modified PHOX ligands, a general synthetic procedure was targeted. The investigation of the steric and electronic properties of the synthesized series of ligands was accomplished in two steps. First, analysis of the physical data obtained by NMR, and CV was performed in order to study an influence of the structure of the compounds on electronic properties. Then, the ligands were applied in the synthesis of new iron complexes. The study of the coordination compounds should allow for an understanding in what ways and how efficiently the electronic properties of the ligands could be translated to the electron density at the iron center. Also, investigation of the steric properties of the ligands could be performed by analyzing relationships between the geometries of the ligands and the structures of their respective metal complexes.

3.2. Introduction

Phosphinooxazolines (PHOX, **Figure 3.1**) are a known class of organic compounds.¹ Since they were first successfully applied as ligands in metal complexes synthesis,²⁻⁴

phosphinooxazolines were effectively employed in a variety of transition metal catalyzed reactions.^{2,5-22}

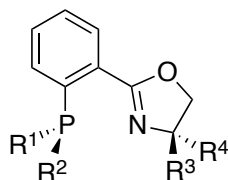


Figure 3.1. Phosphinooxazolines (PHOX)

Phosphinooxazolines serve as P-N bidentate ligands and can be tuned both sterically and electronically in a nearly orthogonal manner. These have been extremely useful characteristics in view of the fact that it is challenging to tune the steric effects of most phosphine and/or nitrogen-donor ligands without effecting the electronic properties and vice versa. PHOX ligands can be electronically tuned by varying the substitution pattern on the benzene ring while steric tuning (and some electronic tuning at nitrogen) can be accomplished by varying the substituents R³ and R⁴ on the oxazoline ring (**Figure 3.1**).

Several synthetic approaches to oxazolines can be found in the literature.²³

Common starting materials are carboxylic acids and their derivatives (acid halides, nitriles or imidates) on one side and β -aminoalcohols on the other side. One step methods are known,^{4,24,25} but usually applicable only for synthesis with limitations concerning the starting materials, and the yields are often moderate. Two step procedures usually give higher overall yields.^{6,26}

3.3. Synthesis of phosphinoxazolines

First, we needed to develop a generally applicable standard protocol for our laboratory to be employed in the synthesis of a variety of PHOX ligands. The main factors in method development were the availability of an assortment of starting materials from commercial sources and the overall yield of the synthesis. A general protocol needed also to be compatible with a variety of functional groups. After comparing existing approaches to the PHOX ligands, a modified literature procedure starting with acid chlorides and aminoalcohols was chosen.²⁶

In order to investigate the impact of steric and electronic tuning, we picked a number of target molecules. Four PHOX ligands with different substituents on the carbon next to the nitrogen atom of the oxazoline ring were selected for studying the steric effects (**Figure 3.2**).

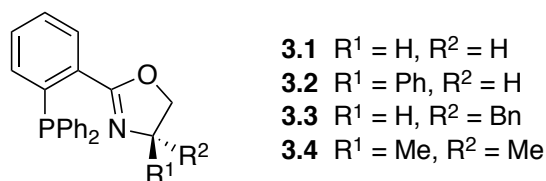


Figure 3.2. Sterically tuned PHOX ligands

To probe the electronic tuning effects, we decided to introduce a series of electron withdrawing and electron donating substituent on the aryl ring. Accordingly, six target molecules were selected (**Figure 3.3**).

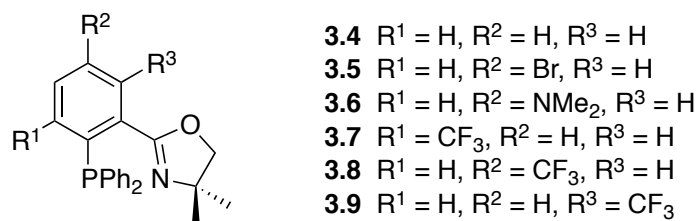


Figure 3.3. Electronically tuned PHOX ligands

The corresponding aminoalcohols and most of the substituted 2-fluorobenzoic acid chlorides required for the synthesis of the target molecules were commercially available. For these cases, a three-step method was developed (**Figure 3.4**).

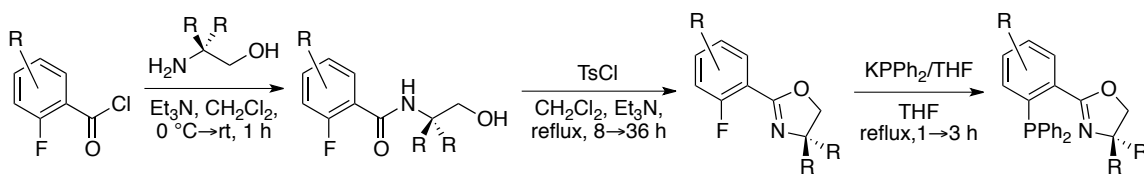


Figure 3.4. General methodology for PHOX syntheses

The synthesis started with the preparation of the amides from the aminoalcohols **3.10-3.13** and the acid chlorides **3.14-3.17** (**Figure 3.5**). The reactions proceeded smoothly and were very “forgiving”. Due to the significant difference in nucleophilicity between the oxygen of the hydroxyl unit and the nitrogen of the amine in the aminoalcohols, we did not observe O-acylated side products under any reaction conditions. Nevertheless, it was found that for the best reproducibility and in order to prevent overheating of the reaction mixture, the reaction should be performed at 0 °C and at relatively high dilution. Accordingly, a solution of the acid chloride (3 mL of CH₂Cl₂ per mmol) was slowly added to a solution of the aminoalcohol (4 mL of CH₂Cl₂ per mmol) at 0 °C with intensive stirring. After the addition was finished, the reaction mixtures were allowed to reach room temperature over a period of one hour. At that time, TLC showed complete

conversions of the aminoalcohols. The hydrochloride of Et₃N was the only byproduct of the synthesis, which was removed by aqueous work up. The obtained products **3.18-3.24** did not show any impurities by either TLC or NMR and were used without further purification for the next step. In order to acquire analytically pure samples for characterization, the compounds were purified by column chromatography or recrystallization. Seven amides **3.18-3.24** were prepared in 90 to 95% yield as white, crystalline materials (**Figure 3.5**).

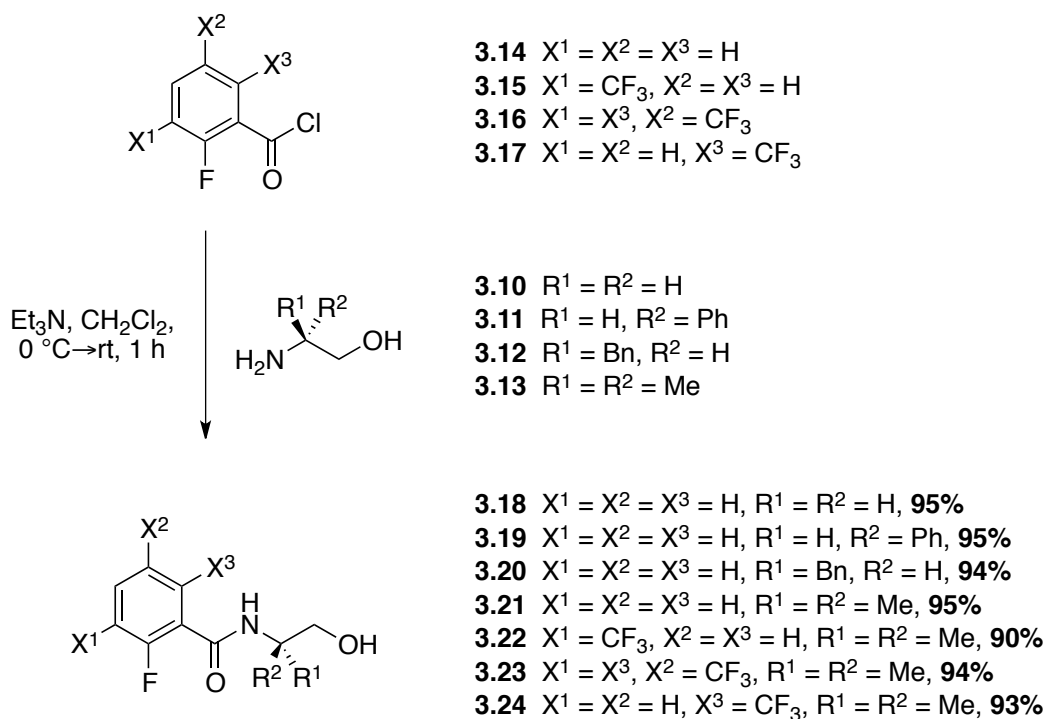


Figure 3.5. Synthesis of the amides

In the next step, intramolecular cyclization of the amides **3.18-3.24** led to the construction of the oxazoline rings in the molecules (**Figure 3.6**). This transformation was performed by converting the hydroxyl unit of the amides to a better leaving group followed by a base assisted, intramolecular nucleophilic substitution at elevated temperatures. Tosylate was chosen as an efficient leaving

group to accomplish the substitution at a relatively low temperature without the need of an additional strong base to help complete the cyclization. Thus, we were able to carry out the transformation in CH_2Cl_2 at reflux using Et_3N as the base (**Figure 3.6**). However, substitution on the carbon atom next to the nitrogen atom of the amides had a significant influence on the time required for the reaction to go to completion. Amide **3.18** that did not have any substituents on the carbon next to the nitrogen showed nearly complete conversion to the oxazoline **3.25** after a few hours of reflux and the reaction went to completion after around 8 hours. When amides with one substituent (**3.19** and **3.20** with phenyl and benzyl substituents, respectively) were employed, the reaction time needed to be increased to 16 hours. Only then, no more starting materials **3.19** or **3.20** and their corresponding tosylate intermediates were observed in the reaction mixture. The cyclization of the amides **3.21-3.24** containing two methyl groups next to the nitrogen atom was the most challenging. For those compounds, it was found that the maximum conversion to the target compounds **3.28-3.31** could be achieved after 36 hours of reflux. After that time, small amounts of uncyclized materials were usually still present but further reflux lead to decomposition of the already formed products **3.28-3.31**. An attempt to change CH_2Cl_2 to a higher boiling solvent such as dichloroethane did result in a shorter reaction time but also led to significantly higher amounts of side products, and, thus, the overall yield was not improved and purification became more difficult. Despite the differences in the reaction times, all cyclizations proceeded similarly. In order to decompose the excess of TsCl at the end of the reaction, 1 mL of H_2O was added to the reaction mixtures and reflux was continued

for one more hour. Et₃N and its ammonium salts were removed from the reaction mixtures during work up that consisted of washing the CH₂Cl₂ phase with H₂O, 2 M aqueous NaHSO₄ and saturated aqueous NaHCO₃. Purification of the obtained brown, oilish crude material by column chromatography resulted in the desired products **3.25-3.31** in 78 to 94 % yield as colorless oils (**Figure 3.6**).

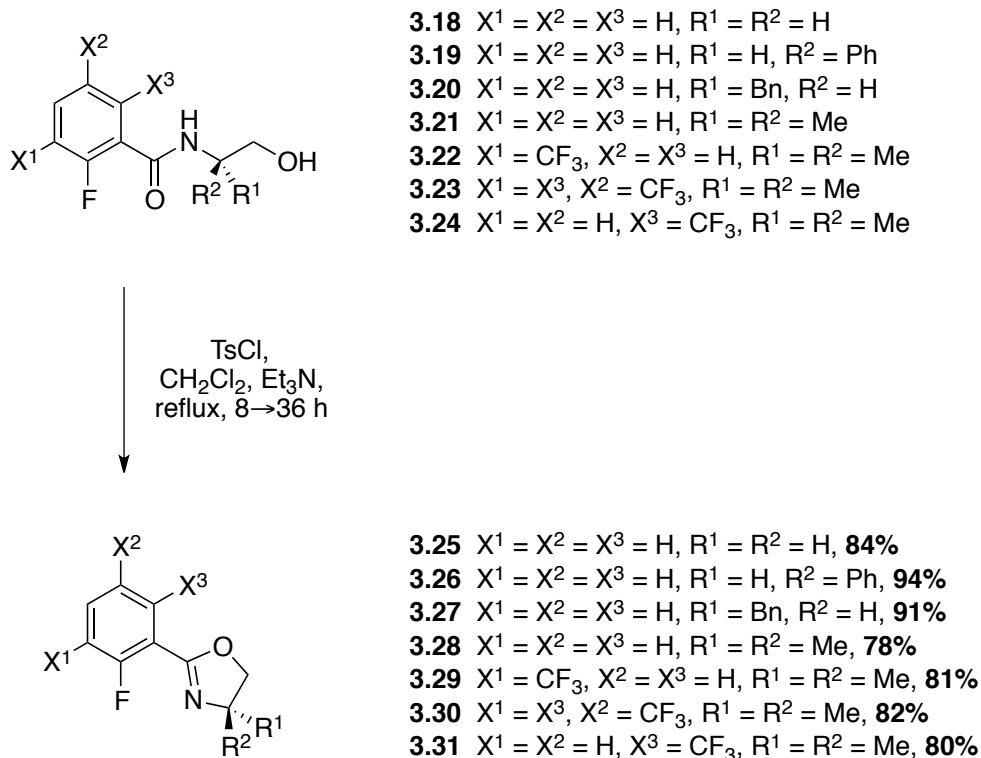


Figure 3.6. Cyclization of the amides 3.18-2.24 to the oxazoline compounds

3.25-3.31

At that point, the compounds **3.25-3.31** were ready for introduction of the diphenylphosphino group through nucleophilic substitution of the fluorine atom on the aryl ring. The reactions were carried out by using a commercial THF solution of the potassium salt of diphenylphosphide (KPPH₂) as nucleophile that was added to the fluorophenyloxazolines **3.25-3.31** in THF. After 3 hours of reflux, the

conversions were complete. As was expected, we observed differences in the rate of the substitution depending on the structure of the oxazoline starting materials. Compounds **3.25–3.28** differed from each other only by the substituents on the oxazoline ring, that were far enough from the reaction center in order to not cause any steric interactions. On the other side, electron densities on the benzene rings were nearly identical, thus no differences were found in the reaction times required for these compounds. After three hours reaction time, no more starting materials **3.25–3.28** were detected in the reaction mixtures. Significant changes in the reactivity were observed for the oxazolines **3.29–3.31** that bear highly electron withdrawing CF_3 groups on the aryl rings. For those compounds, formation of the products was seen immediately after addition of the reagent, as the red color of the KPPH_2 solution quickly disappeared. Upon an hour of reflux, the substitutions were complete. The PHOX ligands were purified by column chromatography and isolated as colorless oils, which solidified over time, in 70 to 86% yields (**Figure 3.7**). The successful introduction of the PPh_2 group was best seen in the ^{31}P NMR spectra, where signals between -4 and 5 ppm were observed.

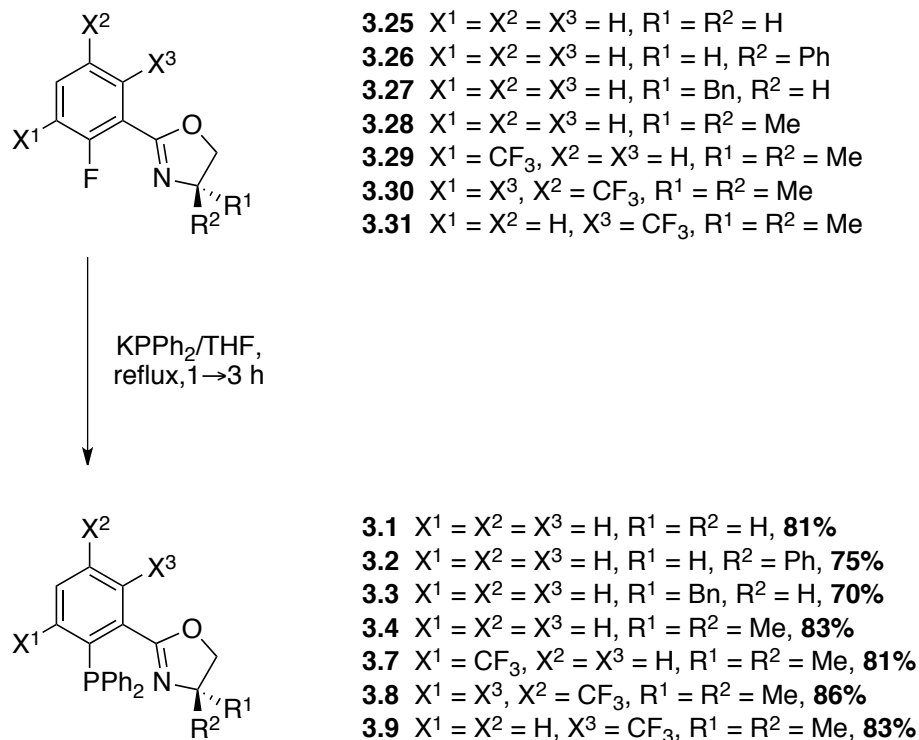


Figure 3.7. Introduction of the PPh₂ groups

At that point, seven PHOX ligands **3.1-3.4, 3.7-3.9** were synthesized from commercially available starting materials. However, we were interested in readily accessing PHOX ligands with other types of substituents, especially compounds with electron donating or withdrawing groups on the aryl ring of the ligands. We sought access to two of our initial targets **3.5** and **3.6** (PHOX with bromine and dimethylamino substituents, respectively). The most convenient starting material that allows not only the introduction of bromo and dimethylamino groups but also for other possible functionalization is 2-fluorobenzoic acid **3.32** (**Figure 3.8**). It is relatively cheap and it can undergo electrophilic aromatic substitutions with a variety of reagents. However, the presence of two electron withdrawing substituents on the benzene ring requires harsher conditions for the reaction. In

order to apply our general procedure for phosphinooxazolines syntheses to obtain compound **3.5**, the acid chloride **3.33** was prepared (**Figure 3.8**).

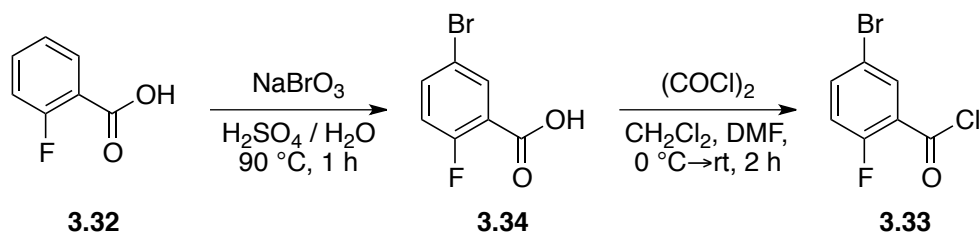


Figure 3.8. Synthesis of the starting material 3.33 for the preparation of the PHOX ligand 3.5

Bromination of **3.32** was performed using the *in situ* formation of a bromonium ion from NaBrO_3 under acidic conditions at elevated temperature. The brominated product **3.34**, which precipitated out of the reaction mixture, was separated by filtration in spectroscopically pure form in 88% yield. Subsequently, conversion of the substituted acid **3.34** into the acid chlorides **3.33** was performed using oxalyl chloride with a catalytic amount of DMF. Upon addition of the DMF catalyst to the reaction mixture, vigorous gas formation was observed. When the reaction was performed on a large scale, control of the temperature at the beginning of the reaction was necessary to prevent uncontrollable boiling of the mixture. The transformation was clean and went to completion within 2 hours. After removal of the solvents, thorough drying of the crude materials under high vacuum in order to remove excess of the reagents and volatile side products lead to the crude product **3.33** that was spectroscopically pure and, thus, was used immediately without further purification.

At this point, the starting material for our standard methodology was obtained. The acid chloride **3.33** was converted to the PHOX ligand **3.5** according to the three-step procedure described above (**Figure 3.4**). However, a slight modification of the reaction conditions was required for the last step of the synthesis (**Figure 3.9**). During the nucleophilic substitution employing the diphenylphosphide anion, a competition between the two halogens was observed in the molecule **3.36** with substitution of the fluorine being the major product of the reaction. The fluorine is a significantly better leaving group for the nucleophilic aromatic substitution. On the other side, the bromine is located in a *para*- position to the fluorine where the negatively charged intermediate of the substitution is highly stabilized by the strongly electron withdrawing fluorine. It appeared that we were looking at a case of kinetic versus thermodynamic control of the product formation. Adjusting the condition of the reaction favoring the kinetic product should favor the desired fluoride substitution product **3.5**. Low temperatures typically result in kinetic control. Accordingly, lowering the temperature resulted in a significant increase of the time required for complete conversion, but did not improve the ratio between the desired compound **3.5** and the side product. It was found that optimal conditions for the transformation featured the same temperature as the standard method but a shorter reaction time. The best yield (61%) of the desired PHOX ligand **3.5** was achieved after one hour at reflux.

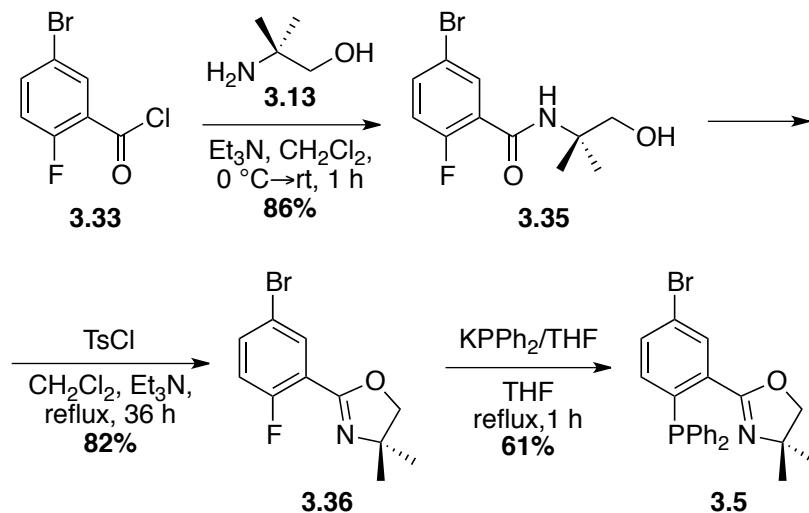


Figure 3.9. Synthesis of a PHOX ligand with a bromine substituent

The last target molecule to be synthesized was the PHOX ligand **3.6** with an electron donating dimethylamino group. In order to establish that functionality in the final molecule employing our standard methodology, a seven-step synthesis was developed (**Figure 3.10**).

Even though the strong electron withdrawing nitro group would have facilitated nucleophilic substitution of the fluorine in the phosphorylation step, we decided to convert it first to the dimethylamino functionality in order to prevent a competition between the phosphorus atom and the amino group during the alkylation of the NH₂ group. First, the nitro group in compound **3.40** was reduced to NH₂ employing H₂ at atmospheric pressure and 10% Pd on carbon as a heterogeneous catalyst. The reaction was complete after 16 hours and after filtration of the reaction mixture through a pad of Celite®, the spectroscopically pure amine **3.41** was obtained in 97% yield as a slightly brown oil. Next, the amino group needed to be alkylated. That step became slightly more challenging than was expected. The choice of alkylation methods was significantly narrowed down due to the presence of the oxazoline ring in the molecule that is sensitive to either acidic or basic conditions. Reductive amination reactions employing NaBH₄ and NaBH(OAc)₃ with a series of different aldehydes resulted in poor conversions, and significant amounts of decomposition products were observed. Attempts to employ various combinations of alkyl halides and mild bases were not successful either. In some cases monoalkylated products were detected, but efforts to push those reactions to completion resulted in very low yields of the dialkyl derivatives. Finally, we were able to introduce two methyl groups to the nitrogen atom using dimethyl sulfate as the alkylating agent and K₂CO₃ as a heterogeneous base in MeCN. That method produced compound **3.42** in 50% yield as a colorless oil. For the last step of the synthesis, our standard conditions for the fluorine substitution were employed. While presence of the electron donating NMe₂ group rendered the starting material

less reactive towards nucleophilic substitution, only the reaction time was adjusted in order to achieve complete conversion. It was found that after 3 hours all the starting material was consumed and the desired PHOX ligand **3.6** was formed. Following aqueous work up and purification of the crude product by column chromatography resulted in compound **3.6** in 78% yield as white solid. The overall yield of the ligand **3.6** in the seven steps synthesis starting from the 2-fluorobenzoic acid **3.32** was 23%. At this point, nine new as well as known PHOX ligands were synthesized and we proceeded to investigate their properties.

3.4. Analysis of the ligands' properties

To study the steric and electronic properties of the synthesized PHOX ligands, the following techniques were employed: (1) X-ray structure analysis of their iron complexes to determine bond distances and angles, (2) cyclic voltammetry to determine the oxidation potentials, (3) IR spectroscopy to determine the ν_{CO} stretching frequencies after conversion to iron carbonyl complexes, and (4) NMR spectroscopy to determine ^{31}P - ^{77}Se coupling constants of their selenides. The investigation included direct approaches based on studying the free ligands and indirect methods analyzing the physical data of metal complexes bearing the ligands studied. The series of the available PHOX ligands was intensively applied in our laboratory for the syntheses of a variety of metal complexes.^{27,28} A new class of coordination compounds with iron metal centers was studied in order to obtain additional information about steric and electronic properties of the PHOX ligands.

3.4.1. New iron phosphinooxazoline complexes^{27,28}

The initial application of the synthesized compounds **3.1-3.9** in synthesis of the new iron complexes was based on an exchange of the iodide and one of the carbonyl ligands in the starting material [FeCpI(CO)₂] (**3.43**) with the new PHOX ligands (**Figure 3.11**).²⁸

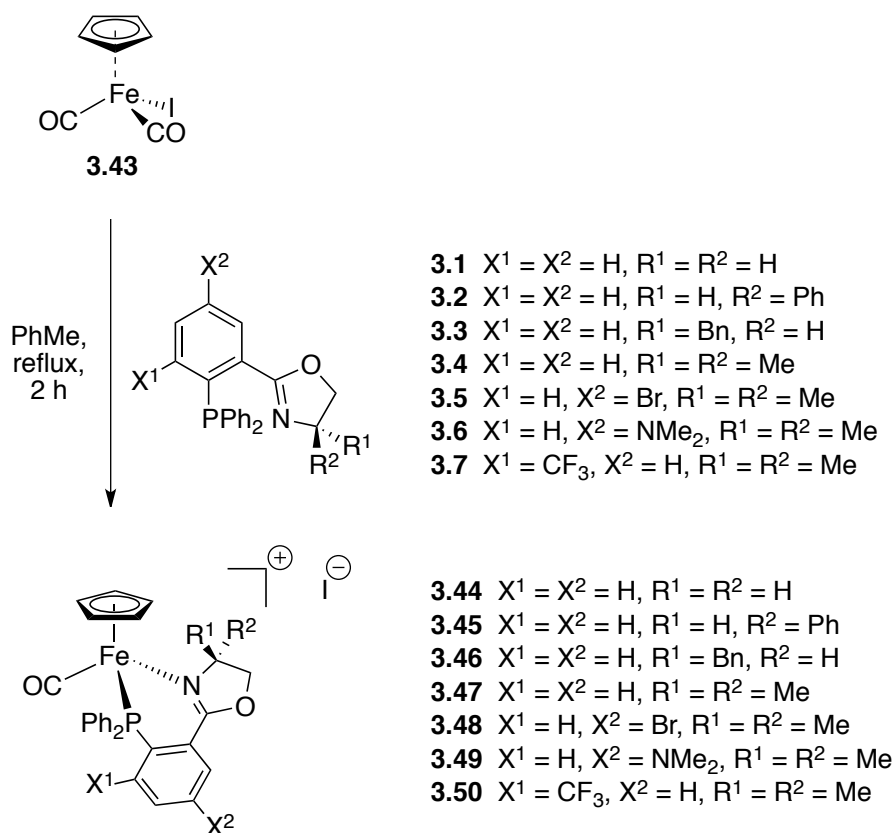


Figure 3.11. Synthesis of new iron PHOX complexes

The complex **3.43** had been used in the literature for preparation of half-sandwich cationic iron complexes by reaction with monodentate^{29,30} and bidentate³¹⁻³³ ligands. It was expected that our PHOX ligands would react similarly to form a new class of iron complexes. A general method applied for the synthesis featured reflux of a PhMe solution of the precursor **3.43** and a PHOX ligand for 2 hours. At that

point, the crude product precipitated out and upon recrystallization from $\text{CH}_2\text{Cl}_2/\text{Et}_2\text{O}$, the desired complexes were obtained. Unpredicted chemical behavior was observed for compound **3.7**. Under the standard condition, the red precipitate expected for product **3.50** did not form; a very dark colored solution was obtained instead. Analysis of the mixture by mass spectrometry, IR and ^{31}P NMR showed presence of the desired complex **3.50** along with large amounts of side products. Any further attempts to isolate the iron complex resulted in decomposition. One of the major signals seen in the crude ^{31}P NMR was a peak at -57.3 ppm. The resonance could indicate ligand decomposition during the reaction with displacement of the PPh_2 group. The decomposition pathway could be facilitated due to activation of the phenyl ring in compound **3.7** by the CF_3 substituent towards nucleophilic substitution of the PPh_2 unit with the iodide counterion. This unusual reactivity of ligand **3.7** stimulated interest in investigation of coordination chemistry of two other molecules **3.8** and **3.9** with CF_3 groups. In a follow up study performed by Matt Lenze, the PHOX ligands **3.8** and **3.9** were applied in the synthesis of related iron complexes bearing an indenyl ligand (**Figure 3.12**).²⁷ Out of the three PHOX molecules with CF_3 substituents, compound **3.8** with the CF_3 group being the furthest away from the phosphorus atom was the only ligand that gave a corresponding iron complex **3.54**. Ligand **3.7** did not show either conversion or decomposition and PHOX **3.9** reacted slowly and did not result in an isolable iron complex.

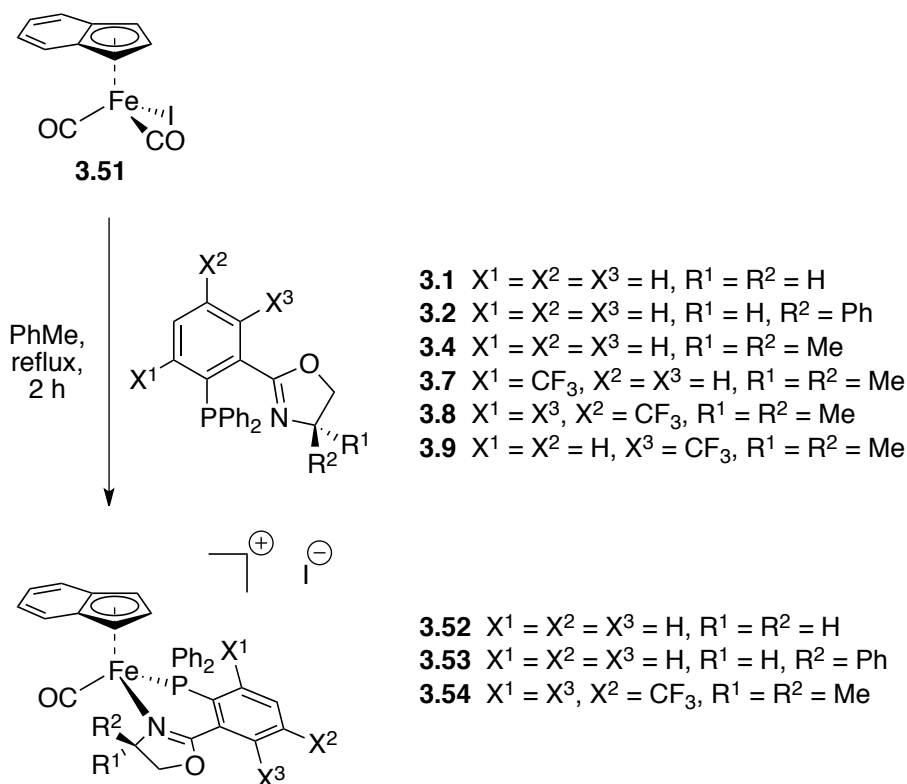


Figure 3.12. New iron indenyl complexes²⁷

A trend for the reactivity of the PHOX ligands **3.7-3.9** containing strongly electron withdrawing CF_3 groups was observed during their application in the iron complex syntheses. Compound **3.7** with CF_3 group in the *ortho*- position to the phosphorus atom was shown to be the least capable of forming coordination bonds to the iron center, but was very susceptible to decomposition through a nucleophilic attack on the phenyl ring by the iodide counterion. The PHOX molecule **3.8** featuring a CF_3 group in *para*- position to the PPh_2 was successfully applied in the synthesis of the iron complex **3.54**. The presence of the CF_3 group in the *meta*- position in compound **3.9** resulted in average reactivity towards formation of the coordination bonds to the iron compared to the ligands **3.7** and **3.8**, not resulting in isolable material. This trend can be linked to the influence of the CF_3 groups on the electron

density at the phosphorus atoms of the ligands **3.7-3.9** by inductive electron withdrawing, which is a distance dependent effect. Therefore, with an increasing number of bonds separating the CF₃ groups from the coordinating atom the electron density at the phosphorus should increase and consequently increase the ability of the ligands to form a metal phosphorus bond. Accordingly, the preliminary data for the compounds **3.7-3.9** indicated that molecule **3.7** was the least electron donating one followed by compound **3.9** and the ligand **3.8** was the most basic out of the three PHOX molecules. This trend was subsequently investigated further.

3.4.2. Electronic properties of the ligands

Investigation of the electronic properties of the free PHOX ligands was performed by NMR. Selenium derivatives of all PHOX molecules were prepared according to the procedure described in the previous chapter. The values of the ³¹P-⁷⁷Se coupling constants are shown in **Table 3.1**. Values for Ph₃P,³⁴ (PhO)₃P³⁵ and (MeO)₃P³⁶ are included for comparison.

Table 3.1. ³¹P-⁷⁷Se coupling constants for the PHOX ligand derivatives

Compound	¹ J(³¹ P- ⁷⁷ Se), Hz	Compound	¹ J(³¹ P- ⁷⁷ Se), Hz
3.1	742	3.7	785
3.2	745	3.8	757
3.3	745	3.9	769
3.4	747	Ph ₃ P	735 ³⁴
3.5	752	(PhO) ₃ P	1025 ³⁵
3.6	729	(MeO) ₃ P	954 ³⁶

As explained in **Chapter II**, these values can be used to judge the relative electron donating properties (or basicity) of phosphorus atoms.^{34,36-42} Analysis of the data supported our initial hypothesis about the influence of the substituents on the electron density at the phosphorus atoms. In the series of electronically tuned ligands **3.4-3.9**, we observed an increase of the $^1J(^{31}\text{P}-^{77}\text{Se})$ coupling constants with increasing electron-withdrawing abilities of the substituents. Accordingly, compound **3.6** with strong electron donating NMe_2 group was the most basic ($^1J(^{31}\text{P}-^{77}\text{Se}) = 729$ Hz) and the compound **3.7** with CF_3 substituent right next to the phosphorus atom was found to be the least basic ligand ($^1J(^{31}\text{P}-^{77}\text{Se}) = 785$ Hz). The other ligands fell in between these two extreme values. As expected, ligands **3.1-3.4**, featuring different substituents on the oxazoline ring rather than the phenyl ring, have very similar electronic properties at the phosphorus. The minor differences in the $^1J(^{31}\text{P}-^{77}\text{Se})$ coupling constants of their selenium derivatives could be due to slight variations of the compounds' geometry. This effect is known in literature.³⁴ Overall, the PHOX ligands were found to be less basic than Ph_3P , except compound **3.6** bearing a NMe_2 group, but significantly more basic than either $(\text{PhO})_3\text{P}$ or $(\text{MeO})_3\text{P}$, which were reported to give $^1J(^{31}\text{P}-^{77}\text{Se})$ coupling constants of 1025 and 954 Hz, respectively.

Analysis of the physical data of the new iron complexes in **Figure 3.11**²⁸ and **Figure 3.12**²⁷ can give additional insight in the electronic properties of the ligands.

Therefore, spectroscopic data were collected and analyzed to identify the influence of different ligands on carbonyl stretching frequencies and the oxidation potentials of the complexes.

It is known from the literature that in a series of structurally similar complexes containing CO ligands, trends for ν_{CO} stretching frequencies and CO bond distances can be correlated to the electron donating properties of phosphine type ligands.⁴³ It was shown that more basic ligands increase electron density at a metal center, which transfers some of the electron density to the π^* orbital of a CO ligand through back bonding interactions, effectively increasing the CO bond distance and at the same time decreasing the ν_{CO} stretching frequency. The data for the CO ligands in the iron PHOX complexes **3.44-3.49** (**Figure 3.11**) were collected by means of IR spectroscopy and X-ray structure analysis and are presented in **Table 3.2**.²⁸

Table 3.2. Carbonyl stretching frequencies and bond distances

Complex	3.44	3.45	3.47	3.48	3.49
ν_{CO} , cm^{-1}	1971	1967	1944	1947	1951
C \equiv O bond distance, Å	1.138(3)	1.142(3)	1.150(3)	1.159(13)	1.16(2)

The ν_{CO} stretching frequencies did not show the anticipated dependency on the electron donating abilities of the PHOX ligands. Compound **3.44**, which does not bear any substituents on either the aryl or the oxazoline ring of the ligand, showed the highest IR stretching frequency (1971 cm^{-1}), followed by compound **3.45** that had a phenyl substituent on the oxazoline ring (1967 cm^{-1}). The PHOX ligand **3.6** with NMe_2 group was found to be the most electron-donating as judged by the ^{31}P - ^{77}Se coupling constant, but in the metal complex **3.49** it did not show the expected influence on the ν_{CO} stretching frequency, which is higher than for complex **3.47** without a NMe_2 group. Generally, the data demonstrated greater impacts caused by

sterically tuned ligands **3.1-3.4** rather than the electronically tuned ligands **3.4-3.6**. That conclusion can be rationalized by two main differences between the iron complexes **3.44-3.49** and literature model systems. First, the PHOX ligands are P-N bidentate, and all ligands previously analyzed towards their ν_{CO} stretches in the IR were monodentate phosphorus compounds. While electronic properties of the phosphorus atoms in the PHOX molecules could follow the expected trends, the nitrogen atom of the oxazoline ring simultaneously plays a dual role as a σ -donor and a π -acceptor. Hence, the nitrogen could disturb changes in electron density on the metal center caused by the phosphorus atom. The second explanation is based on the dependency of the complexes' structures on the ligands. X-ray structural analysis confirmed that all our complexes have slightly different geometries.²⁸ However, comparative studies of ν_{CO} stretching frequencies in the literature are based on systems with almost identical geometries.⁴³⁻⁴⁵ Therefore, our results could exhibit deviations from the previously published trends as the complexes **3.44-3.49** showed structural differences.

Finally, cyclic voltammetry was employed to determine the oxidation potentials of the ligands and the iron complexes. The linear dependency of the ν_{CO} stretching frequency on the reduction potential of related iron carbonyl complexes has been investigated in the literature as a probe to analyze the electron donating properties of monodentate phosphorus ligands.⁴³ The linear increase of the oxidation potentials of structurally related iron carbonyl complexes was shown to result in a decrease of the ν_{CO} stretching frequencies in a similarly linear manner that was connected to a decline of the electron donating abilities of their respective ligands.

The cyclic voltammetry data for PHOX ligands **3.1-3.6** and the new iron complexes **3.44-3.49** are shown in **Table 3.3**.

Table 3.3. Electrochemical data for the PHOX ligands and the iron complexes

Complex	Ligand	$\Delta E_{red/ox}, V$	E_{pa}, V	E_{pa}, V, ligand
3.44	3.1	0.43	1.21	0.92
3.45	3.2	0.35	1.18	0.82
-	3.3	-	-	1.09
3.47	3.4	0.36	1.46	0.86
3.48	3.5	0.24	1.32	1.13
3.49	3.6	0.33	1.18	0.87

In the cyclic voltammograms of the ligands, a varying number of oxidation waves were seen and no reduction waves on the reverse scans were observed. Increasing scan rates did not result in better reversibility, suggesting that complex and irreversible reactions were taking place upon oxidation of the ligands.⁴⁶ The first oxidation potential of the PHOX molecules ranged from 1.13 to 0.82 V and little dependency on the anticipated electronic properties was observed. Still, the presence of an electron-withdrawing bromine functionality in the ligand **3.5** made it the most difficult to oxidize ($E_{pa} = 1.13 V$).

The electrochemical data for the metal complexes showed much better reversibility of the first oxidation wave with peak current ratios $i_c/i_a \geq 0.9$, while a very large separation between oxidation and reduction peaks ($\Delta E = 0.24$ to $0.43 V$) suggested sluggish electron transfer. The $E_{1/2}$ values of the first oxidation potentials for our

complexes were recorded between 1.28 and 1.00 V. The reversibility of the oxidations for the metal complexes but not for the ligands indicated a one-electron oxidation/reduction process with the electron coming from the HOMO of the complexes. However, the similarity of the oxidation potentials of the free ligands and the iron complexes suggested that the HOMO is ligand-centered. This could explain why we did not observe the trends described in literature for the oxidation potentials of monodentate iron phosphine complexes where the HOMO might be metal centered.⁴³

3.4.3. Steric properties of the ligands

Evaluation of steric tuning of the PHOX ligands was performed by X-ray structure analysis. Crystal structures of the five complexes **3.44**, **3.45**, **3.47-3.49** were obtained and their geometries were analyzed.²⁸ According to our assumptions, steric tuning of the ligand should be taking place at the position α to the coordinating nitrogen atom of the oxazoline ring. Thus, complexes **3.44**, **3.45** and **3.47** were of high interest due to implementation of the hypothetically sterically tuned ligand **3.1**, **3.2** and **3.4**, respectively.

The ideal geometry for the new iron PHOX complexes should be octahedral, but the actual structural data showed distortion from the theoretical as seen by comparing the bond angles around the iron center described below. Therefore, analysis of magnitudes of the complexes' structural deviations from the ideal octahedral coordination geometry was employed to study the steric tuning of the ligands. Relevant structural data for the analysis of the complexes **3.44**, **3.45**, **3.47-3.49** are compiled in the **Table 3.4**.

Table 3.4. Selected structural data for the complexes 3.44, 3.45, 3.47-3.49

Complex		3.44	3.45	3.47	3.48	3.49
Bond angles, °	O≡C-Fe-N	92.62(12)	91.57(14)	100.00(8)	99.4(4)	99.2(6)
	N-Fe-P	85.23(7)	86.92(9)	83.38(5)	84.2(3)	83.2(3)
	O≡C-Fe-P	92.32(9)	92.90(11)	93.58(7)	96.2(4)	96.5(5)
	O≡C-Fe	176.6(3)	176.2(3)	174.64(19)	173.6(10)	170.7(16)

The concept of bite angles⁴⁷ was applied first to characterize the steric properties of the ligands. The values obtained for N-Fe-P angles were all very similar and ranged from 83.2° to 86.92°. Unexpectedly, regardless of a diminished steric repulsion, the smallest bite angle was not found for the ligand **3.1** with no substituents on either the oxazoline or the phenyl rings. However, the largest bite angle was found for the ligand **3.2** with a large phenyl substituent in the α position to the nitrogen atom on the oxazoline ring.

Another indicative set of parameters to assess the steric properties of the ligands is the bond angles around the iron center. The values ranged from 83.2° for the N-Fe-P to 100.00° for the O≡C-Fe-P angles. The O≡C-Fe-P angles for the complexes **3.47-3.49** bearing two methyl substituents on the oxazoline ring (99.2° to 100.0°) showed the largest deviations from the ideal 90° values. The same three complexes featured a significant loss of linearity of the O≡C-Fe bond angles. The angles O-C-Fe were observed in the range from 170.7° to 174.64°.

Overall, the presence of substituents in the α position to the nitrogen atom of the oxazoline ring in the PHOX ligands was found to influence the geometry of the corresponding metal complexes. Therefore, steric tuning can be achieved by varying the size of these substituents.

3.5. Conclusion

An investigation of the intended steric and electronic tuning of PHOX ligands was performed. For that purpose, nine ligands **3.1-3.9** were synthesized. The compounds **3.5-3.9** were prepared for the first time. The electronic properties of the ligands were examined employing a variety of techniques. Direct studies of the PHOX ligands were performed utilizing NMR spectroscopy and cyclic voltammetry. In an indirect approach, analysis of physical data obtained by NMR, IR and CV for new iron complexes bearing the PHOX ligands synthesized in our laboratory was performed. Overall, it was found that the electronic tuning of the PHOX ligands is possible by varying the substituents on the phenyl ring. However, the tuning was observed to have unexpected and often only a minor influence on the electronic properties of their respective metal complexes due to their P,N chelating nature. The possibility of steric tuning was investigated by evaluation of the data from X-ray structure analysis of the new iron PHOX complexes. It was shown that the presence of substituents in the position α to the nitrogen atom of the oxazoline ring influenced the geometries of the corresponding metal complexes. The phosphinooxazolines **3.4-3.6** having tertiary carbon atoms (two methyl

substituents) in those positions afforded the greatest deviations from the ideal octahedral geometries of the iron complexes **3.47-3.49**.

3.6. References

- (1) Helmchen, G.; Pfaltz, A. *Acc. Chem. Res.* **2000**, *33*, 336.
- (2) Sprinz, J.; Helmchen, G. *Tetrahedron Lett.* **1993**, *34*, 1769.
- (3) Matt, P. v.; Pfaltz, A. *Angew. Chem., Int. Ed.* **1993**, *32*, 566.
- (4) Dawson, G. J.; Frost, C. G.; Williams, J. M. J.; Coote, S. J. *Tetrahedron Lett.* **1993**, *34*, 3149.
- (5) Geisler, F. M.; Helmchen, G. *J. Org. Chem.* **2006**, *71*, 2486.
- (6) García-Yebra, C.; Janssen, J. P.; Rominger, F.; Helmchen, G. *Organometallics* **2004**, *23*, 5459.
- (7) Zehnder, M.; Schaffner, S.; Neuburger, M.; Plattner, D. A. *Inorg. Chim. Acta* **2002**, *337*, 287.
- (8) Helmchen, G. *J. Organomet. Chem.* **1999**, *576*, 203.
- (9) Ogasawara, M.; Yoshida, K.; Kamei, H.; Kato, K.; Uozumi, Y.; Hayashi, T. *Tetrahedron: Asymmetry* **1998**, *9*, 1779.
- (10) Janssen, J. P.; Helmchen, G. *Tetrahedron Lett.* **1997**, *38*, 8025.
- (11) Keith, J. A.; Behenna, D. C.; Mohr, J. T.; Ma, S.; Marinescu, S. C.; Oxgaard, J.; Stoltz, B. M.; Goddard III, W. A. *J. Am. Chem. Soc.* **2007**, *129*, 11876.
- (12) Loiseleur, O.; Hayashi, M.; Keenan, M.; Schmees, N.; Pfaltz, A. *J. Organomet. Chem.* **1999**, *576*, 16.
- (13) Loiseleur, O.; Hayashi, M.; Schmees, N.; Pfaltz, A. *Synthesis* **1997**, 1338.

- (14) Bell, S.; Wüstenberg, B.; Kaiser, S.; Menges, F.; Netscher, T.; Pfaltz, A. *Science (Washington, DC, U.S.)* **2006**, *311*, 642.
- (15) Liu, D.; Tang, W.; Zhang, X. *Org. Lett.* **2004**, *6*, 513.
- (16) Lightfoot, A.; Schnider, P.; Pfaltz, A. *Angew. Chem., Int. Ed.* **1998**, *37*, 2897.
- (17) Naud, F.; Malan, C.; Spindler, F.; Rüggeberg, C.; Schmidt, A. T.; Blaser, H. U. *Adv. Synth. Catal.* **2006**, *348*, 47.
- (18) Langer, T.; Helmchen, G. *Tetrahedron Lett.* **1996**, *37*, 1381.
- (19) Carmona, D.; Vega, C.; García, N.; Lahoz, F. J.; Elipe, S.; Oro, L. A.; Lamata, M. P.; Viguri, F.; Borao, R. *Organometallics* **2006**, *25*, 1592.
- (20) Carmona, D.; Lahoz, F. J.; Elipe, S.; Oro, L. A.; Lamata, M. P.; Viguri, F.; Sánchez, F.; Martínez, S.; Cativiela, C.; López-Ram de VÍu, M. P. *Organometallics* **2002**, *21*, 5100.
- (21) Hiroi, K.; Watanabe, K. *Tetrahedron: Asymmetry* **2002**, *13*, 1841.
- (22) Stangeland, E. L.; Sammakia, T. *Tetrahedron* **1997**, *53*, 16503.
- (23) Frump, J. A. *Chem. Rev.* **1971**, *71*, 483.
- (24) Katagiri, K.; Danjo, H.; Yamaguchi, K.; Imamoto, T. *Tetrahedron* **2005**, *61*, 4701.
- (25) Allen, J. V.; Dawson, G. J.; Frost, C. G.; Williams, I. M. J.; Coote, S. J. *Tetrahedron* **1994**, *50*, 799.
- (26) Peer, M.; Jong, J. C. d.; Kiefer, M.; Langer, T.; Rieck, H.; Schell, H.; Sennhenn, P.; Sprinz, J.; Steinhagen, H.; Wiese, B.; Helmchen, G. *Tetrahedron* **1996**, *52*, 7547.

- (27) Lenze, M.; Sedinkin, S. L.; Rath, N. P.; Bauer, E. B. *Tetrahedron Lett.* **2010**, *51*, 2855.
- (28) Sedinkin, S. L.; Rath, N. P.; Bauer, E. B. *J. Organomet. Chem.* **2008**, *693*, 3081.
- (29) Palazzi, A.; Stagni, S.; Bordoni, S.; Monari, M.; Selva, S. *Organometallics* **2002**, *21*, 3774.
- (30) Ashby, M. T.; Enemark, J. H.; Lichtenberger, D. L. *Inorg. Chem.* **1988**, *27*, 191.
- (31) Nakanishi, S.; Goda, K.; Uchiyama, S.; Otsuji, Y. *Bull. Chem. Soc. Jpn.* **1992**, *65*, 2560.
- (32) Coville, N. J.; Darling, E. A.; Hearn, A. W.; Johnston, P. *J. Organomet. Chem.* **1987**, *328*, 375.
- (33) Vierling, P.; Riess, J. G.; Grand, A. *Inorg. Chem.* **1986**, *25*, 4144.
- (34) Pinnell, R. P.; Megerle, C. A.; Manatt, S. L.; Kroon, P. A. *J. Am. Chem. Soc.* **1973**, *95*, 977.
- (35) Socol, S. M.; Verkade, J. G. *Inorg. Chem.* **1984**, *23*, 3487.
- (36) Kroshefsky, R. D.; Weiss, R.; Verkade, J. G. *Inorg. Chem.* **1979**, *18*, 469.
- (37) Suárez, A.; Méndez-Rojas, M. A.; Pizzano, A. *Organometallics* **2002**, *21*, 4611.
- (38) Jeulin, S.; De Paule, S. D.; Ratovelomanana-Vidal, V.; Genêt, J. P.; Champion, N.; Dellis, P. *Angew. Chem., Int. Ed.* **2004**, *43*, 320.
- (39) Bilenko, V.; Spannenberg, A.; Baumann, W.; Komarov, I.; Börner, A. *Tetrahedron: Asymmetry* **2006**, *17*, 2082.

- (40) Adams, D. J.; Bennett, J. A.; Duncan, D.; Hope, E. G.; Hopewell, J.; Stuart, A. M.; West, A. J. *Polyhedron* **2007**, *26*, 1505.
- (41) Enthaler, S.; Erre, G.; Junge, K.; Schröder, K.; Addis, D.; Michalik, D.; Hapke, M.; Redkin, D.; Beller, M. *Eur. J. Org. Chem.* **2008**, 3352.
- (42) Erre, G.; Junge, K.; Enthaler, S.; Addis, D.; Michalik, D.; Spannenberg, A.; Beller, M. *Chem.-Asian J.* **2008**, *3*, 887.
- (43) Rahman, M. M.; Liu, H. Y.; Eriks, K.; Prock, A.; Giering, W. P. *Organometallics* **1989**, *8*, 1.
- (44) Rahman, M. M.; Liu, H. Y.; Prock, A.; Giering, W. P. *Organometallics* **1987**, *6*, 650.
- (45) Golovin, M. N.; Rahman, M. M.; Belmonte, J. E.; Giering, W. P. *Organometallics* **1985**, *4*, 1981.
- (46) Geiger, W. E. In *Laboratory Techniques in Electroanalytical Chemistry* 1996, p 684.
- (47) Casey, C. P.; Whiteker, G. T. *Israel J. Chem.* **1990**, *30*, 299.

Chapter III

Experimental Section

General methods

Chemicals were treated as follows: THF, toluene, diethyl ether, distilled from Na/benzophenone; CH₂Cl₂, distilled from CaH₂. 2-Fluorobenzoic acid (Aldrich), Ethanolamine **3.10** (Aldrich), (*R*)-2-amino-2-phenylethanol **3.11** (Aldrich), (*S*)-2-amino-3-phenylpropan-1-ol **3.12** (Aldrich), 2-Amino-2-methyl-1-propanol **3.13** (Aldrich), NaBrO₃ (Flinn Scientific Inc.), (COCl)₂ (Acros), TsCl (Aldrich), DMAP (Aldrich), KPPH₂ (Aldrich, 0.5 M in THF), Potassium carbonate (Fisher Scientific), dimethyl sulfate ((CH₃)₂SO₄, Aldrich), Pd/C (5%, Lancaster), Celite® 512 medium (Fluka), Silica gel, 200-400 mesh, 60 Å (Sigma-Aldrich), used as received.

NMR spectra were obtained at 300 K on a Bruker Avance 300 MHz or a Varian Unity Plus 300 MHz instrument and referenced to the signal of TMS; all assignments are tentative. Exact masses were obtained on JEOL MStation (JMS-700) Mass spectrometer. Melting points are uncorrected and were taken on an Electrothermal 9100 instrument. Elemental analyses were performed by Atlantic Microlab Inc., Norcross, GA, USA.

Syntheses

2-Fluoro-*N*-(2-hydroxyethyl)benzamide (3.18). To a stirred solution of the ethanolamine **3.10** (0.57 g, 0.56 mL, 9.3 mmol) in CH₂Cl₂ (30 mL), Et₃N (1.7 g, 2.4 mL, 17 mmol) was added. The resulting solution was cooled to 0 °C (ice bath) and a solution of the acid chloride **3.14** (1.0 mL, 1.3 g, 8.4 mmol) in CH₂Cl₂ (25 mL) was added dropwisely. The reaction mixture was stirred at 25 °C for 2 hours and then

diluted with CH₂Cl₂ (50 mL). The organic layer was washed with H₂O (50 mL), 0.2 M solution of aqueous NaHSO₄, H₂O, a saturated aqueous solution of NaHCO₃ and H₂O. The combined organic layers were dried over MgSO₄ and concentrated *in vacuo*. The crude product was purified by flash column chromatography on SiO₂ (2 × 20 cm column; eluted with 1:0 v/v toluene/EtOAc → 7:3 v/v toluene/EtOAc) to obtain the product **3.18** (1.47 g, 8.01 mmol, 95%) as a colorless oil.

NMR (δ, CDCl₃) ¹H 8.05–7.89 (m, 1 H, aromatic), 7.45–7.31 (m, 1 H, aromatic), 7.24–7.10 (m, 2 H, Ph, NH), 7.07–6.98 (m, 1 H, aromatic), 3.78–3.72 (m, 2 H, CH₂O), 3.61–3.53 (m, 2 H, CH₂N), 2.95 (s, 1 H, OH); ¹³C{¹H} 164.4 (d, ³J_{CF} = 3.3 Hz, C=O), 160.6 (d, ¹J_{CF} = 248.1 Hz, CF), 133.4 (d, ³J_{CF} = 9.3 Hz, aromatic), 131.9 (d, ³J_{CF} = 2.2 Hz, aromatic), 124.7 (d, ³J_{CF} = 3.3 Hz, aromatic), 120.8 (d, ³J_{CF} = 12.1 Hz, aromatic), 116.0 (d, ³J_{CF} = 24.7 Hz, aromatic), 62.0 (s, CH₂O), 42.8 (s, CH₂N); ¹⁹F{¹H} – 113.9 (s).

2-Fluoro-N-[(1R)-2-hydroxy-1-phenylethyl]benzamide (3.19). Acid chloride **3.14** (2.67 g, 2.00 mL, 16.9 mmol) was converted to **3.19** (4.15 g, 16.0 mmol, 95%, white powder) as described above for **3.18**.

NMR (δ, CDCl₃) ¹H 8.04–7.91 (m, 1 H, aromatic), 7.49–7.11 (m, 8 H, Ph+NH), 7.10–6.98 (m, 1 H, aromatic), 5.31–5.17 (m, 1 H, CHN), 3.88 (br s, 2 H, CH₂), 2.63 (br s, 1 H, OH); ¹³C{¹H} 163.5 (d, ³J_{CF} = 3.3 Hz, C=O), 160.7 (d, ³J_{CF} = 247.5 Hz, CF), 138.9 (s, aromatic), 133.5 (d, ³J_{CF} = 9.3 Hz, aromatic), 132.0 (d, ³J_{CF} = 2.2 Hz, aromatic), 128.9 (s, aromatic), 127.9 (s, aromatic), 126.7 (s, aromatic), 124.8 (d, ³J_{CF} = 3.3 Hz, aromatic), 116.0 (d, ³J_{CF} = 24.7 Hz, aromatic), 66.5 (s, CH₂), 56.2 (s, CHN).

***N*-[(1*S*)-1-benzyl-2-hydroxyethyl]-2-fluorobenzamide (3.20).** Acid chloride

3.14 (1.70 g, 1.27 mL 10.7 mmol) was converted to **3.20** (2.75 g, 10.1 mmol, 94%, colorless oil) as described above for **3.18**.

NMR (δ , CDCl₃) ¹H 8.06–7.91 (m, 1 H, aromatic), 7.46–7.32 (m, 1 H, aromatic), 7.31–7.10 (m, 6 H, aromatic), 7.07–6.97 (m, 1 H, aromatic), 6.94 (br s, 1 H, NH), 4.45–4.27 (m, 1 H, CHN), 3.81–3.56 (m, 2 H, CH₂O), 2.92 (dd, $J = 7.2, J = 0.9$ Hz, 2 H, PhCH₂), 2.67 (br s, 1 H, OH); ¹³C{¹H} 161.3 (d, $J_{CF} = 3.1$ Hz, C=O), 137.4 (s, aromatic), 133.5–133.3 (m, aromatic), 132.0 (d, $J_{CF} = 2.2$ Hz, aromatic), 129.3 (s, aromatic), 128.7 (s, aromatic), 126.7 (s, aromatic), 124.8 (d, $J_{CF} = 3.3$ Hz, aromatic), 116.0 (d, $J_{CF} = 24.7$ Hz, aromatic), 64.2 (s, CH₂O), 53.5 (s, CHN), 37.1 (s, PhCH₂); ¹⁹F{¹H} – 113.6 (s).

2-Fluoro-*N*-(2-hydroxy-1,1-dimethylethyl)benzamide (3.21). Acid chloride

3.14 (2.67 g, 2.00 mL, 16.9 mmol) was converted to **3.21** (3.40 g, 16.1 mmol, 95%, colorless oil) as described above for **3.18**.

NMR (δ , CDCl₃) ¹H 7.91 (td, $^4J_{HF} = 7.9, ^4J_{HH} = 1.9$ Hz, 1 H, H-6 aromatic), 7.41–7.33 (m, $J = 8.3, 7.3, 5.3, 2.0$ Hz, 1 H, aromatic), 7.15 (td, $J = 7.5, J = 1.1$ Hz, 1 H, aromatic), 7.01 (ddd, $J = 12.1, J = 8.2, J = 0.9$ Hz, 1 H, aromatic), 6.82 (d, $^5J_{HF} = 13.2$ Hz, 1 H, NH), 4.72 (br s, 1 H, OH), 3.58 (br s, 2 H, CH₂O), 1.33 (s, 6 H, 2CH₃); ¹³C{¹H} 163.7 (d, $J_{CF} = 3.3$ Hz, C=O), 160.2 (d, $J_{CF} = 247.0$ Hz, CF), 133.2 (d, $J_{CF} = 9.3$ Hz, aromatic), 131.6 (d, $J_{CF} = 1.7$ Hz, aromatic), 124.7 (d, $J_{CF} = 3.3$ Hz, aromatic), 121.5 (d, $J_{CF} = 11.5$ Hz, aromatic), 115.9 (d, $J_{CF} = 24.7$ Hz, aromatic), 56.4 (s, CH₂), 24.4 (s, 2CH₃); ¹⁹F{¹H} – 113.7 (s).

2-Fluoro-*N*-(2-hydroxy-1,1-dimethylethyl)-3-(trifluoromethyl)benzamide

(3.22). Acid chloride **3.15** (3.59 g, 2.40 mL, 15.8 mmol) was converted to **3.22** (4.00 g, 14.3 mmol, 90%, of colorless oil) as described above for **3.18**.

NMR (δ , CDCl₃) ¹H{¹⁹F} 7.98 (dd, ³J_{HH} = 7.8, ⁴J_{HH} = 1.7 Hz, 1 H, H-6 aromatic), 7.58 (dd, ³J_{HH} = 7.7, ⁴J_{HH} = 1.9 Hz, 1 H, H-4 aromatic), 7.21 (t, ³J_{HH} = 7.7 Hz, 1 H, H-5 aromatic), 6.92 (br s, 1 H, NH), 4.64 (br s, 1 H, OH), 3.53 (d, ³J_{HH} = 4.6 Hz, 2 H, CH₂), 1.31 (s, 6 H, 2CH₃); ¹³C{¹H} 162.6 (d, ³J_{CF} = 2.7 Hz, C=O), 157.4 (dq, ¹J_{CF} = 256.9, ³J_{CF} = 2.2 Hz, C-2 aromatic), 135.5 (quin, ⁴J_{CF} = 1.7 Hz, C-5 aromatic), 130.0 (m, ³J_{CF} = 4.4, ³J_{CF} = 2.2 Hz, C-4 aromatic), 124.6 (d, ³J_{CF} = 4.4 Hz, C-6 aromatic), 124.0 (d, ²J_{CF} = 12.1 Hz, C-1 aromatic), 122.3 (q, ¹J_{CF} = 272.6 Hz, CF₃), 119.8–118.1 (m, C-3 aromatic), 69.9 (s, CH₂), 56.6 (s, C(CH₃)₂), 24.0 (s, 2CH₃); ¹⁹F{¹H} – 61.8 (d, ⁴J_{FF} = 13.4 Hz, CF₃), – 117.2 (q, ⁴J_{FF} = 13.4 Hz, PhF).

2-Fluoro-N-(2-hydroxy-1,1-dimethylethyl)-5-(trifluoromethyl)benzamide

(3.23). Acid chloride **3.16** (1.05 mL, 1.57 g, 6.93 mmol) was converted to **3.23** (1.81 g, 6.48 mmol, 94%) as described above for **3.18**.

NMR (δ , CDCl₃) ¹H 8.15 (m, 1 H, aromatic), 7.53 (m, 1 H, aromatic), 7.39 (m, 1 H, aromatic), 6.86 (d, ⁵J_{HF} = 3.3 Hz, 1 H, NH), 4.25 (t, ³J_{HH} = 5.7, 1 H, OH), 3.70 (d, ³J_{HH} = 5.7 Hz, 2 H, CH₂), 1.43 (s, 6 H, 2CH₃); ¹³C{¹H} 162.3 (d, ³J_{CF} = 3.3 Hz, C=O), 159.8 (d, ¹J_{CF} = 249.2 Hz, CF), 135.5–134.8 (m), 132.9 (d, ³J_{CF} = 2.2 Hz), 125.0 (d, ³J_{CF} = 11.0 Hz), 121.9–121.4 (m, ³J_{CF} = 3.7, ³J_{CF} = 3.7, ³J_{CF} = 3.6, ³J_{CF} = 3.3 Hz, aromatic), 122.7 (qd, ³J_{CF} = 272.3 Hz, ³J_{CF} = 2.7 Hz, CF₃), 114.2–113.4 (m, aromatic), 70.1 (s, CH₂O), 56.8 (s, C(CH₃)₂), 24.5 (s, 2CH₃); ¹⁹F{¹H} – 63.6 (s, 3 F, CF₃), – 111.9 (s, 1 F, PhF).

MS (EI, *m/z*): 248 ([**(3.23)** – OH]⁺, 20%), 191 ([**(2.23)** – NHC(CH₃)₂OH]⁺, 100%), 163 (C₆H₄F(CF₃), 20%).

2-Fluoro-N-(1-hydroxy-2-methylpropan-2-yl)-6-(trifluoromethyl)benzamide

(3.24). Acid chloride **3.17** (0.50 mL, 0.78 g, 3.47 mmol) was converted to **3.24**

(0.87 g, 3.24 mmol, 93%) as described above for **3.18**.

NMR (δ , CDCl₃) ¹H 7.57 (m, 1 H, aromatic), 7.40 (m, 1 H, aromatic), 7.34 (m, 1 H, aromatic), 6.91 (d, ⁵J_{HF} = 3.0 Hz, 1 H, NH), 4.23 (t, ³J_{HH} = 5.5, 1 H, OH), 3.65 (d, ³J_{HH} = 5.5 Hz, 2 H, CH₂), 1.45 (s, 6 H, 2CH₃); ¹³C{¹H} 163.0 (d, ³J_{CF} = 3.2 Hz, C=O), 160.0 (d, ¹J_{CF} = 250.0 Hz, CF), 136.0–135.7 (m), 131.9 (d, J_{CF} = 2.1 Hz), 125.3 (d, J_{CF} = 10.0 Hz), 123.0–122.8 (m, aromatic), 120.7 (qd, J_{CF} = 272.5 Hz, J_{CF} = 3.7 Hz, CF₃), 114.2–113.4 (m, aromatic), 71.1 (s, CH₂O), 56.3 (s, C(CH₃)₂), 23.5 (s, 2CH₃); ¹⁹F{¹H} – 62.7 (s, 3 F, CF₃), – 112.3 (s, 1 F, PhF).

2-(2-Fluorophenyl)-4,5-dihydro-1,3-oxazole (3.25).

To a stirred solution of **3.18** (1.54 g, 8.43 mmol) in CH₂Cl₂ (85 mL), Et₃N (2.56 g, 3.55 mL, 25.3 mmol), TsCl (3.21 g, 16.9 mmol) and DMAP (0.103 g, 0.843 mmol) were added. The resulting solution was stirred at reflux for 16 hours. H₂O (0.5 mL) was added to the reaction mixture and it was refluxed for one more hour. After the reaction mixture cooled down to 25 °C, it was diluted with CH₂Cl₂ (30 mL) and washed with H₂O, a 0.2 M solution of aqueous NaHSO₄, H₂O, a saturated solution of NaHCO₃ and H₂O. The combined organic layers were dried over MgSO₄ and concentrated *in vacuo*. The crude product was purified by flash column chromatography on SiO₂ (2 × 20 cm column; eluted with 9:1 v/v toluene/EtOAc) to obtain the product **3.25** (1.17 g, 7.07 mmol, 84%) as a colorless oil.

NMR (δ , CDCl₃) ¹H 7.85–7.71 (m, 1 H, aromatic), 7.41–7.27 (m, 1 H, aromatic), 7.15–6.94 (m, 2 H, aromatic), 4.39–4.21 (m, 2 H, CH₂O), 4.00 (t, J = 9.3 Hz, 2 H, CH₂N);

$^{13}\text{C}\{^1\text{H}\}$ 161.1 (d, $J_{\text{CF}} = 5.5$ Hz, C=N), 161.0 (d, $J_{\text{CF}} = 258.0$ Hz, CF), 132.6 (d, $J_{\text{CF}} = 8.8$ Hz, aromatic), 130.8 (d, $J_{\text{CF}} = 1.7$ Hz, aromatic), 123.8 (d, $J_{\text{CF}} = 3.8$ Hz, aromatic), 116.5 (d, $J_{\text{CF}} = 22.5$ Hz, aromatic), 115.8 (d, $J_{\text{CF}} = 9.9$ Hz, aromatic), 66.9 (s, CH_2O), 55.0 (s, CH_2N); $^{19}\text{F}\{^1\text{H}\}$ – 110.1 (s).

(4R)-2-(2-fluorophenyl)-4-phenyl-4,5-dihydro-1,3-oxazole (3.26). Benzamide **3.19** (1.50 g, 5.79 mmol) was converted to **3.26** (1.31 g, 5.44 mmol, 94%, colorless oil) as described above for **3.25**.

NMR (δ , CDCl_3) ^1H 7.94–7.78 (m, 1 H, aromatic), 7.40–6.90 (m, 8 H, aromatic), 5.27 (t, $J = 9.1$ Hz, 1 H, aromatic), 4.71–4.52 (m, 2 H, CH_2), 4.09 (t, $J = 8.3$ Hz, 1 H, CHN); $^{13}\text{C}\{^1\text{H}\}$ 161.5 (d, $J_{\text{CF}} = 5.5$ Hz, C=N), 161.2 (d, $J_{\text{CF}} = 258.5$ Hz, CF), 142.2 (s, aromatic), 133.1 (d, $J_{\text{CF}} = 8.8$ Hz, aromatic), 131.3 (d, $J_{\text{CF}} = 1.7$ Hz, aromatic), 128.7 (s, aromatic), 127.6 (s, aromatic), 126.7 (s, aromatic), 124.0 (d, $J_{\text{CF}} = 3.8$ Hz, aromatic), 116.7 (d, $J_{\text{CF}} = 22.0$ Hz, aromatic), 115.9 (d, $J_{\text{CF}} = 10.4$ Hz, aromatic), 74.5 (s, CH_2), 70.1 (s, CHN).

(4S)-4-benzyl-2-(2-fluorophenyl)-4,5-dihydro-1,3-oxazole (3.27). Benzamide **3.20** (2.65 g, 9.70 mmol) was converted to **3.27** (2.26 g, 8.85 mmol, 91%, colorless oil) as described above for **3.25**.

NMR (δ , CDCl_3) ^1H 7.77–7.66 (m, 1 H, aromatic), 7.28–6.89 (m, 8 H, aromatic), 4.52–4.38 (m, 1 H), 4.11 (t, $J = 9.0$ Hz, 1 H), 3.99–3.90 (m, 1 H), 3.10 (dd, $J = 13.7$, $J = 5.0$ Hz, 1 H, PhCHH'), 2.59 (dd, $J = 13.7$, $J = 8.8$ Hz, 1 H, PhCHH'); $^{13}\text{C}\{^1\text{H}\}$ 161.1 (d, $J_{\text{CF}} = 258.0$ Hz, CF), 137.8 (s, aromatic), 132.8 (d, $J_{\text{CF}} = 8.8$ Hz, aromatic), 131.1 (d, $J_{\text{CF}} = 2.2$ Hz, aromatic), 129.3 (s, aromatic), 128.5 (s, aromatic), 128.6 (d, $J_{\text{CF}} = 60.4$ Hz, aromatic), 126.5 (s, aromatic), 123.8 (d, $J_{\text{CF}} = 3.8$ Hz, aromatic), 116.6 (d, $J_{\text{CF}} = 22.0$ Hz, aromatic), 71.3 (s, CH_2O), 68.0 (s, CHN), 41.6 (s, PhCH_2); $^{19}\text{F}\{^1\text{H}\}$ – 109.5 (s).

2-(2-Fluorophenyl)-4,4-dimethyl-4,5-dihydro-1,3-oxazole (3.28). Benzamide **3.21** (1.55 g, 7.34 mmol) was converted to **3.28** (1.10 g, 5.69 mmol, 78%, white foam) as described above for **3.25**.

NMR (δ , CDCl₃) ¹H 7.95–7.81 (m, 1 H, aromatic), 7.50–7.34 (m, 1 H, aromatic), 7.23–7.03 (m, 2 H, aromatic), 4.09 (s, 2 H, CH₂), 1.40 (s, 6 H, 2CH₃); ¹³C{¹H} 160.9 (d, J_{CF} = 256.3 Hz, CF), 158.7 (d, J_{CF} = 4.4 Hz, C=N), 132.6 (d, J_{CF} = 8.8 Hz, aromatic), 131.0 (d, J_{CF} = 1.7 Hz, aromatic), 123.7 (d, J_{CF} = 2.2 Hz, aromatic), 116.4 (d, J_{CF} = 22.0 Hz, aromatic), 78.6 (s, CH₂), 67.6 (s, C(CH₃)₂), 28.2 (s, 2CH₃); ¹⁹F{¹H} – 110.0 (s).

2-[2-Fluoro-3-(trifluoromethyl)phenyl]-4,4-dimethyl-4,5-dihydro-1,3-oxazole (3.29). Benzamide **3.22** (3.98 g, 14.2 mmol) was converted to **3.29** (3.00 g, 11.5 mmol, 81%, colorless oil) as described above for **3.25**.

NMR (δ , CDCl₃) ¹H 7.97 (m, 1 H, H-6 aromatic), 7.60 (m, 1 H, H-4 aromatic), 7.18 (m, 1 H, H-5 aromatic), 4.03 (s, 2 H, CH₂), 1.31 (s, 6 H, 2CH₃); ¹³C{¹H} 157.9 (d, $^3J_{CF}$ = 4.9 Hz, C=N), 158.5 (dq, $^1J_{CF}$ = 267.9, $^3J_{CF}$ = 2.2 Hz, C-2 aromatic), 135.1 (dq, $^4J_{CF}$ = 2.2, $^3J_{CF}$ = 1.1 Hz, C-5 aromatic), 129.9–129.4 (m, C-4 aromatic), 123.9 (d, $^3J_{CF}$ = 4.9 Hz, C-6 aromatic), 122.5 (q, $^1J_{CF}$ = 272.4 Hz, CF₃), 118.8–120.5 (m, C-3 aromatic), 118.2 (d, $^2J_{CF}$ = 10.4 Hz, C-1 aromatic), 79.1 (s, CH₂), 68.2 (s, C(CH₃)₂), 28.3 (s, 2CH₃); ¹⁹F{¹H} – 62.1 (d, $^4J_{FF}$ = 13.4 Hz, CF₃), – 111.8 (q, $^4J_{FF}$ = 13.4 Hz, PhF).

2-[2-Fluoro-5-(trifluoromethyl)phenyl]-4,4-dimethyl-4,5-dihydro-1,3-oxazole (3.30). Benzamide **3.23** (0.940 g, 3.37 mmol) was converted to **3.30** (0.723 g, 2.77 mmol, 82%) as described above for **3.25**.

NMR (δ , CDCl₃) ¹H 8.02 (m, 1 H, aromatic), 7.50–7.35 (m, 2 H, aromatic), 4.14 (s, 2 H, CH₂), 1.42 (s, 6 H, 2CH₃); ¹³C{¹H} 162.8 (d, $^1J_{CF}$ = 264.6 Hz, CF), 157.7 (d, $^3J_{CF}$ = 5.5 Hz,

C=N), 129.9–129.6 (m), 129.0 (quin, $J_{CF} = 3.6$ Hz), 127.1–126.5 (m, aromatic), 123.4 (q, $^1J_{CF} = 272.2$ Hz, CF_3), 117.5 (d, $J_{CF} = 23.6$ Hz), 117.3 (d, $J_{CF} = 11.5$ Hz, aromatic), 79.1 (s, CH_2O), 68.2 (s, $C(CH_3)_2$), 28.3 (s, $2CH_3$); $^{19}F\{^1H\} - 63.9$ (s, 3 F, CF_3), $- 107.3$ (s, 1 F, PhF).

MS (EI, m/z): 261 ($[(3.30)]^+$, 5%), 246 ($[(3.30) - CH_3]^+$, 70%), 191 ($[(3.30) - NC(CH_3)_2CH_2]^+$, 100%).

2-(2-fluoro-6-(trifluoromethyl)phenyl)-4,4-dimethyl-4,5-dihydrooxazole

(3.31). Benzamide **3.24** (1.034 g, 3.71 mmol) was converted to **3.31** (0.776 g, 2.97 mmol, 80%) as described above for **3.25**.

NMR (δ , $CDCl_3$) 1H 7.53–7.35 (m, 3 H, aromatic), 4.17 (s, 2 H, CH_2), 1.39 (s, 6 H, $2CH_3$); $^{13}C\{^1H\}$ 161.0 (d, $^1J_{CF} = 263.2$ Hz, CF), 157.8 (d, $^3J_{CF} = 5.4$ Hz, $C=N$), 130.0–129.5 (m), 128.1 (quin, $J_{CF} = 3.7$ Hz), 127.4–126.7 (m, aromatic), 123.3 (q, $^1J_{CF} = 270.2$ Hz, CF_3), 118.5 (d, $J_{CF} = 26.3$ Hz), 117.8 (d, $J_{CF} = 12.5$ Hz, aromatic), 78.8 (s, CH_2O), 68.0 (s, $C(CH_3)_2$), 28.2 (s, $2CH_3$); $^{19}F\{^1H\} - 63.3$ (s, 3 F, CF_3), $- 109.1$ (s, 1 F, PhF).

2-[2-(Diphenylphosphino)phenyl]-4,5-dihydro-1,3-oxazole (3.1). A Schlenk flask was charged with the aryl fluoride **3.25** (1.17 g, 7.07 mmol) and THF (15 mL). $KPPH_2$ (0.5 M in THF, 14.9 mL, 7.43 mmol) was added dropwise with stirring. The resulting reddish solution was refluxed for 2 hours. The reaction mixture was diluted with CH_2Cl_2 (200 mL) and poured into a saturated aqueous solution of $NaHCO_3$ (150 mL). The organic layer was separated, washed with H_2O and dried over $MgSO_4$. The solution was concentrated *in vacuo* and the crude product purified by flash column chromatography on SiO_2 (2×35 cm column; eluted with 1:0 v/v

toluene/EtOAc → 9:1 v/v toluene/EtOAc) to obtain **3.1** (1.90 g, 5.73 mmol, 81%) as a white solid.

NMR (δ , CDCl₃) ¹H 7.71–7.59 (m, 1 H, aromatic), 7.21–6.95 (m, 12 H, aromatic), 6.77–6.64 (m, 1 H, aromatic), 3.87–3.72 (m, 2 H, CH₂O), 3.59–3.45 (m, 2 H, CH₂N); ¹³C{¹H} 164.1 (d, J_{CP} = 2.7 Hz, C=N), 138.8 (d, J_{CP} = 25.3 Hz, aromatic), 137.8 (d, J_{CP} = 11.5 Hz, aromatic), 134.0 (s, aromatic), 133.7 (s, aromatic), 133.5 (d, J_{CP} = 2.2 Hz, aromatic), 131.7 (d, J_{CP} = 19.2 Hz, aromatic), 130.2 (s, aromatic), 129.6 (d, J_{CP} = 3.3 Hz, aromatic), 128.4 (s, aromatic), 128.3 (s, aromatic), 128.2 (s, aromatic), 127.8 (s, aromatic), 66.9 (s, CH₂O), 54.7 (s, CH₂N); ³¹P{¹H} – 4.6 (s).

(4R)-2-[2-(diphenylphosphino)phenyl]-4-phenyl-4,5-dihydro-1,3-oxazole

(3.2). Compound **3.26** (1.00 g, 4.14 mmol) was converted to **3.2** (1.27 g, 3.11 mmol, 75%, white solid) as described above for **3.1**.

NMR (δ , CDCl₃) ¹H 8.19–8.07 (m, 1 H, aromatic), 7.53–7.21 (m, 16 H, aromatic), 7.11–6.97 (m, 2 H, aromatic), 5.3 (t, J = 9.6 Hz, 1 H), 4.6 (dd, J = 10.1, J = 8.2 Hz, 1 H), 4.04 (dd, J = 9.0, J = 8.3 Hz, 1 H); ¹³C{¹H}; 164.4 (d, J_{CP} = 2.7 Hz, C=N), 141.8 (s, aromatic), 139.2 (s, aromatic), 137.9 (d, J_{CP} = 12.6 Hz, aromatic), 137.7 (d, J_{CP} = 9.9 Hz, aromatic), 134.3 (s, aromatic), 134.0 (s, aromatic), 133.8 (s, aromatic), 133.7 (s, aromatic), 133.6 (s, aromatic), 131.3 (d, J_{CP} = 19.2 Hz, aromatic), 130.5 (s, aromatic), 130.1 (d, J_{CP} = 2.7 Hz, aromatic), 128.8 (d, aromatic), 128.5 (s, aromatic), 128.4 (s, aromatic), 128.3 (d, J_{CP} = 2.2 Hz, aromatic), 128.2 (d, aromatic), 128.0 (s, aromatic), 127.9 (s, aromatic), 126.9 (s, aromatic), 126.4 (s, aromatic), 125.1 (s, aromatic), 74.1 (s, CH₂), 69.9 (s, CHN); ³¹P{¹H} – 4.8.

(4S)-4-benzyl-2-[2-(diphenylphosphino)phenyl]-4,5-dihydro-1,3-oxazole

(3.3). Compound **3.27** (1.99 g, 7.81 mmol) was converted to **3.3** (2.30 g, 5.46 mmol, 70%, white foam) as described above for **3.1**.

NMR (δ , CDCl₃) ¹H 7.70 (dd, $J = 7.1, J = 3.1$ Hz, 1 H, aromatic), 7.26–6.80 (m, 17 H, aromatic), 6.73 (dd, $J = 7.5, J = 4.1$ Hz, 1 H, aromatic), 4.27–4.06 (m, 1 H), 3.80 (t, $J = 8.9$ Hz, 1 H), 3.56 (t, $J = 7.9$ Hz, 1 H), 2.72 (dd, $J = 13.9, J = 5.2$ Hz, 1 H, PhCHH'), 1.96 (dd, $J = 13.9, J = 9.0$ Hz, 1 H, PhCHH'); ¹³C{¹H} 163.4 (d, $J_{CP} = 3.3$ Hz, C=N), 138.8 (d, $J_{CP} = 25.8$ Hz, aromatic), 137.9–138.0 (m, aromatic), 137.8 (d, $J_{CP} = 2.2$ Hz, aromatic), 134.3 (s, aromatic), 134.0 (s, aromatic), 133.8 (s, aromatic), 133.5 (s, aromatic), 133.4 (d, $J_{CP} = 2.2$ Hz, aromatic), 131.4 (d, $J_{CP} = 18.7$ Hz, aromatic), 130.3 (s, aromatic), 129.7 (d, $J_{CP} = 2.7$ Hz, aromatic), 128.9 (s, aromatic), 128.8 (s, aromatic), 128.5 (s, aromatic), 128.3 (s, aromatic), 128.24 (d, $J_{CP} = 1.7$ Hz, aromatic), 128.20 (s, aromatic), 128.16 (s, aromatic), 128.0 (s, aromatic), 127.7 (s, aromatic), 126.1 (s, aromatic), 71.2 (s, CH₂), 67.8 (s, CHN), 40.9 (s, PhCH₂); ³¹P{¹H} – 4.2 (s).

2-[2-(Diphenylphosphino)phenyl]-4,4-dimethyl-4,5-dihydro-1,3-oxazole (3.4).

Compound **3.28** (0.510 g, 2.64 mmol) was converted to **3.4** (0.790 g, 2.20 mmol, 83%, white solid) as described above for **3.1**.

NMR (δ , CDCl₃) ¹H 8.01–7.93 (m, 1 H, aromatic), 7.49–7.15 (m, 12 H, aromatic), 6.99–6.90 (m, 1 H, aromatic), 3.80 (s, 2 H, CH₂), 1.14 (s, 6 H, 2CH₃); ¹³C{¹H} 161.7 (d, $J_{CP} = 2.2$ Hz, C=N), 138.3 (d, $J_{CP} = 25.2$ Hz, aromatic), 137.6 (d, $J_{CP} = 11.5$ Hz, aromatic), 133.7 (d, $J_{CP} = 20.9$ Hz, aromatic), 133.4 (d, $J_{CP} = 17.0$ Hz, aromatic), 131.5 (d, $J_{CP} = 18.1$ Hz, aromatic), 129.9 (s, aromatic), 129.5 (d, $J_{CP} = 2.7$ Hz, aromatic),

128.2 (s, aromatic), 128.0 (d, $J_{CP} = 7.7$ Hz, aromatic), 127.4 (s, aromatic), 78.2 (s, CH_2), 67.2 (s, $C(CH_3)_2$), 27.5 (s, 2 CH_3); $^{31}P\{^1H\} - 4.0$ (s).

2-[2-(diphenylphosphino)-3-(trifluoromethyl)phenyl]-4,4-dimethyl-4,5-dihydro-1,3-oxazole (3.7). Aryl fluoride **3.29** (1.562 g, 5.98 mmol) was converted and worked up as described above for **3.1** to obtain **3.7** (2.07g, 4.84mmol, 81%) as slightly yellowish crystals. Anal. Calc. for $C_{24}H_{21}F_3NOP$: C, 67.44; H, 4.95. Found: C, 67.42; H, 5.02%.

NMR (δ , $CDCl_3$) 1H 7.85–7.98 (m, 2 H, H-4, H-6 aromatic), 7.57 (t, $^3J_{HH} = 7.8$ Hz, 1 H, H-5 aromatic), 7.24–7.39 (m, 10 H, $P(C_6H_5)_2$), 3.46 (s, 2 H, CH_2O), 1.01 (s, 6 H, 2 CH_3); $^{13}C\{^1H\}$ 163.1 (d, $^3J_{CP} = 2.2$ Hz, $C=N$), 137.6 (d, $J = 8.8$ Hz, aromatic), 137.6–136.1 (m, C-3 aromatic), 135.6 (s, aromatic), 135.3 (dd, $J = 13.5$, $J = 1.4$ Hz, aromatic), 135.2 (d, $J = 41.7$ Hz, aromatic), 132.6 (d, $J = 20.3$ Hz, aromatic), 129.5 (s, C-6 aromatic), 129.4–129.0 (m, aromatic), 128.04 (d, $J = 6.6$ Hz, aromatic), 128.03 (s, aromatic), 123.8 (q, $^1J_{CF} = 275.5$ Hz, CF_3), 78.3 (s, CH_2O), 67.1 (s, $C(CH_3)_2$), 27.8 (s, $C(CH_3)_2$); $^{31}P\{^1H\}$ 0.6 (q, $^4J_{PF} = 46.4$ Hz); $^{19}F\{^1H\} - 55.7$ (d, $^4J_{FP} = 46.4$ Hz, CF_3).

MS (FAB, 3-NBA, m/z) 466 ($[3.7+O+Na]^+$, 100%), 450 ($[3.7+Na]^+$, 19%); IR (cm^{-1} , neat) $\nu_{C=N}$ 1644 (s).

2-[5-Trifluoromethyl-2-(diphenylphosphino)phenyl]-4,4-dimethyl-4,5-dihydro-1,3-oxazole (3.8). Aryl fluoride **3.30** (0.467 g, 1.79 mmol) was converted and worked up as described above for **3.1** to obtain **3.8** (0.659 g, 1.54 mmol, 86%) as a white solid.

NMR (δ , $CDCl_3$) 1H 8.19–8.09 (m, 1 H, aromatic), 7.49 (d, $^3J_{HH} = 7.9$ Hz, 1 H, aromatic), 7.41–7.25 (m, 10 H, aromatic), 6.95 (dd, $^3J_{HH} = 8.0$, $J_{PH} = 3.7$ Hz, 1 H, aromatic), 3.75

(s, 2 H, CH_2), 1.05 (s, 6 H, $2CH_3$); $^{13}C\{^1H\}$ 161.1 (d, $^3J_{CP} = 3.3$ Hz, $C=N$), 144.2 (d, $J = 30.2$ Hz, aromatic), 136.9 (d, $J = 11.0$ Hz, aromatic), 134.2 (d, $J = 22.0$ Hz, aromatic), 133.8 (d, $J = 3.8$ Hz, aromatic), 132.3 (d, $J = 17.0$ Hz, aromatic), 130.0 (d, $J = 32.4$ Hz, aromatic), 129.1 (s, aromatic), 128.7 (d, $J = 7.7$ Hz, aromatic), 126.9–126.4 (m, aromatic), 123.8 (q, $^1J_{CF} = 272.2$ Hz, CF_3), 79.0 (s, CH_2O), 67.9 (s, $C(CH_3)_2$), 27.9 (s, CH_3); $^{19}F\{^1H\} - 63.5$ (d, $^6J_{FP} = 2.1$ Hz, CF_3); $^{31}P\{^1H\} - 3.1$ (s).

HRMS calcd for $C_{24}H_{22}F_3NOP$ 428.1391, found 428.1375; IR (cm^{-1} , neat solid) $\nu_{C=N}$ 1655 (m).

2-(2-(diphenylphosphino)-6-(trifluoromethyl)phenyl)-4,4-dimethyl-4,5-dihydrooxazole (3.9). Aryl fluoride **3.31** (0.560 g, 2.15 mmol) was converted and worked up as described above for **3.1** to obtain **3.9** (0.763 g, 1.78 mmol, 83%) as a white solid.

NMR (δ , $CDCl_3$) 1H 7.51 (d, $^3J_{HH} = 7.5$ Hz, 1 H, aromatic), 7.44–7.26 (m, 11 H, aromatic), 6.96 (dd, $^3J_{HH} = 8.1$, $J_{PH} = 3.6$ Hz, 1 H, aromatic), 3.77 (s, 2 H, CH_2), 1.00 (s, 6 H, $2CH_3$); $^{13}C\{^1H\}$ 162.1 (d, $^3J_{CP} = 3.3$ Hz, $C=N$), 144.3 (d, $J = 30.0$ Hz, aromatic), 137.2 (d, $J = 11.6$ Hz, aromatic), 135.1 (d, $J = 21.8$ Hz, aromatic), 131.7 (d, $J = 3.5$ Hz, aromatic), 130.6 (d, $J = 16.2$ Hz, aromatic), 129.4 (d, $J = 31.3$ Hz, aromatic), 129.1 (s, aromatic), 128.3 (d, $J = 7.5$ Hz, aromatic), 126.8–126.5 (m, aromatic), 124.4 (q, $^1J_{CF} = 270.5$ Hz, CF_3), 79.2 (s, CH_2O), 67.5 (s, $C(CH_3)_2$), 28.2 (s, CH_3); $^{19}F\{^1H\} - 64.6$ (d, $^6J_{FP} = 2.1$ Hz, CF_3); $^{31}P\{^1H\} - 2.5$ (s).

5-Bromo-2-fluorobenzoic acid (3.34). To a stirred solution of 2-fluorobenzoic acid **3.32** (2.00 g, 14.3 mmol) and $NaBrO_3$ (2.15 g, 14.3 mmol) in H_2O (10 mL), concentrated H_2SO_4 (3.7 mL) was added dropwise at 90 °C. The reaction mixture

was stirred at 90 °C for 1 hour, cooled down to 25 °C and diluted with H₂O (100 mL).

A precipitate formed which was separated by filtration and dried to obtain **3.34**

(1.10 g, 4.42 mmol, 88%) as white powder.

NMR (δ , CDCl₃) ¹H 10.01 (br s, 1 H, COOH), 8.11 (dd, ⁴J_{HF} = 6.4, ⁴J_{HH} = 2.6 Hz, 1 H, H-6 aromatic), 7.73–7.61 (m, 1 H, H-4 aromatic), 7.09 (dd, ³J_{HF} = 10.2, ³J_{HH} = 8.9 Hz, 1 H, H-3 aromatic); ¹³C{¹H} 164.1 (d, ³J_{CF} = 3.8 Hz, C=O), 160.8 (d, ¹J_{CF} = 261.3 Hz, CF), 137.0 (d, ³J_{CF} = 8.8 Hz, C-4 aromatic), 134.6 (d, ³J_{CF} = 1.1 Hz, C-6 aromatic), 120.0 (d, ¹J_{CF} = 11.0 Hz, aromatic), 118.5 (d, ¹J_{CF} = 24.2 Hz, aromatic), 115.9 (d, ¹J_{CF} = 3.8 Hz, aromatic); ¹⁹F{¹H} – 106.7 (s).

Typical procedure for preparation of acid chloride (3.33). To a stirred suspension of the carboxylic acid **3.34** in CH₂Cl₂, a catalytic amount of DMF (0.05 eq) was added. The reaction mixture was cooled to 0 °C (ice bath) and (COCl)₂ (1.5 eq) was added dropwisely. The resulting solution was stirred at 0 °C for 30 min and for 2 hours at 25 °C. The solvent was removed from the reaction mixture. The residue was dried in high vacuum and was dissolved in CH₂Cl₂ (3 mL/mmol) and used for preparation of the benzamide without further purification.

5-Bromo-2-fluoro-N-(2-hydroxy-1,1-dimethylethyl)benzamide (3.35). Acid **3.34** (1.19 g, 5.43 mmol) was converted to **3.35** (1.35 g, 4.65 mmol, 86% for two steps, colorless oil) as described above for **3.18**.

NMR (δ , CDCl₃) ¹H 7.87 (dd, ⁴J_{HF} = 6.8, ⁴J_{HH} = 2.6 Hz, 1 H, H-6 aromatic), 7.39 (ddd, ³J_{HH} = 8.8, ⁴J_{HF} = 4.4, ⁴J_{HH} = 2.8 Hz, 1 H, H-4 aromatic), 7.10–6.97 (m, 1 H, NH), 6.88 (dd, ³J_{HF} = 10.9, ³J_{HH} = 8.9 Hz, 1 H, H-3 aromatic), 4.85 (br s, 1 H, OH), 3.54 (d, ³J_{HH} = 4.3 Hz, 2 H, CH₂), 1.33 (s, 6 H, 2CH₃); ¹³C{¹H} 162.0 (d, ³J_{CF} = 3.3 Hz, C=O), 158.7 (d,

$^1J_{CF} = 248.1$ Hz, CF), 135.3 (d, $^3J_{CF} = 9.3$ Hz, C-4 aromatic), 133.5 (d, $^3J_{CF} = 2.2$ Hz, C-6 aromatic), 123.5 (d, $^2J_{CF} = 13.7$ Hz, C-1 aromatic), 117.6 (d, $^2J_{CF} = 26.4$ Hz, C-3 aromatic), 116.9 (d, $^4J_{CF} = 2.7$ Hz, C-5 aromatic), 69.3 (s, CH₂), 55.9 (s, C(CH₃)₂), 23.6 (s, 2CH₃); $^{19}F\{^1H\} - 115.9$ (s).

2-(5-Bromo-2-fluorophenyl)-4,4-dimethyl-4,5-dihydro-1,3-oxazole (3.36).

Benzamide **3.35** (0.935 g, 3.22 mmol) was converted to **3.36** (0.715 g, 2.63 mmol, 82%, colorless oil) as described above for **3.25**.

NMR (δ , CDCl₃) 1H 7.89 (dd, $^4J_{HF} = 6.4$, $^4J_{HH} = 2.6$ Hz, 1 H, H-6 aromatic), 7.39 (ddd, $^3J_{HH} = 8.7$, $^4J_{HF} = 4.2$, $^4J_{HH} = 2.7$ Hz, 1 H, H-4 aromatic), 6.90 (dd, $^3J_{HF} = 10.1$, $^3J_{HH} = 9.0$ Hz, 1 H, H-3 aromatic), 3.98 (s, 2 H, CH₂), 1.27 (s, 6 H, 2CH₃); $^{13}C\{^1H\}$ 159.9 (d, $^1J_{HF} = 258.5$ Hz, CF), 157.5 (d, $^3J_{CF} = 5.5$ Hz, C=N), 135.2 (d, $^3J_{CF} = 8.8$ Hz, C-4 aromatic), 133.5 (d, $^3J_{CF} = 2.2$ Hz, C-6 aromatic), 118.3 (d, $^2J_{CF} = 23.6$ Hz, C-3 aromatic), 116.2 (d, $^4J_{CF} = 3.8$ Hz, CBr), 78.8 (s, CH₂), 67.7 (s, C(CH₃)₂), 28.1 (s, 2CH₃); $^{19}F\{^1H\} - 111.7$ (s).

2-[5-bromo-2-(diphenylphosphino)phenyl]-4,4-dimethyl-4,5-dihydro-1,3-oxazole (3.5).

A Schlenk flask was charged with the aryl fluoride **3.36** (0.552 g, 2.029 mmol) and KPPPh₂ (0.5 M in THF, 4.5 mL, 2.3 mmol) was added dropwisely with stirring. The resulting reddish solution was refluxed for 1 h. The reaction mixture was diluted with CH₂Cl₂ (50 mL) and poured into a saturated aqueous solution of NaHCO₃ (25 mL). The organic layer was separated, washed with H₂O and dried over MgSO₄. The solution was concentrated *in vacuo* and the crude product purified by flash column chromatography on SiO₂ (1 × 15 cm column; eluted with 1:0 v/v toluene/EtOAc → 7:3 v/v toluene/EtOAc) to obtain the product (0.540 g, 1.23 mmol, 61%) as an oil which solidified over the course of several weeks to give a

white solid. Anal. Calc. for $C_{23}H_{21}BrNOP$: C, 63.03; H, 4.83. Found: C, 62.75; H, 4.86%.

NMR (δ , $CDCl_3$) 1H 8.02 (t, $^4J_{HH} = 2.6$ Hz, 1 H, H-6 aromatic), 7.38 (dd, $^3J_{HH} = 8.4$, $^4J_{HH} = 2.2$ Hz, 1 H, H-4 aromatic), 7.29–7.34 (m, 10 H, $P(C_6H_5)_2$), 6.67 (dd, $^3J_{HH} = 8.3$, $^3J_{HP} = 4.0$ Hz, 1 H, H-3 aromatic), 3.74 (s, 2 H, CH_2O), 1.04 (s, 6 H, $2CH_3$); $^{13}C\{^1H\}$ 161.1 (d, $^3J_{CP} = 2.7$ Hz, $C=N$), 138.0 (d, $J_{CP} = 26.9$ Hz, aromatic), 137.2 (d, $J_{CP} = 11.0$ Hz, aromatic), 134.9 (d, $J_{CP} = 2.7$ Hz, aromatic), 134.1 (d, $J_{CP} = 21.4$ Hz, aromatic), 133.4 (d, $J_{CP} = 18.1$ Hz, aromatic), 133.3 (s, aromatic), 132.8 (d, $J_{CP} = 2.2$ Hz, aromatic), 128.9 (s, aromatic), 128.6 (d, $J_{CP} = 7.7$ Hz, aromatic), 122.3 (d, $J_{CP} = 1.1$ Hz, aromatic), 78.9 (s, CH_2O), 67.7 (s, $C(CH_3)_2$), 27.9 (s, $2CH_3$); $^{31}P\{^1H\} - 4.7$ (s).

MS (FAB, 3-NBA, m/z) 476 ($[3.5+O+Na]^+$, 100%), 454 ($[3.5+O]^+$, 7%); IR (cm^{-1} , neat) $\nu_{C=N}$ 1643 (s).

2-Fluoro-N-(2-hydroxy-1,1-dimethylethyl)-5-nitrobenzamide (3.39).

Compound **3.37** (1.00 g, 5.40 mmol) was converted to nitrobenzamide **3.39** (1.28 g, 5.01 mmol, 93% for two steps, slightly yellowish oil) as described above for **3.18** and **3.33**.

NMR (δ , $CDCl_3$) 1H 8.65 (dd, $^4J_{HF} = 6.2$, $^4J_{HH} = 2.8$ Hz, 1 H, H-6 aromatic), 8.33–8.23 (m, 1 H, H-4 aromatic), 7.33 (t, $^3J_{HF} = ^3J_{HH} = 9.6$ Hz, 1 H, H-3 aromatic), 7.19 (d, $^5J_{HF} = 9.6$ Hz, 1 H, NH), 4.72 (br s, 1 H, OH), 3.63 (s, 2 H, CH_2), 1.41 (s, 6 H, $2CH_3$); $^{13}C\{^1H\}$ 163.2 (d, $^1J_{CF} = 252.5$ Hz, CF), 161.5 (d, $^3J_{CF} = 3.3$ Hz, $C=O$), 144.4 (d, $^4J_{CF} = 2.7$ Hz, C-5 aromatic), 128.2 (d, $^3J_{CF} = 11.0$ Hz, C-4 aromatic), 127.3 (d, $^3J_{CF} = 4.4$ Hz, C-6 aromatic), 123.9 (d, $^2J_{CF} = 15.4$ Hz, C-1 aromatic), 117.8 (d, $^2J_{CF} = 27.4$ Hz, C-3 aromatic), 69.5 (s, CH_2), 56.6 (s, $C(CH_3)_2$), 23.8 (s, $2CH_3$); $^{19}F\{^1H\} - 103.9$ (s).

2-(2-Fluoro-5-nitrophenyl)-4,4-dimethyl-4,5-dihydro-1,3-oxazole (3.40).

Nitrobenzamide **3.39** (1.95 g, 7.61 mmol) was converted to **3.40** (1.50 g, 6.30 mmol, 81%, slightly yellowish crystals) as described above for **3.25**.

NMR (δ , CDCl₃) ¹H 8.70 (dd, ⁴J_{HF} = 6.1, ⁴J_{HH} = 2.9 Hz, 1 H, H-6 aromatic), 8.25 (ddd, ³J_{HH} = 9.1, ⁴J_{HF} = 4.0, ⁴J_{HH} = 2.9 Hz, 1 H, H-4 aromatic), 7.24 (t, ³J_{HF} = ³J_{HH} = 9.3 Hz, 1 H, H-3 aromatic), 4.07 (s, 2 H, CH₂), 1.34 (s, 6 H, 2CH₃); ¹³C{¹H} 164.0 (d, ¹J_{CF} = 269.5 Hz, CF), 156.6 (d, ³J_{CF} = 6.0 Hz, C=N), 143.6 (d, ⁴J_{CF} = 3.3 Hz, CNO₂), 127.7 (d, ³J_{CF} = 10.4 Hz, C-4 aromatic), 127.0 (d, ³J_{CF} = 3.8 Hz, C-6 aromatic), 117.8 (d, ²J_{CF} = 24.7 Hz, C-3 aromatic), 117.6 (d, ²J_{CF} = 12.6 Hz, C-1 aromatic), 78.9 (s, CH₂), 68.2 (s, C(CH₃)₂), 28.1 (s, 2CH₃); ¹⁹F{¹H} – 98.6 (s).

3-(4,4-Dimethyl-4,5-dihydro-1,3-oxazol-2-yl)-4-fluoroaniline (3.41). To a stirred solution of **3.40** (0.647 g, 2.72 mmol) in EtOAc (20 mL), Pd/C (0.200 g, 5% Pd) was added. The reaction mixture was stirred overnight under an atmosphere of H₂. The reaction mixture was filtered through Celite®, and the filtrate concentrated *in vacuo* and dried in high vacuum to obtain the product **3.41** (0.550 g, 2.64 mmol, 97%) as a slightly brownish oil.

NMR (δ , CDCl₃) ¹H 7.01 (dd, ⁴J_{HF} = 5.8, ⁴J_{HH} = 3.0 Hz, 1 H, H-2 aromatic), 6.75 (dd, ³J_{HF} = 10.5, ³J_{HH} = 8.8 Hz, 1 H, H-5 aromatic), 6.55 (ddd, ³J_{HH} = 8.7, ⁴J_{HF} = 3.9, ⁴J_{HH} = 3.0 Hz, 1 H, H-6 aromatic), 3.93 (s, 2 H, CH₂), 3.74 (br s, 2 H, NH₂), 1.23 (s, 6 H, 2CH₃); ¹³C{¹H} 158.6 (d, ³J_{CF} = 4.9 Hz, C=N), 153.5 (d, ¹J_{CF} = 246.5 Hz, CF), 142.3 (d, ⁴J_{CF} = 2.2 Hz, CNH₂), 118.3 (d, ³J_{CF} = 7.7 Hz, C-6 aromatic), 116.3 (d, ²J_{CF} = 23.1 Hz, C-5 aromatic), 115.5 (d, ³J_{CF} = 1.7 Hz, C-2 aromatic), 115.4 (d, ²J_{CF} = 11.5 Hz, C-3 aromatic), 78.0 (s, CH₂), 66.9 (s, C(CH₃)₂), 27.6 (s, 2CH₃); ¹⁹F{¹H} – 124.6 (s).

3-(4,4-Dimethyl-4,5-dihydro-1,3-oxazol-2-yl)-4-fluoro-N,N-dimethylaniline

(3.42). To a stirred solution of **3.41** (0.64 g, 3.1 mmol) in CH₃CN (6 mL), potassium carbonate (1.3 g, 9.2 mmol) and (CH₃)₂SO₄ (0.42 g, 0.32 mL, 3.4 mmol) were added. The reaction mixture was stirred overnight. It was then diluted with CH₂Cl₂ (40 mL) and washed with saturated aqueous NaHCO₃ and H₂O. The organic layer was dried over MgSO₄ and concentrated *in vacuo*. The crude product was purified by flash column chromatography on SiO₂ (1 × 10 cm column; eluted with 1:0 v/v toluene/EtOAc → 7:3 v/v toluene/EtOAc) to obtain the product **3.42** (0.36 g, 1.5 mmol, 50%) as colorless oil.

NMR (δ, CDCl₃) ¹H 7.14 (dd, ⁴J_{HF} = 5.8, ⁴J_{HH} = 3.3 Hz, 1 H, H-2 aromatic), 7.00 (dd, ³J_{HF} = 10.3, ³J_{HH} = 9.1 Hz, 1 H, H-5 aromatic), 6.76 (dt, ⁴J_{HF} = ³J_{HH} = 9.1, ⁴J_{HH} = 3.6 Hz, 1 H, H-6 aromatic), 4.08 (s, 2 H, CH₂), 2.92 (s, 6 H, N(CH₃)₂), 1.39 (s, 6 H, C(CH₃)₂); ¹³C{¹H} 159.6 (d, ³J_{CF} = 4.9 Hz, C=N), 153.7 (d, ¹J_{CF} = 247.0 Hz, CF), 147.0 (d, ⁴J_{CF} = 2.2 Hz, CN(CH₃)₂), 116.9 (d, ²J_{CF} = 11.5 Hz, C-5 aromatic), 116.7 (d, ³J_{CF} = 3.8 Hz, C-6 aromatic), 116.0 (d, ²J_{CF} = 11.5 Hz, C-3 aromatic), 113.9 (d, ³J_{CF} = 1.1 Hz, C-2 aromatic), 78.7 (s, CH₂), 67.7 (s, C(CH₃)₂), 41.1 (s, N(CH₃)₂), 28.4 (s, C(CH₃)₂); ¹⁹F{¹H} – 126.5 (s).

3-(4,4-dimethyl-4,5-dihydro-1,3-oxazol-2-yl)-4-(diphenylphosphino)-N,N-

dimethylaniline (3.6). Aryl fluoride **3.42** (0.122 g, 0.515 mmol) was converted as described above for **3.1** to obtain **3.6** (0.162 g, 0.403 mmol, 78%) as white powder.

Anal. Calc. for C₂₅H₂₇N₂OP: C, 74.61; H, 6.76. Found: C, 74.56; H, 6.75%.

NMR (δ, CDCl₃) ¹H 7.24–7.38 (m, 10 H, P(C₆H₅)₂), 7.18 (t, ⁴J_{HH} = 2.9 Hz, 1 H, H-2 aromatic), 6.69 (dd, ³J_{HH} = 8.7, ³J_{HP} = 4.3 Hz, 1 H, H-5 aromatic), 6.59 (dd, ³J_{HH} = 8.7,

$^4J_{\text{HH}} = 2.8$ Hz, 1 H, H-6 aromatic), 3.78 (s, 2 H, CH_2O), 2.93 (s, 6 H, $\text{N}(\text{CH}_3)_2$), 1.11 (s, 6 H, 2CH_3); $^{13}\text{C}\{^1\text{H}\}$ 163.2 (d, $^3J_{\text{CP}} = 1.7$ Hz, $\text{C}=\text{N}$), 149.9 (s, aromatic), 139.0 (d, $J_{\text{CP}} = 12.1$ Hz, aromatic), 134.7 (d, $J_{\text{CP}} = 1.7$ Hz, aromatic), 133.8 (d, $J_{\text{CP}} = 20.3$ Hz, aromatic), 133.4 (d, $J_{\text{CP}} = 22.0$ Hz, aromatic), 128.2 (d, $J_{\text{CP}} = 5.4$ Hz, aromatic), 128.1 (s, aromatic), 122.6 (d, $J_{\text{CP}} = 18.1$ Hz, aromatic), 114.0 (s, aromatic), 113.5 (d, $J_{\text{CP}} = 4.4$ Hz, aromatic), 78.7 (s, CH_2O), 67.5 (s, $\text{C}(\text{CH}_3)_2$), 40.1 (s, $\text{N}(\text{CH}_3)_2$), 28.0 (s, $\text{C}(\text{CH}_3)_2$); $^{31}\text{P}\{^1\text{H}\} - 6.8$ (s).
MS (FAB, 3-NBA, m/z) 425 ($[\mathbf{3.6}+\text{Na}]^+$, 68%), 441 ($[\mathbf{3.6}+\text{O}+\text{Na}]^+$, 48%); IR (cm^{-1} , neat) $\nu_{\text{C}=\text{N}}$ 1598 (s).

Chapter IV

Investigation of New Non-Heme Complexes for Iron Catalyzed Oxidation Reactions

4.1. Aim of the chapter

A series of new non-heme type multidentate ligands containing an oxygen donor became a target of interest. The presence of a labile coordinating atom in a chelating ligand could lead to an easier access to an open coordination site at the metal center that is usually required for catalysis. Therefore, a series of multidentate ligands with a different number of coordinating atoms with different arrangements is targeted. Investigation of their structures and catalytic activities is part of a large project studying iron-catalyzed transformations in our laboratory. At the same time, we could be able to introduce new potential catalytic systems for practical applications in oxidation reactions.

4.2. Introduction

Research on iron catalyzed reactions has gained a lot of interest in recent years.¹ It was motivated by several reasons. Most importantly, iron is the second most abundant metal in the Earth's crust and the most produced metal overall,² which makes it cheap and readily accessible. Iron based catalysts are considered relatively non-toxic due to its higher residual concentration (20 ppm) allowed in pharmaceutical products compared to other commonly employed metals such as ruthenium or chromium (5 ppm).³

Iron catalyzed oxidation reactions are seen as great candidates for substitution of current industrial processes for "greener" alternatives. However, an iron complex suitable for industrial catalytic oxidations utilizing peroxide oxidants has yet to be

discovered. An approach to the investigation of the new iron catalysts is based on mimicking enzymes found in nature. Two main types of iron containing enzymes are heme and non-heme oxygenases.⁴ Heme proteins such as cytochrome P450 feature an iron-porphyrin complex as their cofactor and are known to catalyze various oxidation reactions.^{5,6} However, non-heme architectures of ligands can provide broader structural diversity and the possibility for steric and electronic adjustments.⁷ Preliminary research already performed in our laboratory included the study of bidentate N,N donating ligands (**I, Figure 4.1**)^{8,9}.

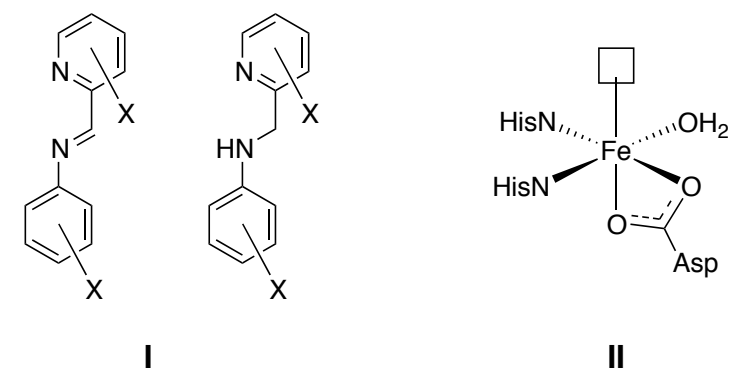


Figure 4.1. Non-heme iron complexes currently investigated in our laboratory^{8,9}

In this chapter, iron complexes mimicking a non-heme enzyme known as Rieske dioxygenase (**II, Figure 4.1**) were targeted. The catalytically active iron center in that enzyme is coordinated by two nitrogen atoms from histidine amino acid residues and two aspartate anion oxygen atoms.¹⁰

4.3. Synthesis of the ligands

Our study of the catalytic activity of the iron chelate complexes mimicking motifs found in nature started with the design of appropriate ligands. To mimic non-heme type structures utilizing artificial iron complexes, the ligand should contain coordinating nitrogen atoms. A combination of pyridyl and amino functionalities were selected as a source for coordinating nitrogen atoms. On the other hand, we intended to probe the influence of oxygen as one of the coordinating atoms on the catalytic activity of the respective iron complexes. It forms weaker coordinating bonds with iron and the presence of a loosely bonded coordinating atom in a complex could lead to open coordination sites required in catalytic cycles.¹¹ Consequently, the final choice included five target ligands **4.1-4.5 (Figure 4.2)**. Three of the structures (**4.1, 4.2, 4.5**) can potentially be tridentate ligands, and the molecule **4.3** can be tetradentate, while target **4.4** can occupy up to five coordination sites at the iron center.

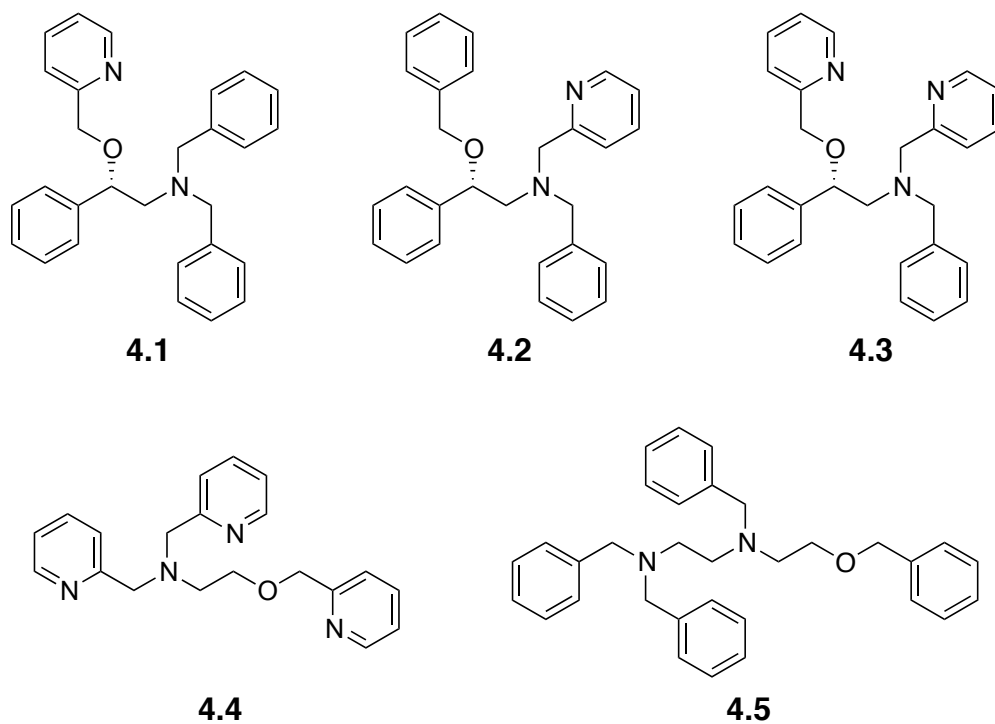


Figure 4.2. Structures of the target ligands 4.1-4.5

An advantage of the selected ligands is that they can be easily synthesized from commercially available starting materials. The core structures of the ligands are aminoalcohols formally protected both at nitrogen and oxygen. Three target structures **4.1-4.3** are derivatives of the same aminoalcohol (**4.6**, **Figure 4.3**). The compound **4.1** bears a picolyl group on the oxygen and a benzyl unit on the nitrogen atom, while the ligand **4.2** exhibits an opposite substitution array. The tetradentate ligand **4.3** contains picolyl groups both at nitrogen and oxygen.

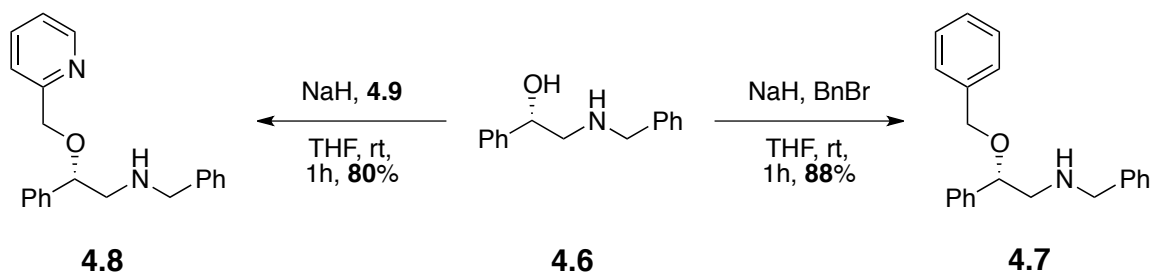


Figure 4.3. First step in the synthesis of the tridentate ligands 4.1 and 4.2

The synthesis of ligands **4.1** and **4.2** is based on a sequence of selective alkylations of the amino and hydroxy functionalities in **4.6**. The two molecules differ in the placement of the picolyl and benzyl groups. The presence of two nucleophilic sites in the aminoalcohol **4.6** required reaction conditions that can differentiate them. Two different approaches were investigated in order to achieve that goal.

It is known that nucleophilicity of an anion is much higher than that of a neutral atom.¹² Hence, in the presence of a strong base, the hydroxyl group would be selectively deprotonated and produce a more reactive alkoxide anion that could be selectively alkylated. To implement that methodology, the aminoalcohol **4.6** was subjected to literature known *O*-alkylation conditions employing NaH as the base.¹³

For the synthesis of ligand **4.1**, the oxygen was first protected with a benzyl group to obtain **4.7** in 88% yield as colorless oil (**Figure 4.3**). The reaction was performed in THF solution at room temperature. Upon addition of NaH to the solution of the starting material, a vigorous formation of hydrogen gas was observed and the color of the mixture gradually changed from transparent to intensely yellow over a period of 30 minutes, which suggested formation of the anion. At that point, benzyl bromide was added and the color disappeared within a few minutes. To ensure complete conversion, the reaction mixture was allowed to stir at room temperature for 30 more minutes. Aqueous work up resulted in the crude product that exhibited high purity, but still contained small amounts of the mineral oil from the NaH emulsion as assessed by ¹H NMR, which exhibited peaks between 1.8 and 0.9 ppm in the aliphatic region. A sample for a final characterization was obtained by purification employing column chromatography on silica. The yield calculated for

the crude product **4.7** was 93%, which dropped after the chromatography to 88%. A similar procedure was applied for synthesis of **4.8**. The required alkylating reagent **4.9** is available from commercial sources as hydrobromide salt (**4.10**, **Figure 4.4**). Therefore, the compound **4.10** was neutralized before usage (**Figure 4.4**), which was performed in a quick biphasic H₂O/CH₂Cl₂ reaction. The aqueous layer contained K₂CO₃ and the salt **4.10**, releasing the free amine **4.9** upon abstraction of HBr by the base. Being more soluble in organic solvents, compound **4.9** accumulated in the CH₂Cl₂ phase. Separation of the organic phase and removal of the solvent afforded the “ready for use” picolyl bromide **4.9**. As a free amine, this compound is not very stable, so it was employed in syntheses immediately after preparation. According to the procedure described above for compound **4.7**, the alkoxide of the aminoalcohol **4.6** was prepared and treated with a THF solution of freshly purified **4.9**. Similar observation of the color change was observed, and the alkylation of **4.6** with the bromide **4.9** was performed the same way as the synthesis of **4.7**. Only one minor modification was performed compared to the initial procedure. The crude material **4.8** contained a significantly larger amount of side products than crude **4.7**, and thus the optional purification by column chromatography was mandatory for the compound **4.8**, which was isolated in 80% yield as an oil.

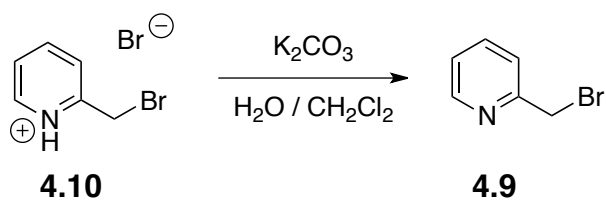


Figure 4.4. Neutralization of the salt 4.10 for the formation of the alkylating agent 4.9

Despite of the relatively high isolated yields obtained for compounds **4.7** and **4.8** by alkylation in the presence of NaH, we were interested in employing an alternative base. Application of DMSO solutions of NaOH or KOH for that purpose is less common due to the limits these bases place on the starting materials to be employed, which have to be able to withstand the presence of basic and nucleophilic hydroxide anions.¹⁴ In cases where hydroxide use is conceivable, the reactions usually are easier to perform, cleaner and higher yielding.¹⁵ The structure of the aminoalcohol **4.6** does not contain any functionalities sensitive to NaOH, thus it was employed in an alternative synthetic pathway to the compounds **4.7** and **4.8** (Figure 4.5).

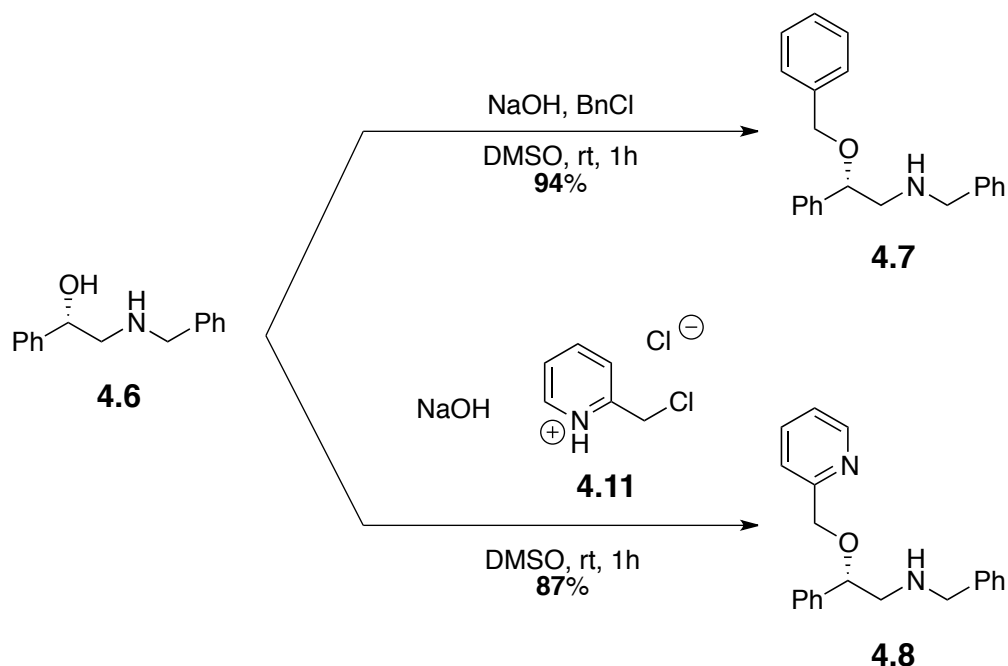


Figure 4.5. Alternative pathways for O-alkylation of the aminoalcohol 4.6

The syntheses started with the preparation of the anion of the compound **4.6**. For this purpose, finely powdered NaOH was mixed with DMSO and vigorously stirred for 20 minutes. Then, a solution of the aminoalcohol **4.6** in DMSO was added to the highly basic mixture. Stirring was continued for 20 more minutes until the reaction gained a colorless, gelatinous appearance. Usually, this indicates formation of an anion, as was observed in the previous synthesis of **4.7** and **4.8**. At that time, the reaction mixture was ready for the addition of the alkylation agents. In order to prevent overheating, the reaction was cooled down with an ice bath. The alkyl bromides were added dropwise as DMSO solutions. Benzyl chloride was employed to perform the synthesis of compound **4.7**, resulting in the introduction of a benzyl group on the oxygen, while the picolyl group in the molecule **4.8** was placed by using the salt **4.11**. After the addition of the reagents, the reactions were allowed to warm up to room temperature over 30 minutes. Work up of the reaction mixtures

containing solvents like DMSO or DMF usually can be very troublesome due to their solubility in H₂O and their high boiling points. But for our syntheses, a convenient procedure to remove the solvent was found. Despite the miscibility of DMSO with many organic solvents, its solubility in non-polar solvents is very low. Therefore, we implemented a two phase separation of the reaction mixtures utilizing toluene and H₂O as immiscible solvents. We did not detect any residual amounts of DMSO in the organic layer after four washes with H₂O. In both cases, the work up led to the crude products **4.7** or **4.8**, which contained only trace quantities of benzyl and picolyl alcohols resulting from hydrolysis of excess amounts of the alkylating agents employed during synthesis. The impurities were removed by column chromatography and the pure compounds **4.7** and **4.8** were obtained as oils in 94% and 87% yields, respectively.

The methodology using NaOH is very similar to the NaH procedure. However, the former was found to have substantial advantages over the latter. The overall process was significantly less sensitive to the quality of the solvents and reagents and the reactions did not require special precautions to exclude moisture. The yields were either comparable to that employing NaH or better. Most significantly, the commercial picolyl chloride salt **4.11** could be employed in synthesis without prior neutralization according to **Figure 4.4**, making the procedure “one pot”.

Finally, another approach for the synthesis of **4.1** and **4.2** was investigated. This method for the selective alkylation was based on different nucleophilicities of amine and hydroxyl groups under neutral or just slightly basic conditions. In absence of a strong base, the nitrogen atom of the aminoalcohol **4.6** is generally more

nucleophilic.¹² Therefore, it should be alkylated at a much higher rate than the oxygen of the hydroxyl group. Accordingly, syntheses of compounds **4.1** and **4.2** were performed by treatment of the aminoalcohol **4.6** with benzyl bromide or freshly prepared picolyl bromide **4.9**, respectively (**Figure 4.4**). The reactions were performed in CH₂Cl₂ solutions at room temperature in presence of Et₃N. Alkylation of the amino functionality was observed in both cases by TLC and NMR but the transformations proceeded very slowly and formation of side products was seen with increasing reaction time. Attempts to increase rate of the reactions and their selectivity by employing heat, a variety of solvents and implementing Bu₄NI as an ion exchange catalyst did not result in a more practical procedure. At this point it was apparent that the method was not going to have any advantages over the other approaches. Thus, its investigation was not pursued further.

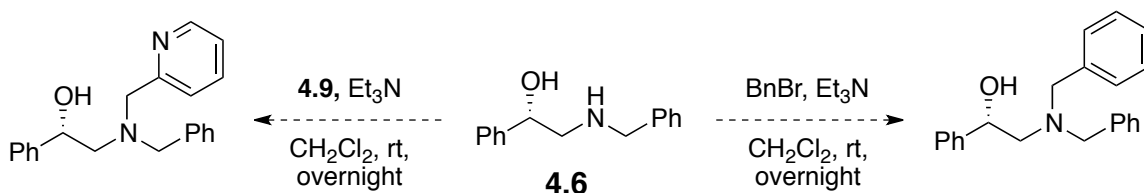


Figure 4.6. Attempted selective *N*-alkylation of the aminoalcohol **4.6**

To complete the conversion of the compounds **4.7** and **4.8** to the tridentate ligands **4.1** and **4.2**, the amino groups of those molecules were converted to the corresponding picolyl and benzyl compounds. The method investigated above for selective *N*-alkylation (**Figure 4.6**) was chosen to accomplish that transformation. Though it was not found to be practical for aminoalcohols previously, on this stage of the synthesis both starting materials **4.7** and **4.8** contained only one nucleophilic site, thus selectivity was not a concern. Accordingly, solutions of the compounds **4.7**

and **4.8** in CH_2Cl_2 were treated with picolyl bromide **4.9** or benzyl bromide, respectively (**Figure 4.7**). The base Et_3N was employed to assist the departure of the proton from the nitrogen atoms, leading to formation of the products **4.1** and **4.2**. As expected based on the previous results of this approach, the conversions were progressing rather slowly. However, formation of only one new compound was observed in both reactions. After 24 hours, the presence of starting materials was not detected by TLC. The reaction mixtures were diluted with CH_2Cl_2 and subjected to work up. Consecutive washing of the organic layer with H_2O and saturated aqueous NaHCO_3 removed excess of Et_3N and salt byproducts. Removal of the solvent resulted in crude **4.1** and **4.2**. Following purification by column chromatography yielded the pure ligands **4.1** and **4.2** in 74% and 82% yield, respectively.

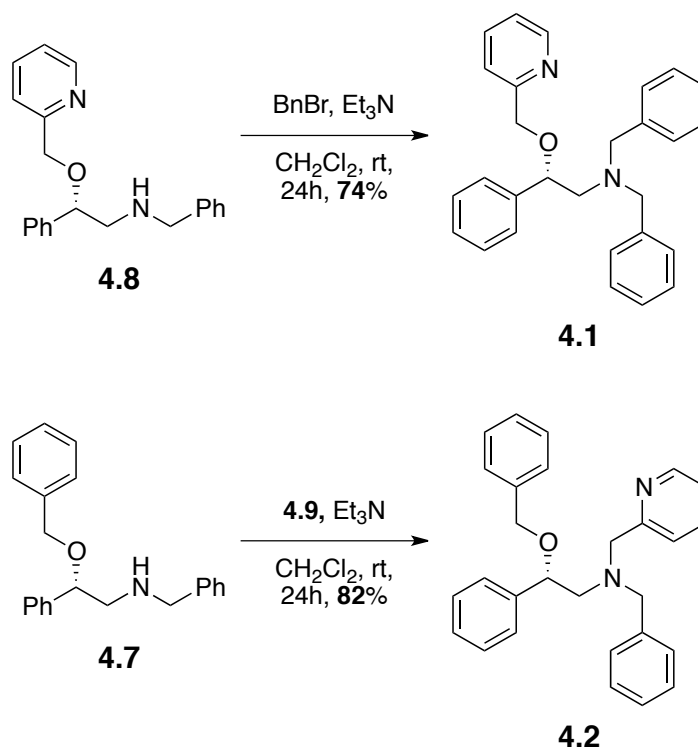


Figure 4.7. Synthesis of ligands **4.1** and **4.2**

In order to convert aminoalcohol **4.6** to the tetradentate ligand **4.3**, both the amine and the hydroxyl were alkylated with the picolyl group. A step-by-step functionalization (pathway **A**, **Figure 4.8**) and a one pot method (pathway **B**, **Figure 4.8**) was employed for the synthesis.

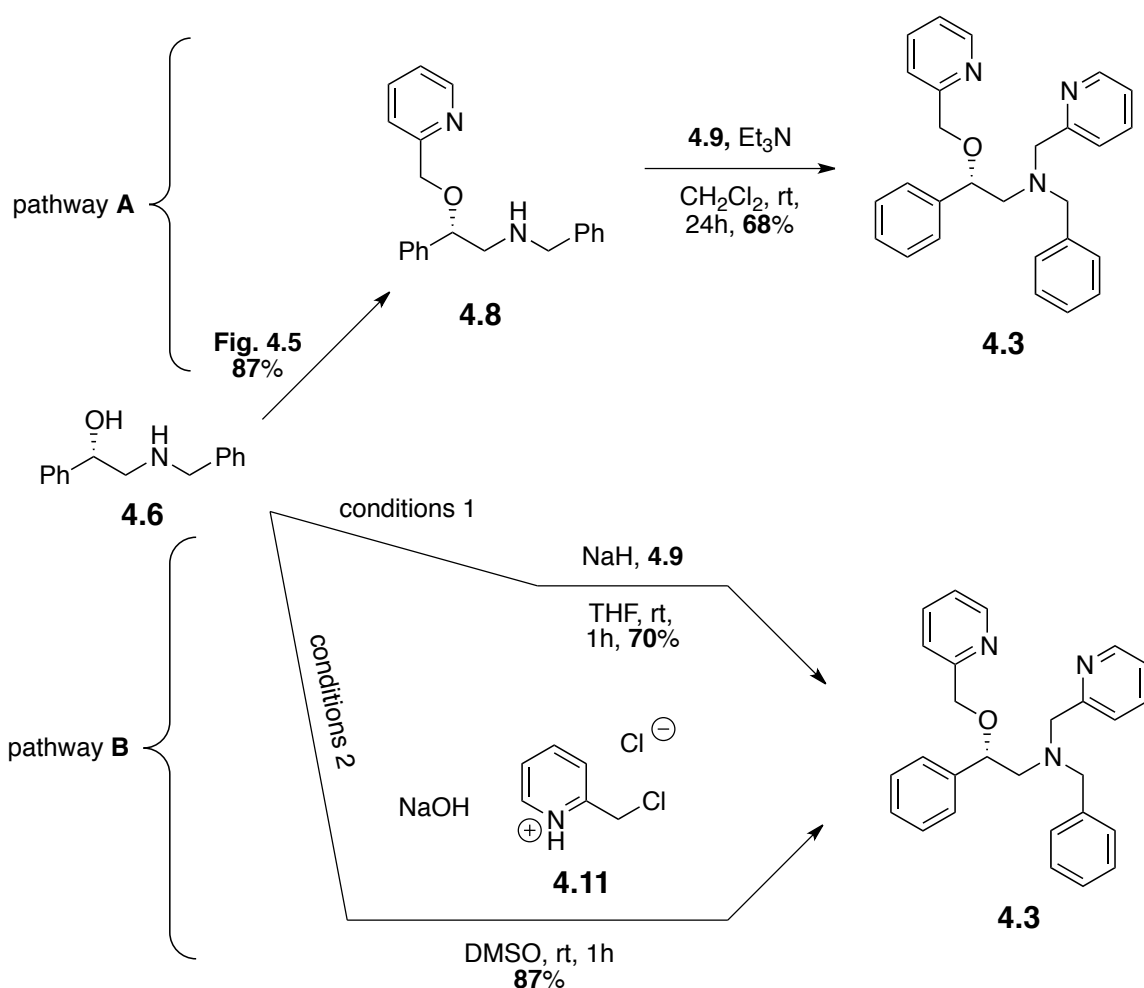


Figure 4.8. Synthesis of the tetradentate ligand 4.3

The pathway **A** (**Figure 4.8**) to the target molecule **4.3** is similar to the approaches investigated above to obtain the tridentate ligands **4.1** and **4.2**. It shared the first step with the synthesis of the compound **4.1** (**Figure 4.3** and **Figure 4.5**), while the following *N*-alkylation was related to that employed in the preparation of the

molecule **4.2** (**Figure 4.7**). Therefore, this procedure was investigated first. The compound **4.8** was already synthesized before in 87% yield (**Figure 4.5**), hence only introduction of the picolyl group on the nitrogen atom was required to obtain the desired product **4.3**. The synthesis was performed according to the procedure described above for the transformation of **4.7** into **4.2** (**Figure 4.7**). The alkylation proceeded as expected and resulted in ligand **4.3** in 68% yield. The overall yield of **4.3** starting from aminoalcohol **4.6** was calculated to be 59%.

The two step preparation of **4.3** has the advantage of sharing the intermediate **4.8** with the synthesis of ligand **4.1**. The divergent approach made the synthesis convenient, but we were still interested in improving the overall yield of the ligand **4.3**. Therefore, a one step procedure was investigated (pathway **B**, **Figure 4.8**). The synthesis required the use of a strong base due to the need for deprotonation of the hydroxyl group. Similar to the preparation of tridentate ligands **4.1** and **4.2**, methods based on employing NaH (conditions 1) and NaOH (conditions 2) were examined. To probe the employment of NaH, a solution of the aminoalcohol **4.6** in THF was treated with a fourfold molar excess of NaH. The amount of the base was required to both completely deprotonate the alcohol and to assist the departure of the proton from the nitrogen. Addition of a 50% excess of freshly prepared picolyl bromide **4.9** resulted in a very dark colored reaction mixture. The crude product was separated from the reaction mixture by an aqueous work up as a dark brown oil. Purification was performed by column chromatography and resulted in the still slightly colored but spectroscopically pure ligand **4.3** in 70% yield. Application of the alternative base NaOH (conditions 2, **Figure 4.8**) by means of the procedure

described above (**Figure 4.5**) improved the yield of the compound **4.3** to 87%. As mentioned before, if applicable the employment of NaOH usually gives better yields. While during synthesis of the compounds **4.7** and **4.8** both conditions performed well (**Figure 4.3** and **Figure 4.5**), a noticeable difference was observed during the preparation of ligand **4.3** (**Figure 4.8**). In addition to improved yields the overall reaction proceeded cleaner for Pathway **B**, conditions 2. The crude material obtained after a work up was nearly colorless and, according to NMR data, contained only the expected product **4.3** with small amounts of picolyl alcohol, which was easily removed by column chromatography. A minor drawback of the method was the relatively high amount of NaOH and the reagent **4.11** employed. It was found that an eightfold excess of NaOH and two equivalents of the alkylating agent **4.11** gave the highest yields. However, both NaOH and the compound **4.11** are much cheaper and easier to handle than NaH and reagent **4.9**.

The studies of the different approaches to alkylate the aminoalcohols helped to select the potentially most suitable method for synthesis of the last two target ligands **4.4** and **4.5** (**Figure 4.9**). Both molecules are derivatives of the commercially available aminoalcohols **4.12** and **4.13**, respectively. These starting materials required introduction of multiple alkyl groups at both the amine and hydroxyl functionalities. It was already shown that the best result for this type of transformation could be expected from employing the NaOH/DMSO methodology for the alkylations described above (**Figure 4.5**). Accordingly, the synthesis of both ligands started with the preparation of a NaOH solution in DMSO. As mentioned before, the best results were achieved with a fourfold excess of NaOH. Hence,

synthesis of the ligand **4.4** required 12 times the amount of the base over the ethanolamine **4.12**, while the starting material **4.13** in the second reaction required 16 moles of NaOH. Use of such large amounts of the base required extra time for the solutions to become mainly homogenous. Thus, they were vigorously stirred for one hour before the addition of the aminoalcohols. Complete benzylation of the compound **4.13** with benzyl chloride resulted in the ligand **4.5** in 93% yield, while introduction of three picolyl groups on the ethanolamine **4.12** employing the picolyl chloride salt **4.11** afforded the expected product **4.4** in 85% yield.

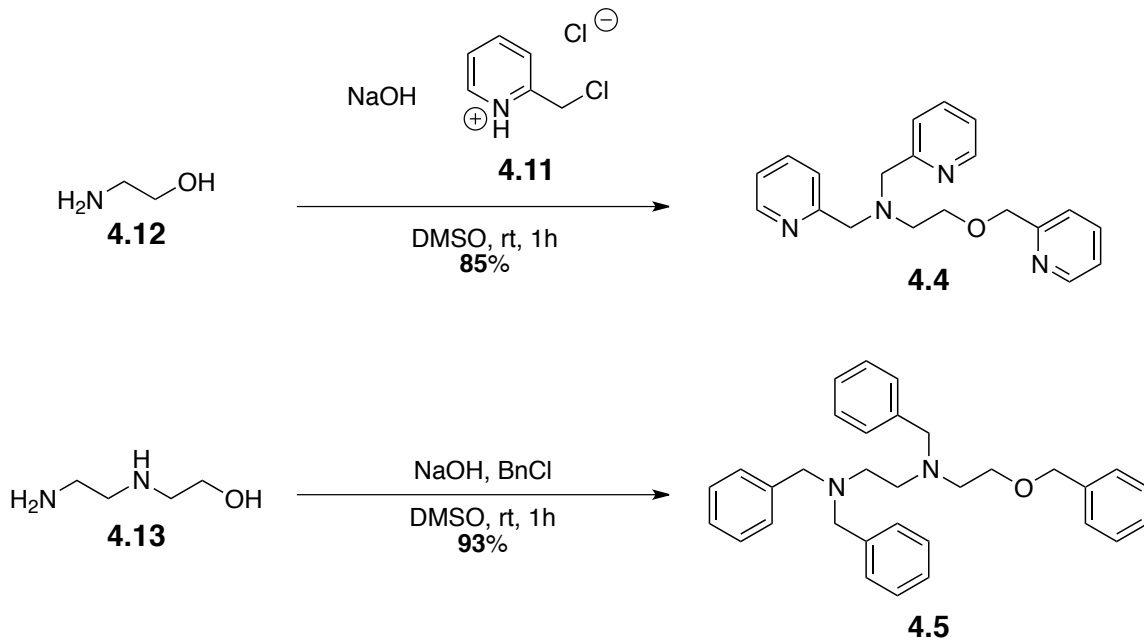


Figure 4.9. Synthesis of the ligands 4.4 and 4.5

4.4. Application of the new ligands in catalysis

There is a couple of principal ways how ligands are applied in catalysis. In one of the approaches, a ligand is employed in preparation of a well defined metal complex. The resulting complex is isolated, purified, characterized and then applied in

synthesis as a catalyst. This method is common for various organic transformations. For example, olefin metatheses can be performed utilizing commercially available ruthenium complexes,¹⁶ and various hydrogenation methods employ preformed coordination compounds.¹⁷ Knowledge of the structure of a complex can help investigating the mechanism of a catalytic cycle and facilitate rational ligand design.¹⁸ Another practical approach involves *in situ* formation of the catalytically active complex. A general procedure consists of setting up a catalytic reaction by combining a metal source and a ligand in solution. The active coordination compound forms *in situ* and then starts, after addition of the reactants, a catalytic cycle. This method found wide application in cross-coupling carbon-carbon and carbon-heteroatom bond forming reactions.¹⁹ Numerous catalytic oxidation reactions also employ a similar methodology.^{20,21} Many iron catalyzed conversions implement an *in situ* formation of the catalytically active compound due to difficulties in isolation and characterization of the corresponding iron complexes. Our goals for this part of the research were to investigate the influence of arrangement, number and type of the coordinating atoms in preformed coordination compounds on the catalytic activity and to introduce a potential new catalytic system based on these ligands.

4.4.1. Preparation of the iron based catalytic systems

The previously synthesized ligands described above were employed in preparation of iron metal complexes. First, we needed to choose an iron source. During previous research in our laboratory, $\text{Fe}(\text{OTf})_2$ and FeCl_2 were successfully employed for this purpose.^{22,23} FeCl_2 is nearly insoluble in most organic solvents to be applied

in the syntheses of the complexes. In addition, the solubility of the coordination compounds obtained from FeCl₂ often is very limited and hampers their application in homogeneous catalysis. On the other side, triflate anions (OTf = CF₃SO₃⁻) afford significantly better solubility of both the initial iron salt and the resulting metal complexes. As mentioned in Chapter I, employment of weakly coordinating counterions (like OTf) assists in the formation of open coordination sites at the metal center, which are required for support of catalytic cycles. Therefore, Fe(OTf)₂ was selected as an iron source for the synthesis of the complexes. A general procedure consisted of a reaction between Fe(OTf)₂ and a ligand in MeCN at room temperature under an inert atmosphere of nitrogen.^{8,9}

First, the three tridentate ligands **4.1**, **4.2** and **4.5** were employed in the synthesis of their respective iron complexes (**Figure 4.10**). The most common coordination number of iron (II) is six. Therefore, two equivalents of the ligands were used for the synthesis. The observations made during the preparation of complexes **4.14** and **4.15** were very similar. The solution of Fe(OTf)₂ in MeCN underwent a transition from colorless to a dark brown upon dropwise addition of a MeCN solution of the ligand. No visual changes were noticed for the reaction mixture after the ligand solutions were completely added. After one hour of stirring at room temperature, the reaction mixtures were layered with Et₂O to precipitate the products from the solutions. Unfortunately, the expected compounds **4.14** and **4.15** did not precipitate. The mixtures of solvents were evaporated from the reaction mixtures and dark brown foams were obtained. A quick washing of the solid materials with Et₂O followed by drying under high vacuum yielded brown

powdered materials that was suitable for the catalytic experiments. The identity of the new complexes will be established below. A completely different outcome was observed when the tridentate ligand **4.5** was employed in synthesis. Formation of a precipitate was observed immediately after addition of a solution of **4.5** in MeCN. Upon completion of the addition, the reaction mixture was entirely heterogeneous. One phase consisted of a colorless liquid and the solid phase was composed of a dark brown flaky material. The solid phase was allowed to settle and the liquid phase was decanted to a separate flask. Evaporation of the solvent did not result in a solid residue. Therefore, the ligand **4.5** fully consumed $\text{Fe}(\text{OTf})_2$ during the reaction to form the tan precipitate **4.16**. Unfortunately, the resulting complex **4.16** did not show notable solubility in any common organic solvent. Thus, the compound is not practical for catalytic applications.

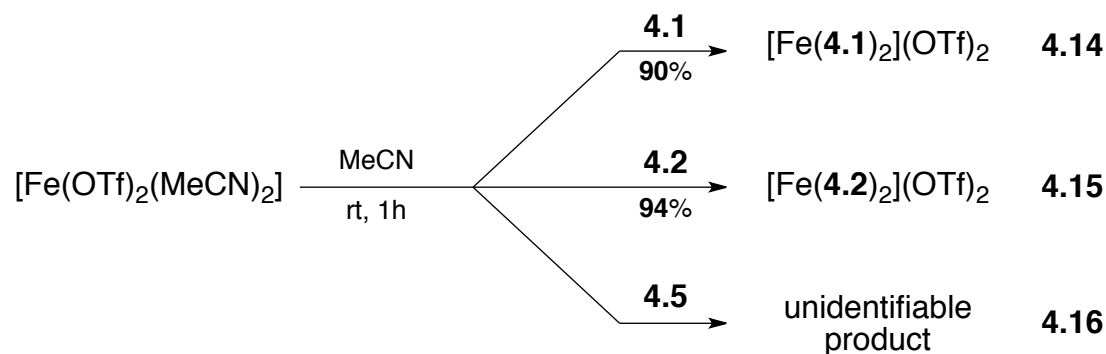


Figure 4.10. Application of the tridentate ligands 4.1, 4.2, 4.5 in the synthesis of iron complexes

Next we moved on to our tetradentate and pentadentate ligands (**4.3** and **4.4**, respectively, **Figure 4.11**). They were reacted with $\text{Fe}(\text{OTf})_2$ according to the procedure described above for the tridentate ligands (**Figure 4.10**). However, only one equivalent of the ligands was required in the synthesis of the corresponding six

coordinate iron complexes **4.17** and **4.18** (**Figure 4.11**). The reactions proceeded without unexpected deviations from the original procedure and resulted in tan solutions after an hour stirring at room temperature. Layering the reaction mixtures with Et₂O did not result in precipitation of the desired complexes **4.17** and **4.18**. Then, after evacuation of the solvents, washing with 5 mL of Et₂O and drying, the compound **4.17** bearing the tetradentate ligand **4.3** and the complex **4.18** carrying the pentadentate ligand **4.4** were obtained as tan powders in 92% and 91% yield, respectively.

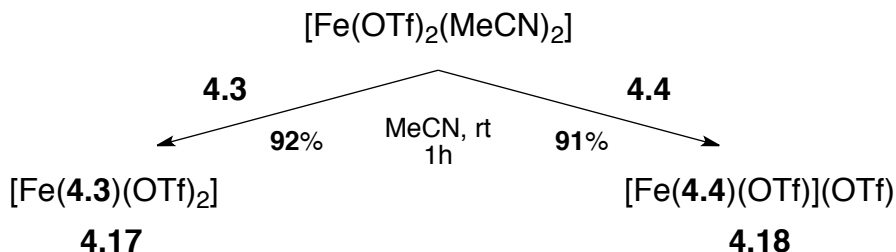


Figure 4.11. Synthesis of new catalysts based on the tetradentate and pentadentate ligands 4.3 and 4.4

Overall, four compounds **4.14**, **4.15**, **4.17**, and **4.18** suitable for catalytic studies were obtained.

4.4.1.1. Characterization of the new iron complexes

Before the investigation of catalytic activities of the synthesized iron complexes, we characterized them and investigated the arrangement of the ligands about the iron center. As was mentioned above, no crystals were obtained for any of the new complexes upon layering the reaction mixtures with Et₂O. Several additional attempts were undertaken to obtain X-Ray quality single crystals. They were based on slow evaporation of the solvent from a solution of the complexes. Also, multiple

binary solvent systems were probed for slow diffusion. Neither experiment produced crystalline material suitable for X-Ray structural analysis. Therefore, the determination of the exact structures by X-ray in the solid state was not possible. Thus, for the analysis of the structures, other physical methods were employed. They included NMR, MS and elemental analysis.

At first, ^1H and ^{13}C NMR spectroscopy was applied for characterization. It is usually problematic to acquire NMR data of iron complexes, as they often are paramagnetic.²⁴⁻²⁶ Accordingly, no NMR data could be obtained for complexes **4.14** and **4.16-4.18**. We were only able to obtain a suitable spectrum for complex **4.15** that was anticipated to contain two tridentate ligands **4.2**. Analysis of the data confirmed the coordination of the ligand **4.2** to the iron center. Upon complexation, the chemical shifts of the aliphatic protons changed. The changes did not follow a common pattern. The CH_2 groups of the picolyl and benzyl functions were shifted slightly upfield from 4.3 ppm and 3.9 ppm to 4.5 ppm and 4.1 ppm, respectively. The protons of the OCHCH_2N unit also had a higher frequency shift from 4.57 ppm to 4.77 ppm for the CH group and from 2.8 ppm to 3.3 ppm for the CH_2 protons. Overall the number of the peaks and their multiplicity matched those of the free ligand. This fact suggested the presence of either one ligand in the structure or a completely symmetrical arrangement of two ligands. It was shown before, that the chemical shift of fluorine in triflate depends on its position in a complex. A free triflate counteranion was reported to resonate around -70 ppm, while a coordinated triflate usually gives downfield shifts around 65 ppm.⁷ This observation was applied to investigate the complex **4.15**. Triflate is a weakly coordinating ligand.

Hence, in order to prevent its possible dissociation and to obtain a reliable fluorine chemical shift, the compound **4.15** was dissolved in a relatively noncoordinating solvent (CDCl_3) and a ^{19}F -NMR spectrum was recorded. The observed chemical shift at -75.9 ppm was in the range consistent with a free triflate. This evidence supported the presence of two ligands **4.2** at the iron center and two non-coordinating triflate counterions. However, additional information from mass spectroscopy and elemental analysis was obtained in order to assign a final structure for the compound **4.15**.

Mass spectrometry provided data for molecular ions and their fragmentation patterns for all iron complexes except the insoluble compound **4.16**. The cations of the compounds **4.14** and **4.15** bearing two tridentate ligands (**4.1** and **4.2**, respectively) at the iron center are twofold positively charged. Two triflate counterions were expected to serve as counterions. Therefore, in the MS data for these compounds, we expected to see peaks corresponding to half of the molecular mass of the complex cations $[(\mathbf{4.1})_2\text{Fe}]^{2+}$ and $[(\mathbf{4.2})_2\text{Fe}]^{2+}$, due to $z = 2$ in the m/z ratio. However, those peaks were not present in the spectra. The most intense signals for both compounds matched the molecular weights of corresponding ligands **4.1** and **4.2**, and less intense peaks according to the fragments with one ligand and one triflate anion ($[(\mathbf{4.1})\text{Fe}(\text{OTf})]^+$ and $[(\mathbf{4.2})\text{Fe}(\text{OTf})]^+$). At the same time we analyzed the MS data for the complexes **4.17** and **4.18** bearing the tetradentate ligand **4.3** and the pentadentate ligand **4.4**, respectively. Both compounds exhibited intense molecular ion peaks consistent with the fragments $[(\mathbf{4.3})\text{Fe}(\text{OTf})]^+$ and $[(\mathbf{4.4})\text{Fe}(\text{OTf})]^+$ formed by loss of a triflate anion. The observed

peaks supported the proposed formulation $[(\mathbf{4.3})\text{Fe}(\text{OTf})_2]$ and $[(\mathbf{4.4})\text{Fe}(\text{OTf})](\text{OTf})$ for the complexes **4.17** and **4.18** (Figure 4.11).

Elemental analysis provided final proof for the formulation of the complexes **4.15**, **4.17** and **4.18**. The obtained results exhibited only slight deviations from the calculated C, H values (<0.5%). The noticeable deviation towards lower values of carbon content was ascribed to the evident hygroscopic properties of the synthesized compounds, which were observed visually and confirmed by IR spectroscopy. Overall, the elemental analyses supported the general formulations for **4.15**, **4.17** and **4.18**. Combination of the NMR and MS findings with the results of the elemental analysis allowed establishing the formulations $[\text{Fe}(\mathbf{4.1})_2](\text{OTf})_2$, $[\text{Fe}(\mathbf{4.2})_2](\text{OTf})_2$, $[(\mathbf{4.3})\text{Fe}(\text{OTf})_2]$ and $[(\mathbf{4.4})\text{Fe}(\text{OTf})](\text{OTf})$ for the synthesized complexes. The iron complex **4.15** was confirmed to form only one isomer in solution by ^1H NMR. However, there are two possible structures to be assigned to this isomer (Figure 4.12), and the physical data are not sufficient to establish the exact structure.

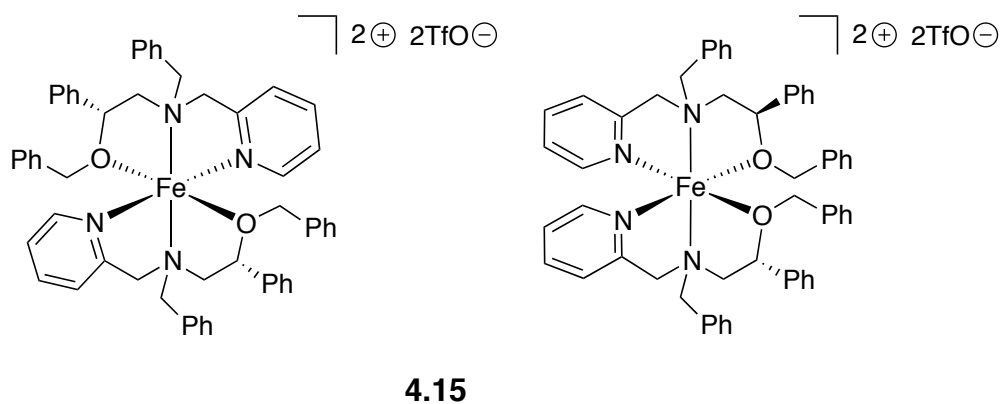


Figure 4.12. The two possible structures of the iron complex **4.15**

4.4.2. Studies of the activities of the catalysts

The relative catalytic activity of the complexes was tested in oxidation reactions utilizing peroxides as the oxidants. Two types of substrates were employed in preliminary studies. The iron catalyzed transformation of activated methylene groups to ketones has been reported in the literature^{7,27} and has already been studied in our laboratory.^{22,23} Accordingly, the first series of test substrates contained activated methylene groups. Several compounds representing different structural features were chosen (**Figure 4.13**).

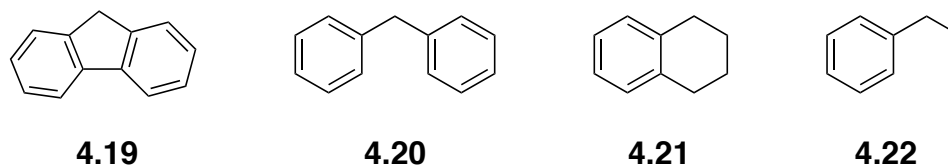


Figure 4.13. Test substrates for the oxidation of activated methylene groups

Another important class of compounds for oxidation studies is alcohols. There are plenty of different methods for the transformation of alcohols into ketones or aldehydes on small scales reported in the literature,²⁸ but only a few of them are applicable for large scale industrial syntheses.²⁹ Catalytic systems, especially those based on cheap metals like iron, are an attractive topic of research.¹ Several alcohols exhibiting different levels of activation were selected for the study (**Figure 4.14**).

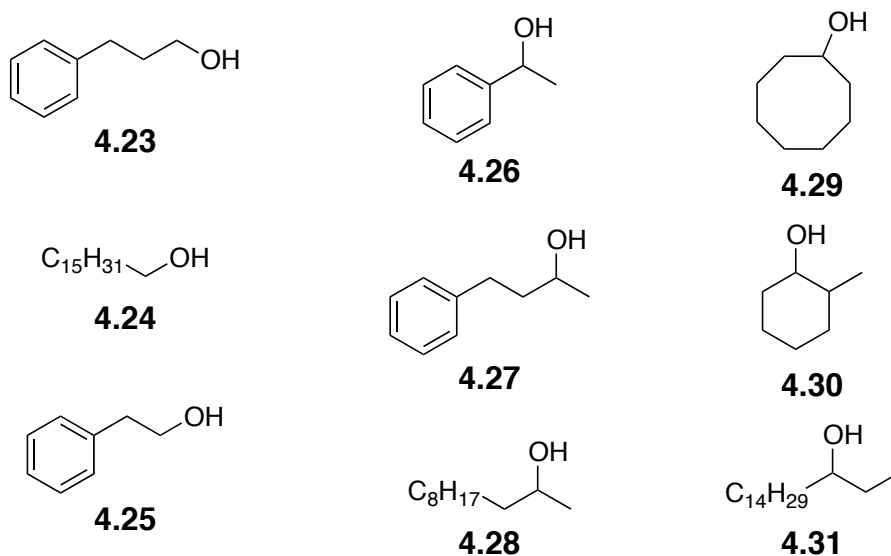


Figure 4.14. Alcohols investigated in catalytic oxidation reactions

4.4.2.1. Comparison of catalytic activities of the complexes

Comparing the activity of the different iron catalysts was the first goal of our study. In order to approach the problem, we needed to create an experiment that would provide reliable data. Furthermore, the conditions of all trials needed to be strictly identical and reproducible for all test reactions. The general protocol employed for the studies is shown in **Figure 4.15**.

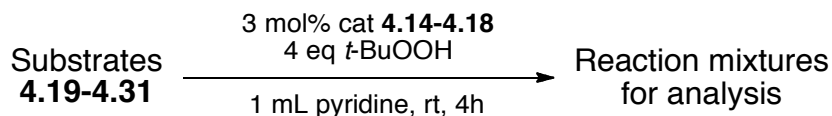


Figure 4.15. General method for comparative catalytic experiments

A similar approach has already been applied in our group before.^{8,9} The method is based on generating a 0.14 M (substrate in pyridine) reaction mixture with constant concentrations of the starting materials, the oxidant and the metal complex in different experiments. It was found that pyridine gives the best results in the

oxidation reactions as has previously been investigated.⁸ Therefore, it was employed as the solvent in all experiments. The standard catalyst load was 3 mol percent, while the oxidizing peroxide agent was employed in a fourfold excess over the starting material. First, the substrate and the catalyst were combined and subsequently the solvent was added. Then, *t*-BuOOH was added the time count was started. Usually, after four hours the conversions of the oxidations were reaching medium to high percentages and flattened. Therefore, the time of the reactions was set to 4 hours as a common, convenient point for obtaining the relative transformations. The samples for determining yields were prepared by filtering 0.3 mL of the reaction mixtures through a short pad of silica gel in order to separate any particles and iron residues. The silica gel was rinsed with 4 mL of CH₂Cl₂, and the combined filtrates were analyzed by GC-MS. With that protocol, batches of 4 experiments at a time were performed employing the same starting material (**4.19-4.31**), but different catalysts (**4.14, 4.15, 4.17, 4.18**). The values for relative conversions of the substrates to the oxidized products are compiled in the **Table 4.1**.

Table 4.1. Data for GC-MS yields in the comparative catalytic experiments

Substrates	Employed catalysts, % GC conversions to ketones or aldehydes			
	4.14	4.15	4.17	4.18
4.19	85	88	89	84
4.20	69	71	72	63
4.21	58	63	60	67
4.22	50	53	47	43
4.23	2	10	4	0
4.24	10	7	8	4
4.25	5	15	3	20
4.26	83	88	80	75
4.27	70	74	80	79
4.28	55	73	68	58
4.29	88	89	98	92
4.30	92	88	95	85
4.31	50	63	70	55

A few unexpected results were obtained after completion of the experiments. First, a large difference in the catalytic activity of the synthesized iron complexes was not observed. We were not able to establish a trend describing the minor changes in conversions observed for different substrates and the catalysts. The slight differences in yields observed for the different catalysts are most likely within experimental error of the GC-MS method. The second unexpected finding concerned

the oxidation of the primary alcohols **4.23-4.25**. These alcohols employed in the catalytic experiments gave almost no conversions with only trace amounts of the corresponding aldehydes along with carboxylic acids and esters, which were observed slightly above baseline levels. The alcohols **4.23** and **4.25** also contained benzylic CH₂ groups that were shown to be oxidized to the ketones in non-alcoholic substrates such as **4.21**. However, the compounds **4.23** and **4.25** did not show oxidation of either the hydroxyl or the methylene groups. Therefore, we assume that primary alcohols are not compatible with our new catalytic systems due to possible decomposition of the metal complexes.

4.4.2.2. Mechanistic considerations of the oxidation reactions

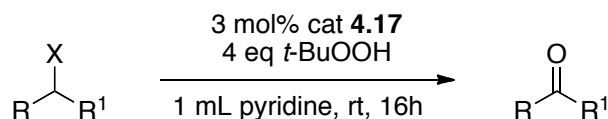
Investigations of mechanisms for iron catalyzed oxidation reactions have been intensively publishing in the literature.^{27,30-35} It was shown that both the mechanism and the participating intermediates depend on a variety of conditions including solvent, and ratios of the reagents and the oxidizing agent.³⁶ However, determination of the exact mechanism for a specific iron catalyzed reaction is a difficult and tedious process. There are two main pathways suggested for iron-catalyzed oxidation reactions employing peroxide oxidants. The first was referred to in the literature as “Oxygenated Fenton Chemistry”³¹ and the alternative one is known as “Gif chemistry”.^{34,37} Usually, analysis of iron catalyzed oxidation reactions allows assignment of their mechanisms to one of those general pathways.³⁸⁻⁴⁰ Regardless of some contradicting publications,^{38,39} “Gif chemistry” is commonly considered to be a non-radical process.^{34,37,40} Therefore, involvement of radical intermediates in “Oxygenated Fenton Chemistry” is the most significant difference

between the two routes.³¹ It was shown that iron catalyzed oxidation reactions employing peroxides as oxidizing agent often follow the radical mechanism.³⁶ During the oxidation of the benzylic methylene groups in substrates **4.19-4.22** utilizing the complexes **4.14**, **4.15**, **4.17**, and **4.18**, corresponding alcohols were never observed in the GC chromatograms of the reaction mixtures. However, formation of trace amounts of dimerized starting materials and pyridyl derivatives of the hydrocarbons **4.19-4.22** were detected along with the expected ketones. Those byproducts could be produced only by participation of radical intermediates in the catalytic cycle. This finding suggested Fenton type chemistry for the mechanism of the catalysis. However, a detailed mechanistic investigation would be needed in order to get more conclusive information about the catalytic cycles for the new iron complexes and possible active species involved.

4.4.2.3. Determination of isolated yields

With the results for the relative activities of the complexes established in **Table 4.1** we moved to the next part of the investigation. The determination of isolated yields is important in order to establish the new catalysts for potential practical applications. As all the synthesized iron complexes showed very similar activity, and the most readily accessible complex **4.17** was selected to determine isolated yields. All four substrates with activated methylene groups **4.19-4.22** were employed for that purpose. Preliminary experiments showed that the primary alcohols **4.23-4.25** did not give significant conversions to the corresponding aldehydes or carboxylic acids. Therefore, four secondary alcohols **4.27**, **4.28**, **4.30**,

4.31 representing different structural features were selected, which gave promising results in preliminary screening (**Table 4.1**).



4.19 Fluorene

4.20 X = H, R = R¹ = Ph

4.21 Tetrahydronaphthalene

4.22 X = H, R = Me, R¹ = Ph

4.27 X = OH, R = Me, R¹ = PhCH₂CH₂

4.28 X = OH, R = Me, R¹ = C₉H₁₉

4.30 2-Methylcyclohexanol

4.31 X = OH, R = Me, R¹ = C₁₄H₂₉

4.32 Fluorenone

4.33 R = R¹ = Ph

4.34 3,4-dihydronaphthalen-1(2*H*)-one

4.35 R = Me, R¹ = Ph

4.36 R = Me, R¹ = PhCH₂CH₂

4.37 R = Me, R¹ = C₉H₁₉

4.38 2-Methylcyclohexanone

4.39 R = Me, R¹ = C₁₄H₂₉

Figure 4.16. General procedure for obtaining isolated yields

The general procedure for the catalytic experiments was based on the conditions established in the comparative experiments described above (**Figure 4.15** and **Table 4.1**) with slight modifications with respect to the time of the reactions (**Figure 4.16**). In the test transformations, where we were looking for differences in conversions after a relatively short period of time (4 hours) to investigate catalytic activity. To obtain isolated yields we were interested in the reactions going to completion. Hence, to achieve full conversion of the starting materials, the oxidations were performed over a period of 16 hours. At this time, the reaction mixtures were filtered through a short pad of silica gel that was rinsed with an excess of CH₂Cl₂. The solvents were removed from the combined filtrates and the desired products were purified by column chromatography on silica. The obtained isolated yields are compiled in **Table 4.2**.

Table 4.2. Isolated yields for the catalytic oxidation reactions

Substrates	4.19	4.20	4.21	4.22	4.27	4.28	4.30	4.31
Desired products	4.32	4.33	4.34	4.35	4.36	4.37	4.38	4.39
Isolated yields, %	89	78	63	74	60	83	57	70

Overall, the catalytic reactions produced good results with isolated yields ranged from 57 to 89%. The oxidations of the activated CH₂ groups in **4.19-4.22** proceeded smoothly and the resulting ketones **4.32-4.35** were easily isolated by column chromatography in high yields (63-89%). However, compound **4.21** containing two benzylic CH₂ groups gave some amount of the overoxidized quinone type product. Therefore, the monoketone **4.34** was obtained with the lowest yield (63%) among the four reactions. Transformation of the alcohols **4.27, 4.28, 4.30, 4.31** to the corresponding ketones gave more diverse results with yields ranging from 57 to 83%. Several factors played a role in the outcome of these catalytic reactions. The best result (83% yield) was obtained for the oxidation of the medium sized, non-functionalized secondary alcohol **4.28**. Elongation of the alkyl chain by several carbon atoms caused a decrease in the yield, as was observed for oxidation of the compound **4.31** to the ketone **4.39** (70% yield), which is possibly due a higher probability of CH₂ group oxidation.

The second problem concerned the possibility of concurrent oxidation reactions of different oxidizable groups in the substrate. It was responsible for the low yield of the ketone **4.36**. The starting alcohol **4.27** contained two reactive sites: the secondary OH group and the benzylic CH₂. Hence, oxidation of both functionalities

was observed during the reaction, with the desired product **4.36** being the major compound in the mixture, which was isolated in 60% yield. The finding suggested that the oxidation of alcohols proceeds at higher rate than that of the activated CH₂ groups.

Lastly, isolation of the relatively low molecular weight ketones, like the compound **4.38**, could be complicated by their high volatility. Thus, the oxidation of the cyclic alcohol **4.30** proceeded with very high conversion and selectivity, but the ketone **4.38** was isolated in only 57% yield.

4.5. Conclusion

Several approaches to a series of new multidentate N, O coordinating ligands were investigated. Overall, five non-heme type ligands were synthesized and characterized. Their coordination chemistry was investigated by preparation of new iron complexes. While the general formulation [Fe(L)₂](OTf)₂, [Fe(L)(OTf)₂] or [Fe(L)(OTf)](OTf) was established for the new complexes, the formation of only one isomer was established only for one of the complexes by ¹H NMR. The catalytic activity of the new compounds was studied in oxidation of activated methylene groups and alcohols utilizing *t*-BuOOH as the oxidant. Although no substantial difference in activity was found, the results were promising and will be investigated further in our laboratory. Consideration of possible mechanisms of the catalysis was presented. Fenton type chemistry was proposed as a mechanism for the catalytic activity for the new iron complexes. However, gathering of more data is required for a thorough investigation of the mechanism. The most readily

accessible iron complex was probed for practical catalytic oxidations under optimized conditions including work up. The corresponding ketone products were isolated in 57 to 89% yield.

Combination of these findings and the previously obtained evidence for different iron based catalytic systems will boost mechanistic studies and hopefully lead to better understanding of ways to improve the outcome of the catalytic transformations described in the chapter.

4.6. References

- (1) Bauer, E. B. *Curr. Org. Chem.* **2008**, *12*, 1341.
- (2) In *CRC Handbook of Chemistry and Physics*; Lide, D. R., Ed.; CRC Press: Boca Raton, Florida, 2005.
- (3) Garrett, C. E.; Prasad, K. *Adv. Synth. Catal.* **2004**, *346*, 889.
- (4) Costas, M.; Chen, K.; Que, L. *Coord. Chem. Rev.* **2000**, *200-202*, 517.
- (5) Geraskin, I. M.; Luedtke, M. W.; Neu, H. M.; Nemykin, V. N.; Zhdankin, V. *V. Tetrahedron Lett.* **2008**, *49*, 7410.
- (6) Ortiz de Montellano, P. R. *Chem. Rev.* **2009**, *110*, 932.
- (7) England, J.; Gondhia, R.; Bigorra-Lopez, L.; Petersen, A. R.; White, A. J. P.; Britovsek, G. J. P. *Dalton Trans.* **2009**, 5319.
- (8) Shejwalkar, P.; Rath, N. P.; Bauer, E. B. *accepted* **2011**.
- (9) Lenze, M.; Rath, N. P.; Bauer, E. B. *in preparation*.
- (10) Bruijnincx, P. C. A.; van Koten, G.; Klein Gebbink, R. J. M. *Chem. Soc. Rev.* **2008**, *37*, 2716.

- (11) Crabtree, R. H. *The Organometallic Chemistry of the Transition Metals*; John Wiley & Sons: New York, 1988.
- (12) Jaramillo, P.; Pérez, P.; Contreras, R.; Tiznado, W.; Fuentealba, P. *J. Phys. Chem. A* **2006**, *110*, 8181.
- (13) *Encyclopedia of Reagents for Organic Synthesis*; J. Wiley & Sons: New York, 2004.
- (14) Trofimov, B. A.; Vasil'tsov, A. M.; Mikhaleva, A. I.; Petrova, O. V.; Polubentsev, A. V. *Russ. Chem. Bull.* **1989**, *38*, 2643.
- (15) Khaibullin, R.; Strobykina, I.; Kataev, V.; Musin, R. *Russ. J. Gen. Chem.* **2009**, *79*, 2197.
- (16) Astruc, D. *New J. Chem.* **2005**, *29*, 42.
- (17) Vries, J. G. d.; Elsevier, C. J. *Handbook of Homogeneous Hydrogenation*; WILEY-VCH Verlag GmbH & Co. KGaA: Weinheim, Germany, 2007.
- (18) Denmark, S. E.; Kalyani, D.; Collins, W. R. *J. Am. Chem. Soc.* **2010**, *132*, 15752.
- (19) Yin, L.; Liebscher, J. *Chem. Rev.* **2006**, *107*, 133.
- (20) Linker, T. *Angew. Chem., Int. Ed.* **1997**, *36*, 2060.
- (21) Katsuki, T.; Sharpless, K. B. *J. Am. Chem. Soc.* **1980**, *102*, 5974.
- (22) Lenze, M.; Bauer, E. B. *J. Mol. Catal. A: Chem.* **2009**, *309*, 117.
- (23) Shejwalkar, P.; Rath, N. P.; Bauer, E. B. *Molecules* **2010**, *15*, 2631.
- (24) De Munno, G.; Julve, M.; Real, J.; Lloret, F.; Scopelliti, R. *Inorg. Chim. Acta* **1996**, *250*, 81.

- (25) Bel'skii, V. K.; Ishchenko, V. M.; Bulychev, B. M.; Protskii, A. N.; Soloveichik, G. L.; Ellert, O. G.; Seifulina, Z. M.; Rakitin, Y. V.; Novotortsev, V. M. *Inorg. Chim. Acta* **1985**, *96*, 123.
- (26) Evangelisti, M.; Bartolom; de Jongh, L. J.; Filoti, G. *Phys. Rev. B: Condens. Matter Mater. Phys.* **2002**, *66*, 144410.
- (27) Rabion, A.; Buchanan, R. M.; Sens, J. L.; Fish, R. H. *J. Mol. Catal. A: Chem.* **1997**, *116*, 43.
- (28) March, J. *Advanced Organic Chemistry: Reactions, Mechanisms, and Structure*; Wiley: New York, 1985.
- (29) Caron, S.; Dugger, R. W.; Ruggeri, S. G.; Ragan, J. A.; Ripin, D. H. B. *Chem. Rev.* **2006**, *106*, 2943.
- (30) Sugimoto, H.; Sawyer, D. T. *J. Am. Chem. Soc.* **1985**, *107*, 5712.
- (31) Sawyer, D. T.; Sobkowiak, A.; Matsushita, T. *Acc. Chem. Res.* **1996**, *29*, 409.
- (32) Walling, C. *Acc. Chem. Res.* **1998**, *31*, 155.
- (33) MacFaul, P. A.; Wayner, D. D. M.; Ingold, K. U. *Acc. Chem. Res.* **1998**, *31*, 159.
- (34) Barton, D. H. R.; Doller, D. *Pure Appl. Chem.* **1991**, *63*, 1567.
- (35) Gelalcha, F. G.; Anilkumar, G.; Tse, M. K.; Brückner, A.; Beller, M. *Chem.-Eur. J.* **2008**, *14*, 7687.
- (36) Gozzo, F. *J. Mol. Catal. A: Chem.* **2001**, *171*, 1.
- (37) Barton, D. H. R. *Tetrahedron* **1998**, *54*, 5805.

- (38) Minisci, F.; Fontana, F.; Araneo, S.; Recupero, F.; Banfi, S.; Quici, S. *J. Am. Chem. Soc.* **1995**, *117*, 226.
- (39) Stavropoulos, P.; Celenligil-Cetin, R.; Tapper, A. E. *Acc. Chem. Res.* **2001**, *34*, 745.
- (40) Schuchardt, U.; Jannini, M. J. D. M.; Richens, D. T.; Guerreiro, M. C.; Spinacé, E. V. *Tetrahedron* **2001**, *57*, 2685.

Chapter IV

Experimental Section

General Methods

Chemicals were treated as follows: THF, toluene, diethyl ether, distilled from Na/benzophenone; CH₂Cl₂, distilled from CaH₂. All reactions were carried out under an atmosphere of nitrogen applying Schlenk techniques if not stated otherwise.

Ethanolamine **4.12**, (*S*)-2-(benzylamino)-1-phenylethanol **4.6**, 2-((2-aminoethyl)amino)ethanol **4.13**, 2-(chloromethyl)pyridin-1-ium chloride **4.11**, NaH 60% suspension in mineral oil, 2-(bromomethyl)pyridin-1-ium bromide **4.10**, NaOH (all Aldrich), Silica gel, 200-400 mesh, 60 Å (Sigma-Aldrich), used as received.

[Fe(OTf)₂(MeCN)₂] was synthesized following a literature procedure.¹

NMR spectra were obtained at room temperature on a Bruker Avance 300 MHz or a Varian Unity Plus 300 MHz instrument (¹H: 300.13 MHz; ¹³C: 75.5 MHz) and referenced to a residual solvent signal; all assignments are tentatively. GC/MS spectra were recorded on a Hewlett Packard GC/MS System Model 5988A. Exact masses were obtained on a JEOL MStation [JMS-700] Mass Spectrometer. Elemental analyses were performed by Atlantic Microlab, GA, USA.

Syntheses

(*S*)-*N,N*-dibenzyl-2-phenyl-2-(pyridin-2-ylmethoxy)ethanamine, (4.1). To a stirred solution of **4.8** (0.610 g, 1.92 mmol) in CH₂Cl₂ (10 mL), Et₃N (0.387 g, 0.535 mL, 2.30 mmol) was added. The resulting solution was cooled to 0 °C (ice/H₂O bath) and BnBr (0.393 g, 0.270 mL, 2.30 mmol) was added dropwise. The reaction mixture was stirred at room temperature for 24 hours. At that time, it was diluted

with CH₂Cl₂ (100 mL) and washed with H₂O, saturated aqueous solution of NaHCO₃ and H₂O. The combined organic layers were dried over MgSO₄ and concentrated *in vacuo*. The crude product was purified by flash column chromatography on SiO₂ (1.5 × 15 cm column; eluted with 9:1 v/v toluene/acetone → 4:1 v/v toluene/acetone) to obtain the product **4.1** (0.580 g, 1.42 mmol, 74%) as a slightly brown oil.

NMR (δ, CDCl₃) ¹H 8.49 – 8.46 (m, 1 H), 7.60 (td, *J* = 7.7, 1.9 Hz, 1 H), 7.50 – 7.46 (m, 1 H), 7.31 – 7.12 (m, 15 H), 7.09 (ddd, *J* = 7.6, 4.9, 1.3 Hz, 1 H), 4.57 (dd, *J* = 6.9, 5.4 Hz, 1 H), 4.55 (d, *J* = 13.8 Hz, 1 H), 4.46 (d, *J* = 13.4 Hz, 1 H), 3.75 (d, *J* = 13.8 Hz, 2 H), 3.60 (d, *J* = 13.8 Hz, 2 H), 2.97 (dd, *J* = 13.6, 7.1 Hz, 1 H), 2.77 (dd, *J* = 13.8, 5.4 Hz, 1 H); ¹³C{¹H} 158.8, 148.8, 140.7, 139.5, 136.4, 128.6, 128.2, 128.1, 128.0, 127.5, 126.9, 126.6, 122.0, 121.2, 81.2, 71.5, 60.2, 59.1.

MS (FAB, 3-NBA, *m/z*) 409 ([**4.1**+H]⁺, 100%), 300 ([**4.1** – PicO]⁺, 19%), 210 ([**4.1** – PicO – PhCH₂]⁺, 3%).

(S)-N-benzyl-2-(benzyloxy)-2-phenyl-N-(pyridin-2-ylmethyl)ethanamine,

(4.2). The compound **4.7** (0.700 g, 2.21 mmol) was reacted with picolyl bromide **4.9** (0.570 g, 3.31 mmol) to yield **4.2** (0.740 g, 1.81 mmol, 82%) as described above for **4.1**.

NMR (δ, CDCl₃) ¹H 8.45 (d, *J* = 4.1 Hz, 1 H), 7.48 (td, *J* = 7.6, 1.4 Hz, 1 H), 7.39 – 7.13 (m, 16 H), 7.09 – 7.01 (m, 1 H), 4.57 (dd, *J* = 6.9, 5.4 Hz, 1 H), 4.45 (d, *J* = 11.7 Hz, 1 H), 4.27 (d, *J* = 11.7 Hz, 1 H), 3.92 (d, *J* = 14.9 Hz, 1 H), 3.80 (d, *J* = 14.9 Hz, 1 H), 3.79 (d, *J* = 13.9 Hz, 1 H), 3.68 (d, *J* = 13.8 Hz, 1 H), 2.98 (dd, *J* = 13.8, 7.2 Hz, 1 H), 2.76 (dd, *J* = 13.7, 5.0 Hz, 1 H); ¹³C{¹H} 160.2, 148.6, 141.0, 139.3, 138.5, 136.2, 128.7, 128.3,

128.2, 128.1, 127.6, 127.6, 127.4, 127.0, 126.8, 122.7, 121.7, 80.2, 70.5, 60.8, 60.7, 59.3.

MS (FAB, 3-NBA, m/z) 409 ([**4.2**+H]⁺, 100%), 318 ([**4.2** – PhCH₂]⁺, 4%), 211 ([**4.2** – PhCH₂O – PhCH₂]⁺, 7%).

(S)-N-benzyl-2-phenyl-2-(pyridin-2-ylmethoxy)-N-(pyridin-2-ylmethyl)ethanamine, (4.3). *Pathway A.* The compound **4.8** (0.800 g, 2.51 mmol) was reacted with picolyl bromide **4.9** (0.650 g, 3.77 mmol) to yield **4.3** (0.700 g, 1.71 mmol, 68%) as described above for **4.1**.

Pathway B, conditions 1. To a stirred solution of **4.6** (0.500 g, 2.10 mmol) in THF (20 mL), NaH (0.211 g, 8.80 mmol, 60% emulsion in mineral oil) was added in small portions. The resulting solution was stirred at room temperature for 30 minutes to yield a bright yellow solution. At that time, picolyl bromide **4.9** (1.14 g, 6.60 mmol) in THF (5 mL) was added dropwise. The reaction mixture was stirred at room temperature for additional 3 hours and then diluted with CH₂Cl₂ (100 mL) and washed with H₂O, a saturated aqueous solution of NaHCO₃ and H₂O. The combined organic layers were dried over MgSO₄ and concentrated *in vacuo*. The crude product was purified by flash column chromatography on SiO₂ (1.5 × 15 cm column; eluted with 9:1 v/v toluene/acetone → 3:2 v/v toluene/acetone) to obtain the product **4.3** (0.630 g, 1.54 mmol, 70%) as a slightly brown oil.

Pathway B, conditions 2. To a flask containing DMSO (20 mL) finely powdered NaOH (1.41 g, 35.2 mmol) was added and the mixture was stirred at room temperature for 30 minutes. A solution of **4.6** (1.00 g, 4.40 mmol) in DMSO (2 mL) was added and the white slurry was stirred at room temperature for additional 30 minutes, upon

which the color changed to yellow. At that time, the reaction flask was placed into an ice/water bath and a solution of picolyl chloride hydrochloride **4.11** (2.90 g, 17.6 mmol) in DMSO (5 mL) was added dropwise. After warming up to room temperature over 30 minutes, the slurry was diluted with PhMe (200 mL). The organic layer was washed three times with H₂O (150 mL), with a saturated aqueous solution of NaHCO₃ and H₂O. The combined organic layers were dried over MgSO₄ and concentrated *in vacuo*. The crude product was purified by flash column chromatography on SiO₂ (2 × 20 cm column; eluted with 9:1 v/v toluene/acetone → 3:2 v/v toluene/acetone) to obtain the product **4.3** (1.57 g, 3.83 mmol, 87%) as a colorless oil.

NMR (δ , CDCl₃) ¹H 8.49 (ddd, J = 4.9, 1.7, 0.9 Hz, 1 H), 8.46 (ddd, J = 4.9, 1.7, 0.9 Hz, 1 H), 7.64 (td, J = 7.7, 1.7 Hz, 1 H), 7.51 (td, J = 7.5, 1.9 Hz, 1 H), 7.35 – 7.19 (m, 12 H), 7.13 (ddd, J = 7.3, 4.9, 1.1 Hz, 1 H), 7.07 (ddd, J = 7.4, 4.9, 1.2 Hz, 1 H), 4.62 (dd, J = 7.1, 5.2 Hz, 1 H), 4.55 (d, J = 13.4 Hz, 1 H), 4.46 (d, J = 13.4 Hz, 1 H), 3.94 (d, J = 14.9 Hz, 1 H), 3.82 (d, J = 14.9 Hz, 1 H), 3.82 (d, J = 13.9 Hz, 1 H), 3.71 (d, J = 13.9 Hz, 1 H), 3.04 (dd, J = 13.8, 7.2 Hz, 1 H), 2.81 (dd, J = 13.7, 5.2 Hz, 1 H); ¹³C{¹H} 160.2, 158.8, 148.9, 148.7, 140.7, 139.3, 136.4, 136.2, 128.7, 128.3, 128.1, 127.7, 127.0, 126.8, 122.7, 122.1, 121.7, 121.2, 81.1, 71.6, 61.0, 60.7, 59.5.

MS (FAB, 3-NBA, m/z) 410 ([**4.3**+H]⁺, 100%), 301 ([**4.3** – PicO]⁺, 50%), 211 ([**4.2** – PicO – PhCH]⁺, 28%).

2-(pyridin-2-ylmethoxy)-*N,N*-bis(pyridin-2-ylmethyl)ethanamine, (4.4).

Ethanolamine **4.12** (0.500 g, 8.19 mmol) was reacted with picolyl chloride

hydrochloride **4.11** (6.04 g, 36.8 mmol) to yield **4.4** (2.33 g, 6.97 mmol, 85%) as described above for **4.3**, *pathway B*, *conditions 2*.

NMR (δ , CDCl₃) ¹H 8.56 – 8.49 (m, 3 H), 7.69 – 7.55 (m, 5 H), 7.42 (d, J = 7.9 Hz, 1 H), 7.19 – 7.10 (m, 3 H), 4.61 (s, 2 H), 3.95 (s, 4 H), 3.74 (t, J = 5.8 Hz, 2 H), 2.93 (t, J = 5.8 Hz, 2 H); ¹³C{¹H} 159.8, 158.6, 148.9, 136.5, 136.3, 122.8, 122.2, 121.9, 121.1, 73.9, 69.4, 60.9, 53.7.

MS (FAB, 3-NBA, m/z) 335 ([**4.4**+H]⁺, 100%), 244 ([**4.4** – Pic + H]⁺, 60%).

***N*¹,*N*¹,*N*²-tribenzyl-*N*²-(2-(benzyloxy)ethyl)ethane-1,2-diamine, (4.5)**. The compound **4.13** (1.00 g, 0.970 mL, 9.60 mmol) was reacted with BnCl (7.29 g, 6.65 mL, 57.6 mmol) to yield **4.5** (4.15 g, 8.93 mmol, 93%) as described above for **4.3**, *pathway B*, *conditions 2*.

NMR (δ , CDCl₃) ¹H ; ¹³C{¹H} 139.7, 139.6, 138.4, 129.0, 128.8, 128.7, 128.3, 128.2, 128.1, 128.0, 127.5, 127.4, 126.7, 126.7, 73.0, 68.9, 59.4, 58.7, 53.6, 52.3, 51.3.

MS (FAB, 3-NBA, m/z) 465 ([**4.5**+H]⁺, 100%), 373 ([**4.5** – PhCH₂]⁺, 5%), 268 ([**4.5** – PhCH₂O – PhCH₂]⁺, 20%).

(S)-*N*-benzyl-2-(benzyloxy)-2-phenylethanamine, (4.7). *Method 1*. To a stirred solution of **4.6** (1.00 g, 4.40 mmol) in THF (40 mL), NaH (0.211 g, 8.80 mmol, 60% emulsion in mineral oil) was added in small portions. The resulting solution was stirred at room temperature for 30 minutes to yield a bright yellow solution. At that time BnBr (0.752 g, 0.523 mL, 4.40 mmol) was added dropwise. The reaction mixture was stirred at room temperature for additional 30 minutes and then it was diluted with CH₂Cl₂ (150 mL) and washed with H₂O, a saturated aqueous solution of NaHCO₃ and H₂O. The combined organic layers were dried over MgSO₄ and

concentrated *in vacuo*. The crude product was purified by flash column chromatography on SiO₂ (2 × 20 cm column; eluted with 9:1 v/v toluene/acetone → 3:2 v/v toluene/acetone) to obtain the product **4.7** (1.23 g, 3.87 mmol, 88%) as a colorless oil that crystallized over a period of time.

Method 2. To a flask containing DMSO (10 mL) finely powdered NaOH (0.352 g, 8.80 mmol) was added and the mixture was stirred at room temperature for 20 minutes. A solution of **4.6** (0.500 g, 2.20 mmol) in DMSO (1 mL) was added and the white slurry was stirred at room temperature for 30 minutes, upon which the color changed to yellow. At that time, the reaction flask was placed into an ice/water bath and a solution of BnCl (0.292 g, 0.265 mL, 2.31 mmol) in DMSO (1 mL) was added dropwise. After warming up to room temperature in over 30 minutes, the slurry was diluted with PhMe (100 mL each). The organic layer was washed three times with H₂O (100 mL), with a saturated aqueous solution of NaHCO₃ and H₂O. The combined organic layers were dried over MgSO₄ and concentrated *in vacuo*. The crude product was purified by flash column chromatography on SiO₂ (2 × 10 cm column; eluted with 9:1 v/v toluene/acetone → 3:2 v/v toluene/acetone) to obtain the product **4.7** (0.655 g, 2.06 mmol, 94%) as a colorless oil that crystallized over a course of several weeks.

NMR (δ , CDCl₃) ¹H 7.38 – 7.33 (m, 4 H), 7.33 – 7.25 (m, 11 H), 4.59 (dd, J = 9.0, 3.8 Hz, 1 H), 4.48 (d, J = 11.5 Hz, 1 H), 4.29 (d, J = 11.5 Hz, 1 H), 3.77 (s, 2 H), 2.98 (dd, J = 12.4, 9.0 Hz, 1 H), 2.75 (dd, J = 12.3, 3.9 Hz, 1 H), 1.94 (br s, 1 H); ¹³C{¹H} 140.5, 140.2, 138.2, 128.5, 128.3, 128.3, 128.0, 127.8, 127.8, 127.6, 126.8, 126.8, 80.7, 70.6, 56.2, 53.6.

(S)-N-benzyl-2-phenyl-2-(pyridin-2-ylmethoxy)ethanamine, (4.8). *Method 1.*

The aminoalcohol **4.6** (0.630 g, 2.77 mmol) was reacted with picolyl bromide **4.9** (0.5 g, 2.91 mmol) to yield **4.8** (0.710 g, 2.23 mmol, 80%) as described above for **4.7**, *method 1*.

Method 2. The aminoalcohol **4.6** (0.500 g, 2.20 mmol) was reacted with picolyl chloride hydrochloride **4.11** (0.379 g, 2.31 mmol) to yield **4.8** (0.610 g, 1.92 mmol, 87%) as described above for **4.7**, *method 2*.

NMR (δ , CDCl₃) ¹H 8.46 (ddd, J = 4.8, 1.6, 0.8 Hz, 1 H), 7.58 (td, J = 7.7, 1.7 Hz, 1 H), 7.44 – 7.15 (m, 12 H), 7.07 (ddd, J = 7.5, 4.9, 0.9 Hz, 1 H), 4.65 (dd, J = 8.9, 3.9 Hz, 1 H), 4.58 (d, J = 13.2 Hz, 1 H), 4.51 – 4.44 (m, J = 13.2 Hz, 1 H), 3.79 (s, 2 H), 3.03 (dd, J = 12.4, 8.9 Hz, 1 H), 2.80 (dd, J = 12.4, 4.0 Hz, 1 H); ¹³C{¹H} 158.0, 148.7, 139.7, 139.6, 136.2, 128.2, 128.0, 127.8, 127.6, 126.6, 126.4, 121.9, 121.2, 81.1, 71.2, 55.6, 53.2.

2-(bromomethyl)pyridine, (4.9). To a 100 mL beaker containing H₂O (25 mL) and CH₂Cl₂ (25 mL) compound **4.10** (1.00 g, 3.95 mmol) and K₂CO₃ (2.73 g, 19.8 mmol) were added. The resulting biphasic mixture was vigorously stirred at room temperature for 30 minutes. At that time the organic layer was separated, dried over MgSO₄, and concentrated *in vacuo*. The product **4.9** (0.620 g, 3.60 mmol, 91%) was obtained as a slightly pink solid and was immediately employed in further syntheses.

NMR (δ , CDCl₃) ¹H 8.56 (d, J = 4.3 Hz, 1 H), 7.71 (td, J = 7.7, 1.4 Hz, 1 H), 7.46 (d, J = 7.7 Hz, 1 H), 7.23 (dd, J = 7.1, 5.2 Hz, 1 H), 4.67 (s, 2 H); ¹³C{¹H} 149.2, 137.0, 122.9, 122.7, 36.8 (CH₂).

[Fe(4.1)₂](OTf)₂, (4.14). A Schlenk flask was charged with [Fe(OTf)₂(MeCN)₂] (0.072 g, 0.165 mmol) and MeCN (4 mL). A solution of the ligand **4.1** (0.135 g, 0.330 mmol) in MeCN (1 mL) was added dropwise with stirring. The resulting tan solution was stirred at room temperature for 1 hour. At that time, the solvent was removed by high vacuum and the residue was washed with Et₂O (3 mL). The solvent was decanted, and the tan residue dried under vacuum to obtain the complex **4.14** (0.175 g, 0.149 mmol, 90%).

NMR (δ , CDCl₃) ¹H 8.64 (br s, 2 H), 8.01 (br s, 2 H), 7.92 – 7.20 (m, 34 H), 7.05 (br s, 2 H), 4.90 – 4.42 (m, 8 H), 4.22 (br s, 6 H), 3.72 – 3.30 (m, 2 H); ¹³C{¹H} 155.2, 146.2, 139.9, 135.2, 131.2, 129.9, 129.0, 128.9, 128.8, 128.7, 126.2, 123.9, 123.0, 68.1, 59.1, 57.2.

MS (FAB, 3-NBA, m/z) 613 ([**4.15** – **4.2** – OTf]⁺, 1%).

[Fe (4.2)₂](OTf)₂, (4.15). The ligand **4.2** (0.230 g, 0.562 mmol) was reacted with [Fe(OTf)₂(MeCN)₂] (0.123 g, 0.282 mmol) to yield complex **4.15** (0.310 g, 0.265 mmol, 94%) as described above for **4.14**. Anal. calcd for C₅₈H₅₆F₆FeN₄O₈S₂: C, 59.49; H, 4.82. Found: C, 58.67; H, 5.07.

NMR (δ , Acetonitrile-d₃) ¹H 8.35 (d, *J* = 2.6 Hz, 2 H), 7.74 (t, *J* = 7.3 Hz, 2 H), 7.12 – 7.39 (m, 34 H), 4.72 (dd, *J* = 9.1, 2.7 Hz, 2 H), 4.40 (d, *J* = 15.6 Hz, 2 H), 4.32 (d, *J* = 15.8 Hz, 2 H), 4.23 (d, *J* = 10.7 Hz, 4 H), 4.12 (d, *J* = 11.5 Hz, 4 H), 3.29 (dd, *J* = 13.2, 2.4 Hz, 2 H), 3.20 (dd, *J* = 13.5, 9.8 Hz, 2 H).

NMR (δ , CDCl₃) ¹H 8.47 (d, *J* = 2.5 Hz, 2 H), 7.67 (t, *J* = 6.1 Hz, 2 H), 7.43 – 7.17 (m, 34 H), 4.77 (dd, *J* = 9.5, 2.7 Hz, 2 H), 4.57 (d, *J* = 15.4 Hz, 2 H), 4.45 (d, *J* = 15.0 Hz, 2 H), 4.42 (d, *J* = 10.9 Hz, 2 H), 4.30 (br s, 4 H), 4.20 (d, *J* = 10.9 Hz, 2 H), 3.50 (dd, *J* = 13.5,

2.7 Hz, 2 H), 3.26 (dd, $J = 13.5, 9.5$ Hz, 2 H); $^{13}\text{C}\{^1\text{H}\}$ 148.0, 138.1, 136.9, 136.8, 129.7, 129.1, 128.9, 128.7, 128.7, 128.2, 127.9, 127.8, 126.7, 123.6, 123.3, 76.1, 70.3, 59.1, 58.8, 57.4; $^{19}\text{F}\{^1\text{H}\} - 75.9$.

MS (FAB, 3-NBA, m/z) 613 ($[\mathbf{4.15} - \mathbf{4.2} - \text{OTf}]^+$, 18%).

$[\text{Fe}(\mathbf{4.5})_2](\text{OTf})_2$, ($\mathbf{4.16}$). The ligand **4.5** (0.640 g, 1.38 mmol) was reacted with $[\text{Fe}(\text{OTf})_2(\text{MeCN})_2]$ (0.300 g, 0.688 mmol) to yield complex **4.16** (0.860 g, 0.670 mmol, 97%) as described above for **4.14**.

MS (FAB, 3-NBA, m/z) 555 ($[\mathbf{4.16} - \mathbf{4.5} - 2\text{OTf} + \text{Cl}]^+$, 0.7%).

$[\text{Fe}(\text{OTf})_2(\mathbf{4.3})]$, ($\mathbf{4.17}$). The ligand **4.3** (0.290 g, 0.711 mmol) was reacted with $[\text{Fe}(\text{OTf})_2(\text{MeCN})_2]$ (0.310 g, 0.711 mmol) to yield complex **4.17** (0.500 g, 0.655 mmol, 92%) as described above for **4.14**. Anal. calcd for $\text{C}_{29}\text{H}_{27}\text{F}_6\text{FeN}_3\text{O}_7\text{S}_2$: C, 45.62; H, 3.56. Found: C, 45.05; H, 3.98.

NMR (δ , Acetonitrile- d_3) ^1H 9.72 (br s), 9.17 (br s), 8.53 – 8.32 (m), 8.23 (br s), 7.92 (br s), 7.83 – 7.65 (m), 7.50 – 7.04 (m), 6.64 (br s), 5.67 (br s), 5.53 (br s), 4.82 (br s), 4.67 (d, $J = 8.5$ Hz), 4.53 (t, $J = 14.8$ Hz), 4.46 – 4.22 (m), 3.36 – 3.21 (m), 3.20 – 3.03 (m); $^{19}\text{F}\{^1\text{H}\} - 66.8$.

HRMS calcd for $\text{C}_{28}\text{H}_{27}\text{F}_3^{56}\text{FeN}_3\text{O}_4\text{S}$ 614.1024, found 614.1030.

$[\text{Fe}(\text{OTf})(\mathbf{4.4})](\text{OTf})$, ($\mathbf{4.18}$). The ligand **4.4** (0.298 g, 0.890 mmol) was reacted with $[\text{Fe}(\text{OTf})_2(\text{MeCN})_2]$ (0.315 g, 0.890 mmol) to yield complex **4.18** (0.560 g, 0.813 mmol, 91%) as described above for **4.14**. Anal. calcd for $\text{C}_{22}\text{H}_{22}\text{F}_6\text{FeN}_4\text{O}_7\text{S}_2$: C, 38.38; H, 3.22. Found: C, 38.19; H, 3.45.

NMR (δ , CDCl_3) ^1H 10.09 (br s, 1 H), 8.81 (d, $J = 2.8$ Hz, 1 H), 8.55 (br s, 3 H), 8.43 (d, $J = 3.2$ Hz, 1 H), 8.01 – 7.94 (m, 1 H), 7.89 (t, $J = 7.3$ Hz, 1 H), 7.81 – 7.64 (m, 4 H), 7.58

– 7.37 (m, 4 H), 7.37 – 7.16 (m, 6 H), 4.76 (br s, 1 H), 4.62 (s, 2 H), 4.45 (br s, 4 H), 4.05 (br s, 1 H), 3.86 (br s, 1 H), 3.52 – 3.35 (m, 3 H).

HRMS calcd for C₂₁H₂₂F₃⁵⁶FeN₄O₄S 539.0658, found 539.0657.

Catalytic experiments

General procedure for comparative catalytic oxidation reaction in Table 4.1.

The substrates **4.19-4.31** (140 μmol) were placed in 7 mL screw-capped vials. Pyridine (1.00 mL) was added to the vials. To the solutions, the iron complexes **4.14-4.18** (4.20 μmol) were added followed by *t*-BuOOH (560 μmol, 70% in H₂O). The sealed vials were shaken for 4 h at room temperature. At that time, samples (0.3 mL) of the reaction mixtures was taken out and filtered through short pads of silica gel. The silica pads were washed with CH₂Cl₂ (4 mL) and the filtrates were analyzed by GC-MS.

Determination of isolated yields

9H-fluoren-9-one, (4.32). 9H-fluorene **4.19** (200 mg, 1.20 mmol) was placed in a 7 mL screw-capped vial. Pyridine (2.00 mL) was added to the vial. Upon dissolving of the substrate, the iron complex **4.17** (27.6 mg, 36.1 μmol) was added followed by *t*-BuOOH (688 μL, 620mg, 4.81 mmol, 70% in H₂O). The sealed vial was shaken for 16 h at room temperature. At that time, the reaction mixture was filtered through a short pad of silica gel. The vial and filter was washed with CH₂Cl₂. The combined filtrates were dried over MgSO₄ and concentrated *in vacuo*. The crude product was purified by flash column chromatography on SiO₂ (1 × 15 cm column; eluted with

9:0 v/v toluene/EtOAc → 19:1 v/v toluene/EtOAc) to obtain the product **4.32** (193 mg, 1.07 mmol, 89%) as white solid.

NMR (δ , CDCl₃) ¹H 7.66 (d, ³J_{HH} = 7.7 Hz, 2 H, H-4 + H-5), 7.64 (d, ³J_{HH} = 7.6 Hz, 2 H, H-1 + H-8), 7.55 (t, ³J_{HH} = 7.6 Hz, 2 H, H-3 + H-6), 7.34 (t, ³J_{HH} = 7.6 Hz, 2 H, H-2 + H-7); ¹³C{¹H} 193.6 (C=O), 143.8 (C-11 + C-12), 134.8 (C-3 + C-6), 133.8 (C-10 + C-13), 129.2 (C-2 + C-7), 124.1 (C-1 + C-8), 120.5 (C-4 + C-5).

Benzophenone, (4.33). The compound **4.20** (200 mg, 1.19 mmol) was oxidized to **4.33** (170 mg, 0.933 mmol, 78%) as described above for **4.19**.

NMR (δ , CDCl₃) ¹H 7.74 (d, ³J_{HH} = 7.7 Hz, 4 H, 2×H-2 + 2×H-6), 7.50 (t, ³J_{HH} = 7.7 Hz, 2 H, 2×H-4), 7.40 (t, ³J_{HH} = 7.6 Hz, 4 H, 2×H-3 + 2×H-5); ¹³C{¹H} 196.1 (C=O), 137.7 (2×C-1), 132.3 (2×C-4), 130.1 (2×C-2 + 2×C-6), 128.2 (2×C-3 + 2×C-5).

3,4-Dihydronaphthalen-1(2H)-one, (4.34). The compound **4.21** (200 mg, 1.51 mmol) was oxidized to **4.34** (140 mg, 0.958 mmol, 63%) as described above for **4.19**.

NMR (δ , CDCl₃) ¹H 7.96 (d, ³J_{HH} = 7.7 Hz, 1 H, H-8), 7.45 (t, ³J_{HH} = 7.5 Hz, 1 H, H-6), 7.25 (m, 2 H, H-5 + H-7), 2.9 (m, 2 H, CH₂), 2.6 (m, 2 H, CH₂), 2.1 (m, 2 H, CH₂); ¹³C{¹H} 198.0 (C=O), 144.4, 133.2, 132.6, 128.7, 127.0, 126.4, 39.0 (CH₂), 29.6 (CH₂), 23.2 (CH₂).

Acetophenone, (4.35). The compound **4.22** (200 mg, 1.88 mmol) was oxidized to **4.35** (168 mg, 1.40 mmol, 74%) as described above for **4.19**.

NMR (δ , CDCl₃) ¹H 7.90 (d, ³J_{HH} = 7.8 Hz, 2 H, 2×H-2), 7.50 (t, ³J_{HH} = 7.7 Hz, 1 H, H-4), 7.41 (t, ³J_{HH} = 7.7 Hz, 2 H, H-3 + H-5), 2.54 (s, 3 H, CH₃); ¹³C{¹H} 197.4 (C=O), 137.1 (C-1), 132.7 (C-4), 128.5, 128.4, 26.0 (CH₃).

4-Phenylbutan-2-one, (4.36). The compound **4.27** (200 mg, 1.33 mmol) was oxidized to **4.36** (118 mg, 0.796 mmol, 60%) as described above for **4.19**.

NMR (δ , CDCl₃) ¹H 7.20 (m, 5 H, Ph), 2.89 (t, ³J_{HH} = 7.0 Hz, 2 H, PhCH₂), 2.73 (t, ³J_{HH} = 7.0 Hz, 2 H, CH₂C=O), 2.00 (s, 3 H, CH₃); ¹³C{¹H} 208.1 (C=O), 141.1 (C-1), 128.5, 128.3, 126.1 (C-4), 45.1 (CH₂C=O), 30.0, 29.8.

Undecan-2-one, (4.37). The compound **4.28** (200 mg, 1.16 mmol) was oxidized to **4.37** (165 mg, 0.969 mmol, 83%) as described above for **4.19**.

NMR (δ , CDCl₃) ¹H 2.39 (t, ³J_{HH} = 15.0 Hz, 2 H, CH₂C=O), 2.11 (s, 3 H, CH₃C=O), 1.32–1.21 (m, 14 H, 7×CH₂), 0.87 (t, ³J_{HH} = 2.7 Hz, 3 H, CH₃); ¹³C{¹H} 208.9 (C=O), 43.7, 31.0, 29.6, 29.4, 29.3, 29.2, 23.8, 22.7, 14.1 (CH₃).

2-Methylcyclohexanone, (4.38). The compound **4.30** (200 mg, 1.75 mmol) was oxidized to **4.38** (112 mg, 0.998 mmol, 57%) as described above for **4.19**.

NMR (δ , CDCl₃) ¹H 2.32 (m, 2 H, CH₂C=O), 2.10 (m, 1 H, CHC=O), 1.98–1.85 (m, 4 H, 2×CH₂), 1.68 (m, 2 H, CH₂), 1.03 (d, ³J_{HH} = 1.5 Hz, 3 H, CH₃); ¹³C{¹H} 212.8 (C=O), 45.2, 41.7, 36.1, 27.4, 25.0, 14.7 (CH₃).

Hexadecan-2-one, (4.39). The compound **4.31** (200 mg, 0.825 mmol) was oxidized to **4.39** (139 mg, 0.578 mmol, 70%) as described above for **4.19**.

NMR (δ , CDCl₃) ¹H 2.38 (t, ³J_{HH} = 17.0 Hz, 2 H, CH₂C=O), 2.10 (s, 3 H, CH₃C=O), 1.33–1.20 (m, 26 H, 13×CH₂), 0.87 (t, ³J_{HH} = 3.2 Hz, 3 H, CH₃); ¹³C{¹H} 209.9 (C=O), 43.9, 32.0, 29.7, 29.60, 29.58, 29.53, 29.5, 29.4, 29.3, 23.9, 22.7, 14.3 (CH₃).

References

- (1) Vos, G.; De Graaff, R. A. G.; Haasnoot, J. G.; Van der Kraan, A. M.; De Vaal, P.; Reedijk, J. *Inorg. Chem.* **1984**, *23*, 2905.